AN ABSTRACT OF THE DISSERTATION OF

Sharon Maley Herbelin for the degree of Doctor of Philosophy presented on July 20, 1999.

Title: Mechanistic Studies of Polyhalogenated Benzenes

Abstract approved:

Redacted for privacy

Peter K. Freeman

Polyhalogenated benzenes have been analyzed by standard electron capture chemical ionization mass spectrometry (ECCI/MS), and electron monochromator mass spectrometer (EM/MS) systems. The EM/MS experiments distinguished electronegative compounds (especially isomers) by transient negative ions (TNIs) of the same mass but differing energies and/or the formation of distinct TNIs of different masses for each electronegative compound. The ECCI/MS results of polybrominated benzenes show that "bromine addition" and hydrogen abstraction reactions occur to form ions with one to three bromines added to the starting material. Computations have given insight into the mechanisms that may be involved in the EM/MS and ECCI/MS experiments. Calculations have also provided qualitative support for the processes that may be occurring in the ECCI/MS experiments, and in non-photochemical and photochemical reactions of polyhalogenated benzenes. Photochemical experiments reveal that a minor, but notable pathway that involves an "*iso*-polychlorobenzene intermediate", is taking part in the photo-dehalogenation of chlorobenzene and hexachlorobenzene.

Mechanistic Studies of Polyhalogenated Benzenes

by

Sharon Maley Herbelin

A DISSERTATION

submitted to

Oregon State University

in partial fulfillment of
the requirements for the
degree of

Doctor of Philosophy

Presented July 20, 1999
Commencement June 2000

Doctor of Philosophy dissertation of Sharon Maley Herbelin presented on July 20, 1999

APPROVED:

Redacted for privacy

Major Professor, representing Chemistry

Redacted for privacy

Chair of Department of Chemistry

Redacted for privacy

Dean of Graduate School

I understand that my dissertation will become part of the permanent collection of Oregon State University libraries. My signature below authorizes release of my thesis to any reader upon request.

Redacted for privacy

Sharon Maley Herbelin, Author

ACKNOWLEDGMENT

I would like to thank Professor Peter K. Freeman for his patience, encouragement, and guidance during my graduate studies. I would also like to thank Professor Max L. Deinzer for allowing me to work with his group and his informative discussions. I am thankful that Dr. Paul Mazurkiewicz and Dr. James A. Laramée ran my samples on the electron monochromator mass spectrometer and for their helpful discussions. Also, I would like to thank to Dr. Donald Griffith for his expertise on mass spectrometry and for his suggestions and advice. I would like to thank the members of the laboratory and chemistry department who offered their help and friendship.

I would also like to thank my husband, Armando L. Herbelin for his scientific advice, love and support.

Finally, a special thanks to the Environmental Health Sciences, Oregon State University Chemistry Department and the N. L. Tarter fellowship for financial support of this research.

CONTRIBUTION OF AUTHORS

The trochoidal electron monochromator mass spectrometer experiments were run in the laboratory of Max L. Deinzer. Two members of this laboratory, James Laramée and Paul Mazurkiewicz conducted the experiments on the trochoidal electron monochromator mass spectrometer system.

TABLE OF CONTENTS

TABLE OF CONTENTS (continued)

Page

TABLE OF CONTENTS (continued)

Page

LIST OF FIGURES

LIST OF FIGURES (continued)

LIST OF TABLES

LIST OF TABLES (continued)

LIST OF TABLES (continued)

LIST OF TABLES (continued)

LIST OF APPENDIX FIGURES

LIST OF SCHEMES

LIST OF SCHEMES (continued)

LIST OF SCHEMES (continued)

LIST OF EQUATIONS

DEDICATION

I would like to dedicate this dissertation to my mother, Jeanne Bell Maley.
May her soul rest in peace.

MECHANISTIC STUDIES OF POLYHALOGENATED BENZENES

Chapter 1: Introduction

Sharon Maley Herbelin

Many polyhalogenated benzenes are prevalent environmental pollutants. Pentachlorobenzene and hexachlorobenzene were used as pesticides in the late 1960's. Pentachlorophenol has been used as a pesticide worldwide and for the protection of wood and wood products against insects and microorganisms. Dioxins have been used as pesticides and are impurities in the manufacturing of chlorophenols.[1-3] Polybrominated benzenes are used as a flame retardant in plastics, paper and electronic manufactured goods, and are bi-products in incineration processes.[4-6]

Since the polyhalogenated benzenes have been found to be toxic and persistent in the environment,[1-6] researchers have been engaged in implementing present analytical techniques and in the development of new analytical methods to analyze trace amounts of polyhalogenated benzenes in "real" samples.[7-9] Many scientists have also been interested in their reaction mechanisms, environmental processes and synthesis. In particular, the photodehalogenation of these compounds and the mechanisms involved in these photochemical reactions are of great interest because a deeper understanding could lead to the development of inexpensive toxic waste disposal methods and/or new applications in synthetic methods.[7, 10-16]

In the following chapters, mechanistic studies have been conducted on the polyhalogenated benzenes. These prevalent environmental pollutants have been analyzed by standard electron capture chemical ionization mass spectrometry, and by an electron monochromator mass spectrometer system. Computations have been undertaken to aid in the understanding of the processes that are occurring in the electron capture chemical ionization mass spectrometry and the electron monochromator mass spectrometry experiments. Calculations have also been performed to provide further insight into the mechanisms participating in non-photochemical and photochemical reactions of the

polyhalogenated benzenes. Finally, experiments were conducted to see if a minor, but important pathway that involves a "π-polychlorobenzene intermediate"[15-16] is taking part in the photodehalogenation of two polychlorinated benzenes, chlorobenzene and hexachlorobenzene.

References

1. Crosby, D.G.; Hamadmad, N.J. *Agr. Food Chem.* **1971**, *19*, 1171.

2. Crosby, D.G.; Moilanen, K.W.; Wong, A.S. *Eniron. Health Perspect.* **1973**, *5*, 259.

3. *Chlorinated Organic Micropollutants*; Hester, R.E., Harrison, R.M., Eds.; Issues in Environmental Science and Technology 6; Royal Society of Chemistry: Cambridge, UK, 1996.

4. Klusmeier, W.; Vögler, P.; Ohrback, K.-H.; Weber, H.; Kettrup, A. *J. Anal. App. Pyrolysis*, **1988**, *13*, 277-285.

5. Watanabe, I.; Kashimoto, T.; Tatsukawa, R. *Bull. Envrion. Contam. Toxicol.*, **1986**, *36*, 778-784.

6. Bieniek, D.; Bahadir, M.; Korte, F. *Heterocycles*, **1989**, *28*, 719-722.

7. Freeman, P.K.; Srinivasa, R.; Campbell, J.-A.; Deinzer, M.L. *J. Am. Chem. Soc.*, **1986**, *108*, 5531-5536.

8. Laramée, M. L.; Kocher, C. A.; Deinzer, M. L. *Analytical Chemistry* **1992,** *64,* 2316-2322.

9. Oster, T.; Kühn, A.; Illenberger, E. *Int. J. Mass Specctrom. Ion Proc.*, **1989**, *89*, 1-72.

10. Freeman, P. K.; Ramnath, N. *J. Org. Chem.* **1988**, *53*, 148-152.

11. Freeman, P. K.; Ramnath, N.; Richardson, A. D. *J. Org. Chem.* **1991**, *56*, 3643-3646.

12. Freeman, P. K.; Ramnath, N. *J. Org. Chem.* **1991**, *56*, 3646-3651.

13. Freeman, P. K.; Jang, J-S.; Haugen, C.M. *Tetrahedron* **1996**, *52*, 8397-8406.

14. Couch, T.L. Ph.D. Thesis, Oregon State University, Corvallis, OR, 1997.

15. Fox, M.A.; Nichols, Jr., W.C; Lemal, D.M. *J. Am. Chem. Soc.* **1973**, *95*, 8164-8166.

16. Arnold, D.R.; Wong, P.C. *J. Am. Chem. Soc.* **99**, *1977*, 3361-3366.

Chapter 2: Analysis of Polyhalogenated Benzenes with a Trochoidal Electron Monochromator Mass Spectrometer System: Mechanistic Study of Polyhalogenated Benzene Radical Anion Cleavage Pathways

Sharon Maley Herbelin, Peter K. Freeman,* M. L. Deinzer, P. Mazurkiewicz, and J. A. Laramée

Department of Chemistry
Oregon State University
Corvallis, OR 97331

Introduction

In standard electron capture chemical ionization mass spectrometry (ECCI/MS) a buffer gas such as methane is used to moderate the electron energy and can cause spurious product ions in the spectra. The Deinzer research group has developed and implemented a trochoidal electron monochromator mass spectrometry (EM/MS) instrument that does not utilize a buffer gas to moderate electron energies. The EM/MS utilizes a magnetic field to confine very low energy electrons and crossed electrical and magnetic fields to produce electrons of differing energies. A series of lenses increases the electron beam intensity by collimating and focusing the energy-selected electrons. The EM/MS is tunable so that very specific energies can be chosen to ionize specific isomers of environmentally prevalent electronegative compounds.[1]

The EM/MS allows for the observation of a variety of different types of ionic processes. Among these are two types of ionic process that are of great interest which are resonance electron capture to form the molecular radical anion and dissociative electron capture which produces fragment ions with the charge residing on either of the two fragments, **Scheme 2.1**.[1,2] These pathways produce transient negative ions (TNIs) that are distinguished by their energy requirements. The minimum energy required for any ion formation is the appearance potential (AP). The AP is the difference in energy of the ground vibrational state of the neutral molecule and the anionic surface within the Born-Oppenheimer formalism, **Figure 2.1**. Franck-Condon factors govern the energetic position and shape of the peak as a function of electron energy that is a reflection of the ground vibrational state wave function of the neutral molecule. These factors hold true as long as the dissociation limit (D_o) and the potential energy along the reaction coordinate lie below

$$AB \xrightarrow{\varepsilon_1} AB:$$

$$AB \xrightarrow{\varepsilon_3} A^- + B^\bullet$$

$$AB \xrightarrow{\varepsilon_2} A^\bullet + B^-$$

Scheme 2.1: Ionic processes observed in EM/MS experiments.

the energy of the anionic surface within the Franck-Condon region, **Figure 2.1**. The peaks of the TNIs may be characterized two ways: the maximum ion production (ε_{max}) which is the topmost position of the ion yield curve measured as a function of electron energy or the centroid energy ($\varepsilon_{centroid}$) which is the energy with 50 % of the ion current above and 50 % of the ion current below the $\varepsilon_{centroid}$, **Figure 2.1**.[1,2]

Experimental Methods

Electron Monochromator Mass Spectrometer System

The Deinzer research group's procedure is a modification of the electron monochromator mass spectrometer (EM/MS) system of Illenberger.[1,2] The electron monochromator is interfaced to a quadrupole mass spectrometer, **Figure 2.2**.[1] Electrons emitted from an exterior rhenium filament are collimated and focused by four electrodes into a magnetic field produced by Helmholtz coils. A small electrical field is applied perpendicular to the electron beam. The electrons are deflected in a perpendicular direction to the magnetic and electrical fields, thus, dispersing in a trochoidal motion

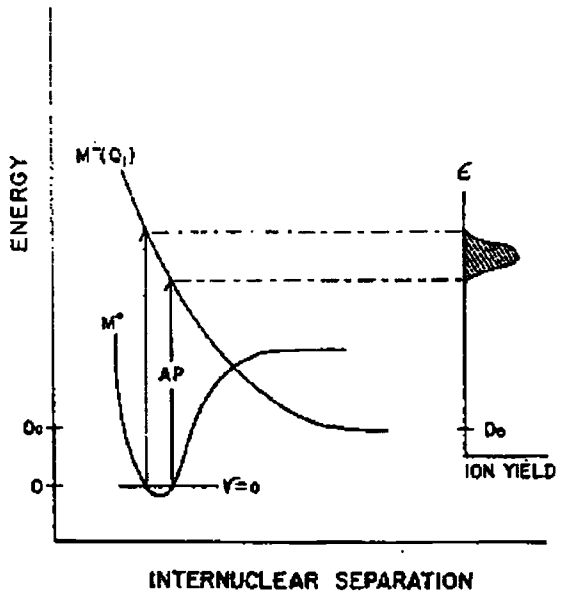

Figure 2.1: **Born-Oppenheimer energy diagram illustrating electron attachment with subsequent electronic dissociation.**[1]

according to their initial kinetic energies. A set of three electrodes right before the ion source function as an einzel lens that focuses the electrons entering the ion source. The positive or negative ions that are formed in the ion source are extracted by a small electrical field and are focused on the entrance aperture of a quadrupole mass spectrometer. Pulses from a Spiraltron ion detector are counted and stored in a multi-channel analyzer. Converting the channel number from the multi-channel analyzer into an analogous voltage signal generates the electron energy potential. The voltage signal is buffered and reshaped and connected via a Wheatstone bridge to a ten-amp filament power supply. The above arrangement allows for a linear conversion between channel number and electron energy. The electron energy scale is calibrated before and after data acquisition by using hexafluorobenzene as a standard that has widely accepted electron attachment energies of 4.5 and 8.3 eV.[1]

The polychlorinated benzenes studied were introduced into the EM/MS by direct probe insertion and the source temperature was 110° C. The polybrominated benzenes were introduced into the electron monochromator via a gas chromatograph with a transfer line set at 270° C, and the source temperature was 98° C.

Chemicals

The chemicals were obtained from commercial sources except for 1, 2, 3, 5- tetrachlorobenzene which was synthesized by a known method.[3] Pentachlorobenzene, 1, 2, 3, 4-tetrachlorobenzene, 1, 2, 4, 5-tetrachlorobenzene, 1, 2, 3-trichlorobenzene, 1, 3, 5-trichlorobenzene, bromobenzene, 1, 3-dibromobenzene, 1, 4-dibromobenzene, 1, 3, 5-tribromobenzene, 1, 2, 3-tribromobenzene, 1, 2, 4-tribromobenzene, 1, 2, 3, 5-tetra-

bromobenzene, and hexabromobenzene were obtained from Aldrich Chemical Co. 1, 4-Di-bromobenzene, 1, 2, 4-tribromobenzene, 1, 2, 3, 5-tetrabromobenzene, and hexabromobenzene were used directly from the manufacturer's bottle. 1, 2, 3-Tri-chlorobenzene and 1, 2, 4-tribromobenzene were crystallized one time each from absolute ethanol. All other compounds were purified by preparative gas chromatography using a Varian 3700 Gas Chromatograph equipped with a thermal conductivity detector. The Varian 3700 gas chromatograph was equipped with a 4′ × 1/8″-10% OV-101 on chromosorb and a 4′ × 1/8″-Chromosorb W on 80/100 solid support reference column. All compounds were found to be greater than 99% pure by analysis on a Varian 3300 and/or a Varian 3400 gas chromatograph equipped with flame ionization detector, and a Varian 3400 gas chromatograph interfaced with a Finnigan 4023 mass spectrometer operating in electron capture chemical ionization mode.

Computations

Ab initio calculations[4] were carried out using the Spartan 4.0-5.0 molecular modeling and Gaussian 92/94 programs.[5,6] The 6-31G*[7-11] and D95[12,13] basis sets were employed. The restricted Hartree-Fock (HF) method and the Moller-Plesset perturbation (MP2) method were used with the 6-31G* basis set. The optimized geometries from lower levels of theory (AM1 and HF/3-21G) were used as starting coordinates for higher-level geometry optimizations. The "/" separates the method from the basis set; and "//" separates the computational level of the energy from the level of the geometry optimization in the following example: B3LYP/D95//B3LYP/D95. Frequency calculations were executed to

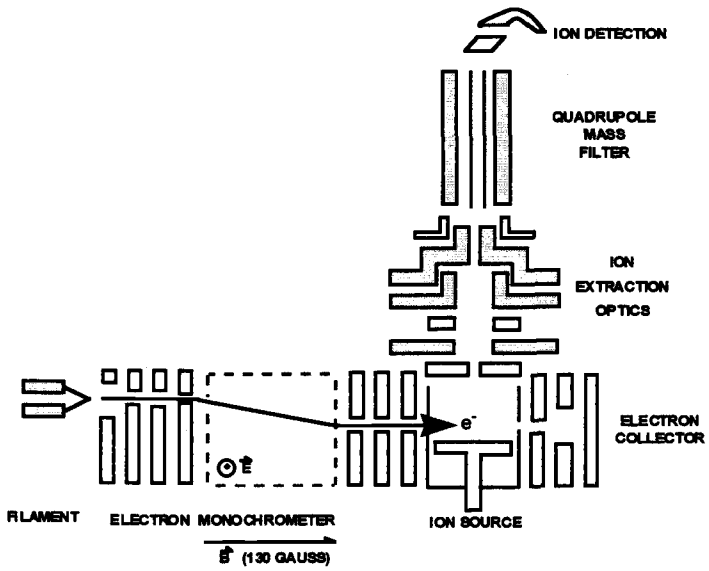

Figure 2.2: **The trochoidal electron monochromator mass spectrometer system schematic diagram.**[1]

ensure that no imaginary frequencies were present in any of the optimized geometries, and, no imaginary frequencies were found for the optimized structures discussed, *vide infra*.

Results and Discussion

Polyhalogenated benzenes that were run on the EM/MS were analyzed via gas chromatographic electron capture chemical ionization mass spectrometry (GC/ECCI/MS) to identify the masses of the most abundant ions. These ions were used as a starting point for direct probe insertion electron monochromator mass spectrometry (DP/EM/MS) and gas chromatographic electron monochromator mass spectrometry (GC/EM/MS) experiments.

Direct probe electron monochromator mass spectrometer experiments were run on the following polychlorinated benzenes: 1, 3, 5-trichlorobenzene, 1, 2, 4-trichlorobenzene, 1, 2, 3, 5-tetrachlorobenzene, 1, 2, 4, 5-tetrachlorobenzene, 1, 2, 3, 4-tetrachlorobenzene and pentachlorobenzene. In the DP/EM/MS experiments most ions that were found in the GC/ECCI/MS experiments of polychlorinated benzenes were observed along with assorted ions formed by resonance and dissociative electron capture processes that were not observed in the latter method. The mass/charge (m/z) ratios, proposed ions for resonance and dissociative electron capture, ε_{max} and $\varepsilon_{centriod}$ values in electron volts (eV) of the TNIs, and population standard deviations are listed in **Tables 2.1**, **2.2**, **2.3**, **2.4**, and **2.5**. The energies corresponding to ε_{max} and $\varepsilon_{centriod}$ are not exactly the same although most are within

Table 2.1: **The ε_{max} and $\varepsilon_{centriod}$ values (eV) of transient negative ions observed in DP/EM/MS experiments on 1, 3, 5-trichlorobenzene and 1, 2, 3-trichlorobenzene.[a,b]**

Compound	m/z	Ion	ε_{max} (eV)[c]	$\varepsilon_{centriod}$ (eV)[c]
1, 3, 5-Trichlorobenzene	180	$M^{-\cdot}$	0.30 ± 0.06	0.37 ± 0.05
	35	Cl^-	0.62 ± 0.11	0.65 ± 0.11
	35	Cl^-	5.25 ± 0.08	5.65 ± 0.12
1, 2, 3-Trichlorobenzene	180	$M^{-\cdot}$	0.15 ± 0.04	0.06 ± 0.03
	79[d]	$(CCl_2)^-$	0.1	0.12
	35	Cl^-	0.19 ± 0.11	0.29 ± 0.05
	35	Cl^-	6.6	

[a]1, 3, 5-Trichlorobenzene and 1, 2, 3-trichlorobenzene were studied in the DP/EM/MS experiments because both were solids. The other isomer, 1, 2, 4-trichlorobenzene, is a liquid and is too volatile resulting in the disappearance of the sample before any results are collected. [b]The trichlorobenzenes were purified by preparative gas chromatography and found to be > 99% pure by gas and GC/ECCI/MS analysis. [c]Averages and standard deviations of two to three experiments run on the EM/MS system. [d]May be an impurity.

Table 2.2: **The ε_{max} and $\varepsilon_{centriod}$ values (eV) of transient negative ions observed in DP/EM/MS experiments on 1, 2, 3, 4-tetrachlorobenzene.[a]**

m/z	Ion	ε_{max} (eV)[b]	$\varepsilon_{centriod}$ (eV)
215	$M^{-\cdot}$	0.17 ± 0.04	0.04 ± 0.04
180	$(M-Cl)^-$	3.70 ± 0.04	3.69 ± 0.01
180	$(M-Cl)^-$	7.74 ± 0.13	7.77 ± 0.15
144	$(M-Cl_2)^-$	6.6 ± 0.07	6.5 ± 0.1
35	Cl^-	0.4 ± 0.02	0.29 ± 0.08
35	Cl^-	6.19 ± 0.73	5.25 ± 1.2

[a]1, 2, 3, 4-Tetrachlorobenzene was purified by preparative gas chromatography and found to be > 99% pure by gas chromatography and GC/ECCI/MS analysis. [b]Averages and standard deviations of three experiments run on the EM/MS system.

Table 2.3: **The ε_{max} and $\varepsilon_{centriod}$ values (eV) of transient negative ions observed in DP/EM/MS experiments on 1, 2, 4, 5-tetrachlorobenzene.[a]**

m/z	Ion	ε_{max} (eV)[b]	$\varepsilon_{centriod}$ (eV)[b]
215	$M^{-\cdot}$	0.18 ± 0.01	0.09 ± 0.03
125	$(M-C_2Cl_2)^-$	0.23 ± 0.13	0.1 ± 0.05
79[c]	$(CCl_2)^-$	0.21 ± 0.2	0.1 ± 0.03
44[c]	$(CCl)^-$	0.08	0.03
35	Cl^-	0.23 ± 0.1	0.26 ± 0.04
35	Cl^-	5.27	5.50

[a]1, 2, 4, 5-Tetrachlorobenzene was purified by preparative gas chromatography and found to be > 99% pure by gas chromatography and GC/ECCI/MS analysis. [b]Averages and standard deviations of three experiments run on the EM/MS system. [c]May be an impurity.

Table 2.4: **The ε_{max} and $\varepsilon_{centriod}$ values (eV) of transient negative ions observed in DP/EM/MS experiments on 1, 2, 3, 5-tetrachlorobenzene.[a]**

m/z	Ion	ε_{max} (eV)[b]	$\varepsilon_{centriod}$ (eV)[b]
215	$M^{-\cdot}$	0.10 ± 0.07	0.04 ± 0.06
215	$M^{-\cdot}$	3.6	
180	$(M-Cl)^-$	0.18 ± 0.10	0.18 ± 0.07
180	$(M-Cl)^-$	3.79 ± 0.11	3.92
195		0.22 ± 0.07	0.19 ± 0.07
160	$(M-Cl+O)^-$	0.20 ± 0.02	0.17 ± 0.07
160	$(M-Cl+O)^-$	3.0	3.06
79[c]	$(CCl_2)^-$	0.1	0.06 ± 0.03
35	Cl^-	0.25 ± 0.11	0.28 ± 0.04
35	Cl^-	5.07	5.55

[a]1, 2, 3, 5-Tetrachlorobenzene was purified by preparative gas chromatography and found to be > 99% pure by gas chromatography and GC/ECCI/MS analysis. [b]Averages and standard deviations of three experiments run on the EM/MS system. [c]May be an impurity.

Table 2.5: **The ε_{max} and $\varepsilon_{centriod}$ values (eV) of transient negative ions observed in DP/EM/MS experiments on pentachlorobenzene.[a]**

m/z	Ion	ε_{max} (eV)[b]	$\varepsilon_{centriod}$ (eV)[b]
250	$M^{-\cdot}$	0.09 ± 0.09	0.03 ± 0.04
215	$(M-Cl)^-$	3.7 ± 0.08	3.81 ± 0.08
204		0.27	0.22
188	$(M-C_2HCl)^-$	0.17	0.2
180	$(M-CCl_2)^-$	6.38 ± 0.09	6.26 ± 0.09
120		0.52 ± 0.14	0.6 ± 0.14
73 or 79[c]	$(CCl_2)^-$	0.27 ± 0.07	0.25 ± 0.14
35	Cl^-	0.24 ± 0.02	0.20 ± 0.08
35	Cl^-	4.41	4.78

[a]Pentachlorobenzene was purified by preparative gas chromatography and found to be > 99% pure by gas chromatography and GC/ECCI/MS analysis. [b]Averages and standard deviations of three or more experiments run on the EM/MS system. [c]May be an impurity.

experimental error. The slope of the anionic yield curve may be skewed from gaussian because the shape of the ion yield curve is a reflection of the ground vibrational state wavefunction bound to the anionic surface, **Figure 2.1**.[1,2]

In general, transient negative ions for resonance electron capture are observed for all the polychlorinated benzenes studied in the DP/EM/MS. Many TNIs were formed from dissociative electron capture where fragment ions are produced with the charge residing on either of the two fragments, **Tables 2.1**, **2.2**, **2.3**, **2.4**, and **2.5**. TNIs due to the loss of one or two chlorine atoms are formed and TNIs are formed from cleavage of the aromatic ring. Since no buffer gas is present in the ion source to relieve excess energy, cleavage of the aromatic ring can be observed. All the polychlorinated benzenes produced chloride ion (Cl^-) with two different resonances and these dual resonances come about from two different dissociative electron capture pathways where the charge resides on the chlorine rather than the aromatic fragment in both cases. Transient negative ions resulting in the additions of oxygen to certain fragments are present. The addition of oxygen could be caused by an oxygen impurity in the system. A variety of TNIs are observed for which no particular ion could be formulated. These spurious dissociative electron capture pathways may be explained by the realization that in direct probe insertion experiments there is a high concentration of the starting compound and very few electrons. Thus, the radical anions or anions that are formed from fragmentation processes can interact with neutral species producing TNIs with unexplained masses. Overall, most TNIs observed have come about from discernable resonance or dissociative electron capture processes.

Gas chromatograph electron monochromator mass spectrometer experiments were conducted on polybrominated benzenes: bromobenzene, 1, 2-dibromobenzene, 1, 3-di-bromobenzene, 1,4-dibromobenzene, 1, 3, 5-tribromobenzene, 1, 2, 3-tribromobenzene,

1, 2, 4-tribromobenzene, and hexabromobenzene. The GC/EM/MS experiments did not produce as many different types of TNIs because the starting compound is slowly bled from the gas chromatograph column resulting in an initial lower concentration of molecules that capture electrons. No molecular ions (M^{-}s) are observed for the dibromobenzenes, **Table 2.6**. The lack of $M^{-\cdot}$ formation could be due to the energy involved in capturing an electron not being dispersed by a buffer gas, resulting in the observation of dissociative electron capture processes. The tribromobenzenes did undergo resonance electron capture to form $M^{-\cdot}$s, **Table 2.6**. 1, 2, 4-Tribromobenzene underwent two different dissociative electron capture processes to form bromide ion (Br^{-}). The other polyhalogenated benzenes may have had two different cleavage pathways to form Br^{-} as well, but the concentrations may have been below the threshold level of the detector. The lack of parent ion formation for hexabromobenzene is not surprising because the $M^{-\cdot}$ was not very intense in the ECCI mass spectra. The TNIs for the loss of one or two bromines may have been formed but the concentrations may have been below the threshold level of the detector.

Overall the results of the EM/MS experiments were very interesting even though some spurious results were observed in the DP/EM/MS experiments for the polychlorinated benzenes **Tables 2.1-2.5**, and a low number of TNIs were observed in the GC/EM/MS experiments of the polybrominated benzenes, **Table 2.6**. The trichlorobenzene, tetrachlorobenzene, dibromobenzene, tribromobenzene, and tetrabromobenzene isomers could be distinguished from each other by the differing energies of their TNIs. Graphically, one can see more clearly that the trichlorobenzene isomers could be distinguished from each other by differing energies of the TNIs responsible for the formation of Cl^{-}, **Figure 2.3**. TNIs with differing energies for the same

Table 2.6: The ε_{max} values in eV of transient negative ions observed in GC/EM/MS experiments on polybrominated benzenes.[a]

Compound	m/z	Ion	ε_{max}[b]
Bromobenzene	79	Br^-	1.2 ± 0.02
1, 2-Dibromobenzene	79	Br^-	0.63 ± 0.20
1, 3-Dibromobenzene	79	Br^-	0.96 ± 0.09
1, 4-Dibromobenzene	79	Br^-	0.84 ± 0.02
1, 3, 5-Tribromobenzene	79	Br^-	0.97 ± 0.02
	314	$M^{-\cdot}$	0.63 ± 0.13
1, 2, 3-Tribromobenzene	79	Br^-	0.74 ± 0.46
	314	$M^{-\cdot}$	1.13 ± 0.18
1, 2, 4-Tribromobenzene	79 Peak #1	Br^-	0.77 ± 0.23
	79 Peak #2	Br^-	4.7
	314	$M^{-\cdot}$	0.31 ± 0.13
1, 2, 3, 5-Tetrabromobenzene	79	Br^-	0.69 ± 0.04
1, 2, 4, 5-Tetrabromobenzene	79	Br^-	0.75 ± 0.10
Hexabromobenzene	79	Br^-	0.61 ± 0.05

[a]Polybrominated benzenes were purified by preparative gas chromatography and/or used directly from the manufacturer's bottle and found to be > 99% pure by gas chromatography and GC/ECCI/MS analysis. [b]Averages and standard deviations of two to three experiments run on the EM/MS system.

mass occur in the EM/MS experiments because each molecule possesses a unique set of virtual orbitals that can capture electrons. The three tetrachlorobenzene isomers 1, 2, 3, 4-tetrachlorobenzene, 1, 2, 4, 5-tetrachlorobenzene, and 1, 2, 3, 5-tetrachlorobenzene can be distinguished by the EM/MS because TNIs are produced with the same mass but differing energies (plus, TNIs with totally different masses), **Figure 2.4**. Pentachlorobenzene produces a variety of TNIs with different masses. These TNIs are produced from electrons being captured in the unique set of virtual molecular orbitals of pentachlorobenzene, **Figure 2.5**. The polybrominated benzenes produced the same TNIs and bromide ion with differing energies, although, some energies were relatively close, **Table 2.6**. In contrast, in standard GC/ECCI/MS experiments that were conducted on the polyhalogenated benzenes to check purity and to look for the most abundant ions in the mass spectrum, isomers could not be distinguished from each other and dual resonances were not observed for the halide ions. Therefore, the EM/MS is a very powerful analytical tool that can be implemented to distinguish electronegative compounds (especially isomers) by observing TNIs of the same mass but differing energies and/or the formation of distinct TNIs of different masses for each electronegative compound.

Resonance electron capture produces $M^{-\cdot}$, and this process occurs at lower energies than those ions produced from dissociative electron capture in the EM/MS experiments. What kinds of orbital are responsible for resonance and dissociative electron processes? The electrons captured in low energy π^* orbitals would result in resonance electron capture to form $M^{-\cdot}$ if 1) the molecule has enough degrees of freedom to survive long enough to be detected;[14,15] 2) the molecule does not undergo pre-dissociation;[15,16] and/or 3) the π^*

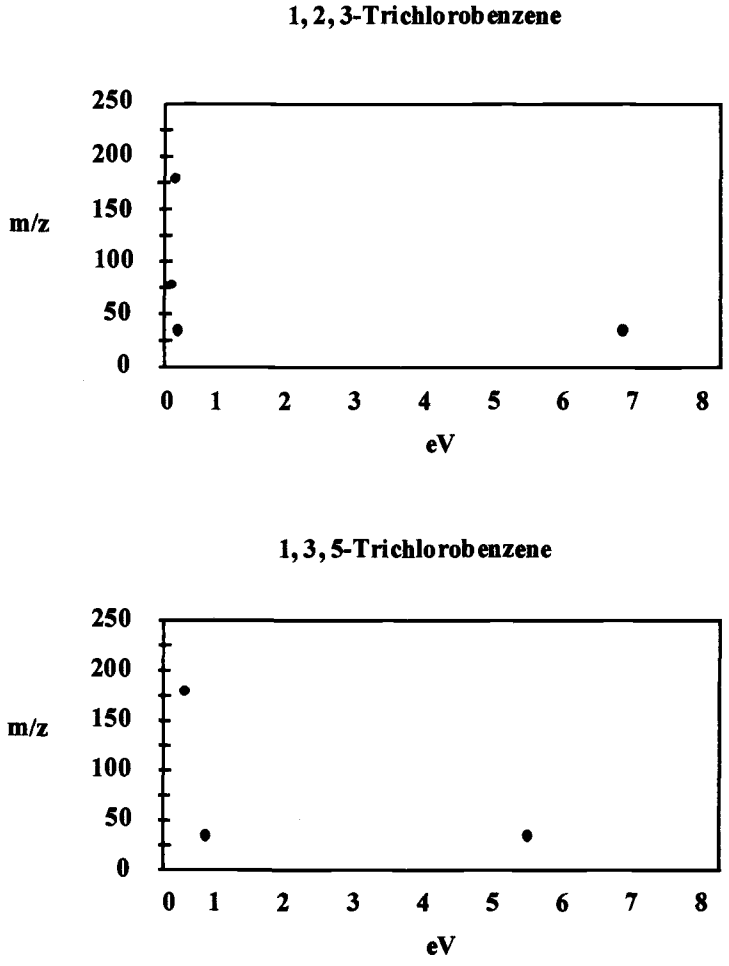

Figure 2.3: **Transient negative ions observed in DP/EM/MS experiments of 1, 3, 5-trichlorobenzene and 1, 2, 3-trichlorobenzene.**

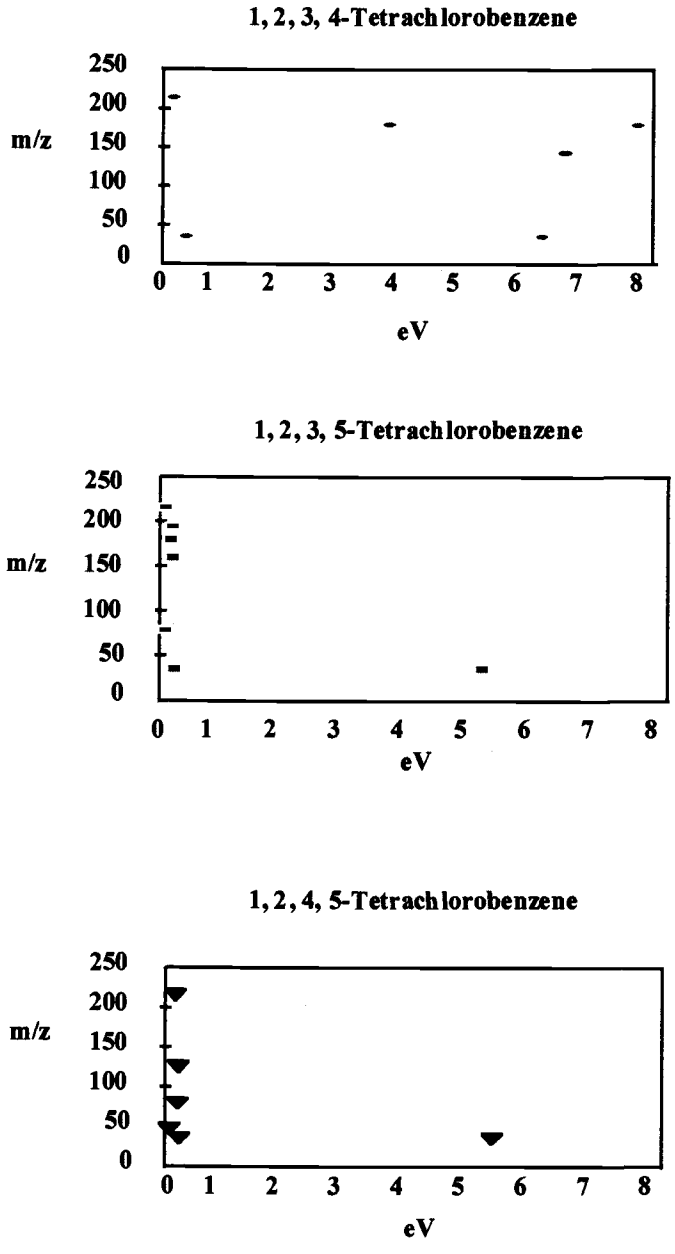

Figure 2.4: **Transient negative ions observed in DP/EM/MS experiments of 1, 2, 3, 4-tetrachlorobenzene, 1, 2, 3, 5-tetrachlorobenzene, and 1, 2, 4, 5-tetrachlorobenzene.**

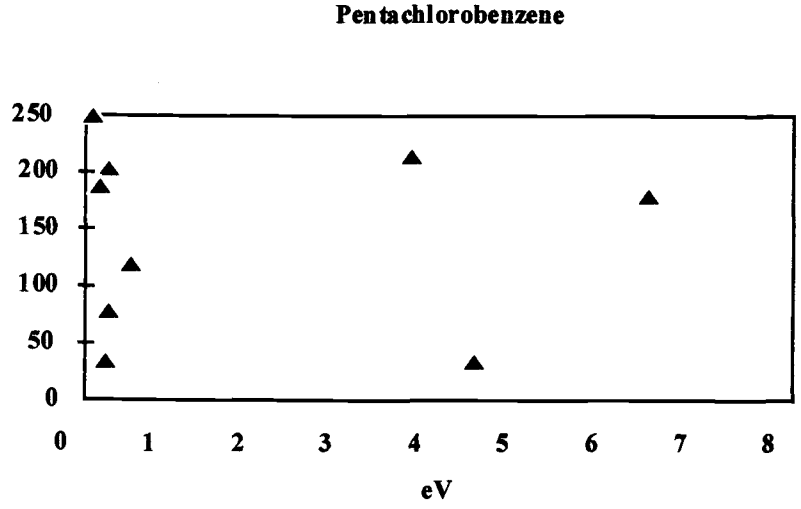

Figure 2.5: **Transient negative ions observed in DP/EM/MS experiments of pentachlorobenzene.**

orbital does not undergo significant mixing with a σ* orbital.[15,17-18] Electrons captured into higher energy σ* orbitals[19] would result in dissociative electron capture to form two fragments with the anionic charge residing on either fragment,[14] **Scheme 2.1**.

Computational studies have been undertaken to see if there is a correlation between a direct comparison of the energies of the virtual molecular orbital eigenvalues and the energies of the polychlorinated benzene TNIs observed in DP/EM/MS experiments. Calculations at the HF/6-31G*//HF/6-31G*, MP2/6-31G*//MP2/6-31G* and B3LYP/D95// B3LYP/D95 levels have been conducted on neutral polychlorinated benzenes. At first, we searched for any kind of relationship between the eigenvalues from the HF/6-31G*//HF/ 6-31G*, MP2/6-31G*//MP2/6-31G* and B3LYP/D95//B3LYP/D95 calculations and the energies of the TNIs and Cl^-. Groups of molecular orbital eigenvalues were found that correlated with the energies of the TNIs, **Tables 2.7**, **2.8**, **2.9**, **2.10**, and **2.11**. The virtual molecular orbitals that were chosen are those orbitals that have eigenvalues that are the closest in energy to the energy of the TNIs observed in the DP/EM/MS experiments. In the comparison of the energies of TNIs vs. molecular orbital eigenvalues, resonance electron capture processes are produced by electron capture in lower energy π* orbitals except for 1, 2, 3, 4-tetrachlorobenzene, 1, 2, 4, 5-tetrachlorobenzene and 1, 2, 3-trichlorobenzene which will be discussed further in subsequent paragraphs. The electrons that are captured by higher energy σ* orbitals generally produced dissociative TNIs and chloride ion.

Pentachlorobenzene underwent both a resonance electron capture process forming the $M^{-\cdot}$ and many different dissociative electron capture processes undergoing bond fission with the charge residing on either fragment. The $M^{-\cdot}$ corresponds to eigenvalues of virtual molecular orbitals 63 and 64, the π* LUMO + 1 and the LUMO + 2, at the HF/6-31G*//

HF/6-31G* and the MP2/6-31G*//MP2/6-31G* levels and the LUMO + 7 and the LUMO + 8 at the B3LYP/D95//B3LYP/D95 level, **Table 2.7**. The TNIs resulting from dissociative electron capture range from approximately 0 eV to > 6 eV corresponding to virtual orbital eigenvalues ranging from LUMO + 3 to LUMO + 116 at the HF/6-31G*//HF/6-31G* and the MP2/6-31G*//MP2/6-31G* levels. Orbitals that corresponded to high energy TNIs (> 6 eV) are not available at the HF/6-31G*//HF/6-31G* and the MP2/6-31G*//MP2/6-31G* levels. This might suggest that these TNIs may come about from electron capture by an excited state parent molecule or fragment ion that has undergone autodetachment losing a captured electron. This process has been found to occur with the triplet states of (*o*, *m* or *p*)-halomethylhalobenzenes (where halo = bromine or chlorine).[3] We do find, however, eigenvalues that correspond to all of the low and high energy TNIs and Cl^- at the B3LYP/D95//B3LYP/D95 level. The B3LYP/D95//B3LYP/D95 orbital coefficients suggest that the higher energy TNIs and the Cl^- (in particular, those that are greater than 3.58 eV which is the bond dissociation energy for a carbon-chlorine bond) are a result of electron capture into a σ^* orbital.[15]

The tetrachlorobenzene isomers underwent resonance and dissociative electron capture in the DP/EM/MS experiments. The transient negative ions for 1, 2, 3, 4-tetrachlorobenzene ranged from approximately 0 eV to > 7 eV corresponding to virtual orbital eigenvalues ranging from LUMO + 3 to LUMO + 106 at the HF/6-31G*//HF/6-31G* and MP2/6-31G*//MP2/6-31G* levels, and the LUMO + 9 to the LUMO + 70 at the B3LYP/D95//B3LYP/D95 level, **Table 2.8**. The M^- of 1, 2, 3, 4-tetrachlorobenzene corresponds directly to a σ^* type orbital. The majority of the transient negative ions of 1, 2, 4, 5-tetrachlorobenzene were < 1 eV and correspond to the LUMO up to LUMO + 5 virtual orbital eigenvalues at the HF/6-31G*//HF/6-31G* and MP2/6-31G*//MP2/6-31G*

levels, and the LUMO + 6 to the LUMO + 13 at the B3LYP/D95//B3LYP/D95 level, **Table 2.9**. Once again, a molecular orbital that corresponds to the high energy TNI (> 5 eV) is not available at the HF/6-31G*//HF/6-31G* and MP2/6-31G*//MP2/6-31G* levels. In contrast, the B3LYP/D95//B3LYP/D95 computations do provide virtual molecular orbital eigenvalues that correspond to the TNIs and chloride ions found in the EM/MS experiments. The resonance and dissociative ion resonances for 1, 2, 3, 5-tetra-chlorobenzene are approximately 0 eV to < 6 eV corresponding to virtual orbital eigenvalues ranging from the LUMO + 1 to LUMO + 116 at the HF/6-31G*//HF/6-31G* and MP2/6-31G*//MP2/6-31G* levels and the LUMO + 8 and the LUMO + 52 at the B3LYP/D95//B3LYP/D95 level. All the virtual molecular orbitals that corresponded to the energies of the TNIs are listed in the output of the 1, 2, 3, 5-tetrachlorobenzene geometry optimization calculations, **Table 2.10**.

The M^-s formed from resonance electron capture for 1, 2, 3, 4-tetrachlorobenzene and 1, 2, 4, 5-tetrachlorobenzene correspond directly to σ^* type orbitals, **Tables 2.8**, and **2.9**, and the total ion yield curves are not very intense for the M^-. In contrast, 1, 2, 3, 5-tetrachlorobenzene M^- resonance corresponds to a π^* type orbital and the total ion yield curve is much more intense. The comparison of the M^- intensities is better represented in three-dimensional plots of electron energy of TNIs vs. m/z vs. relative intensity **Figures 2.6**, **2.7** and **2.8**. Other electrons captured into σ^* type orbitals result in dissociative electron capture. In the future, we may be able to calculate the lifetime for these TNIs by conducting time-of-flight (TOF) experiments.[20-23]

Two trichlorobenzene isomers were studied in DP/EM/MS experiments: 1, 2, 3-trichlorobenzene and 1, 3, 5-trichlorobenzene, and both underwent resonance and dissociative electron capture. The electron capture processes for 1, 2, 3-trichlorobenzene ranged from approximately 0 eV to < 0.5 eV corresponding to the eigenvalues of the LUMO + 2 and the LUMO + 3 at the HF/6-31G*//HF/6-31G* and MP2/6-31G*//MP2/6-31G* levels and the LUMO + 6 and the LUMO + 8 at the B3LYP/D95//B3LYP/D95 level, **Table 2.11**. The TNIs for 1, 3, 5-trichlorobenzene ranged from approximately 0 eV to < 1 eV corresponding to virtual orbital eigenvalues of LUMO + 8 and LUMO + 21 at the HF/6-31G*//HF/6-31G* and MP2/6-31G*//MP2/6-31G* levels and the LUMO + 15 and the LUMO + 33 at the B3LYP/D95//B3LYP/D95 level, **Table 2.12**. As noted above, only the B3LYP/D95//B3LYP/D95 computations list eigenvalues that correspond to all the TNIs and chloride ions found in the DP/EM/MS experiments. The Cl^- = 6.6 eV for 1, 2, 3-trichlorobenzene corresponds to a σ^* orbital which would allow dissociation to take place immediately after electron capture. Although, the Cl^- = 5.28 eV for 1, 3, 5-trichlorobenzene corresponds to a π^* orbital, therefore, pre-dissociation would have to occur before fragmentation could take place.[13,16-18]

More specifically, the energies of the TNIs for the 1, 2, 3-trichlorobenzene molecular ion and for two of the three dissociative electron capture TNIs correspond directly to the LUMO + 2 and LUMO + 3, σ^* type orbitals, **Table 2.11**. The energy of the M^- corresponds to a σ^* orbital at all three levels of computational theory. Resonance electron capture by a σ^* orbital may have competition from other types of processes such as auto-detachment and/or dissociative electron capture.[2] If competition is occurring

Table 2.7: **The energies of transient negative ions and chloride ions (eV) observed in direct probe insertion electron monochromator mass spectrometer experiments for pentachlorobenzene, and virtual molecular orbital eigenvalues (eV) of the pentachlorobenzene optimized geometry[a] at the HF/6-31G*//HF/6-31G*, MP2/6-31G*// MP2/6-31G* and *B3LYP/D95//B3LYP/D95* levels.**

m/z	ε_{max}	MO	HF/6-31G*// HF/6-31G*		MP2/6-31G*// MP2/6-31G*		*MO*	*B3LYP/D95// B3LYP/D95*	
		62	0.08135	π*	0.07903	π*	*68*	*0.04781*	σ*
250	0.09	63	0.08162	π*	0.07937	π*	*69*	*0.08349*	π*
		64	0.11238	σ*	0.11488	σ*	*70*	*0.14925*	σ*
188	0.17	65	0.18558	σ*	0.18755	σ*	*71*	*0.17345*	σ*
		66	0.20113	σ*	0.20141	σ*	*72*	*0.20454*	σ*
		⋮	⋮	⋮	⋮	⋮	⋮	⋮	⋮
		67	0.23039	σ*	0.22865	σ*	*73*	*0.21947*	σ*
35	0.24	68	0.24341	σ*	0.24184	σ*	*74*	*0.25543*	π*
79, 204	0.27	69	0.28982	σ*	0.28592	σ*	*76*	*0.32705*	π*
		70	0.29306	π*	0.28702	π*	*77*	*0.33525*	σ*
		⋮	⋮	⋮	⋮	⋮	⋮	⋮	⋮
		77	0.50652	σ*	0.50581	σ*	*91*	*0.52196*	σ*
120	0.52	78	0.51197	σ*	0.50972	σ*	*92*	*0.52898*	π*
		79	0.56009	σ*	0.5567	σ*	*93*	*0.52956*	σ*
		⋮	⋮	⋮	⋮	⋮	⋮	⋮	⋮
		⋮	⋮	⋮	⋮	⋮	*121*	*1.36697*	σ*
215	3.7	176	3.62134	σ*	3.5849	σ*	*122*	*5.90442*	σ*
		177	4.38865	σ*	4.37729	σ*	*123*	*5.91118*	π*
35	4.41	178	4.41397	σ*	4.40994	σ*	*124*	*5.93270*	σ*
		179	4.44866	σ*	4.44254	σ*	*125*	*5.93575*	π*
		⋮	⋮	⋮	⋮	⋮	*126*	*5.94718*	σ*
		187	5.05327	σ*	5.043	σ*	⋮	⋮	⋮
		⋮	⋮	⋮	⋮	⋮	*136*	*6.08255*	σ*
180	6.38	⋮	⋮	⋮	⋮	⋮	*137*	*8.71330*	σ*
		⋮	⋮	⋮	⋮	⋮	*138*	*8.92335*	σ*

[a]The optimized geometry of pentachlorobenzene contains no imaginary frequencies.

Table 2.8: **The energies of transient negative ions and chloride ions (eV) observed in direct probe insertion electron monochromator mass spectrometer experiments for 1, 2, 3, 4-tetrachlorobenzene, and virtual molecular orbital eigenvalues (eV) of the 1, 2, 3, 4-tetrachlorobenzene optimized geometry[a] at the HF/6-31G*//HF/6-31G*, MP2/6-31G*//MP2/6-31G* and *B3LYP/D95//B3LYP/D95* levels.**

m/z	ε_{max}	MO	HF/6-31G*// HF/6-31G*		MP2/6-31G*// MP2/6-31G*		*MO*	*B3LYP/D95// B3LYP/D95*	
		55	0.09279	π*	0.09065	π*	⋮	⋮	⋮
		56	0.12847	σ*	0.13068	σ*	*62*	*0.15255*	*σ**
215	0.17	57	0.19916	σ*	0.20035	σ*	*63*	*0.20264*	*σ**
		58	0.22697	σ*	0.22614	σ*	*64*	*0.20498*	*σ**
		⋮	⋮	⋮	⋮	⋮	⋮	⋮	⋮
		63	0.39646	σ*	0.3943	σ*	*76*	*0.26118*	*σ**
35	0.4	64	0.40597	σ*	0.40212	σ*	*77*	*0.40293*	*σ**
		65	0.42179	σ*	0.42179	σ*	*78*	*0.41480*	*π**
		⋮	⋮	⋮	⋮	⋮	⋮	⋮	⋮
		159	3.37879	σ*	3.36228	σ*	*110*	*1.41828*	*σ**
180	3.7	160	3.66498	σ*	3.62684	σ*	*111*	*5.91386*	*σ**
		161	4.39999	σ*	4.38961	σ*	*112*	*5.91386*	*π**
		⋮	⋮	⋮	⋮	⋮	⋮	⋮	⋮
		170	5.06051	σ*	5.04965	σ*	⋮	⋮	⋮
		⋮	⋮	⋮	⋮	⋮	*121*	*6.01185*	*σ**
35	6.19	⋮	⋮	⋮	⋮	⋮	*122*	*6.07676*	*σ**
144	6.56	⋮	⋮	⋮	⋮	⋮	*123*	*8.75418*	*σ**
179	7.74	⋮	⋮	⋮	⋮	⋮	*124*	*8.94573*	*σ**

[a]The optimized geometry of 1, 2, 3, 4-tetrachlorobenzene contains no imaginary frequencies.

Table 2.9: **The energies of transient negative ions and chloride ions (eV) observed in direct probe insertion electron monochromator mass spectrometer experiments for 1, 2, 4, 5-tetrachlorobenzene, and virtual molecular orbital eigenvalues (eV) of the 1, 2, 4, 5-tetrachlorobenzene optimized geometry[a] at the HF/6-31G*//HF/6-31G*, MP2/6-31G*//MP2/6-31G* and *B3LYP/D95//B3LYP/D95* levels.**

m/z	ε_{max}	MO	HF/6-31G*//HF/6-31G*		MP2/6-31G*//MP2/6-31G*		*MO*	*B3LYP/D95//B3LYP/D95*	
			⋮	⋮	⋮	⋮	⋮	0.05195	σ*
44	0.08	54	0.09108	π*	0.08816	π*	60	0.09083	π*
		55	0.09111	π*	0.08944	π*	61	0.14593	σ*
		56	0.13325	σ*	0.13428	σ*	⋮	⋮	⋮
		⋮	⋮	⋮	⋮	⋮	⋮	0.17228	σ*
215	0.18	57	0.19069	σ*	0.19257	σ*	64	0.19028	σ*
79, 125	0.21, 0.22	58	0.21239	σ*	0.21171	σ*	65	0.22222	σ*
35	0.23	59	0.24543	σ*	0.24384	σ*	66	0.26193	π*
		60	0.27993	σ*	0.27587	σ*	67	0.28356	σ*
		⋮	⋮	⋮	⋮	⋮	⋮	⋮	⋮
		170	5.05723	σ*	5.04601	σ*	⋮	⋮	⋮
		⋮	⋮	⋮	⋮	⋮	110	1.39592	σ*
35	5.27	⋮	⋮	⋮	⋮	⋮	111	5.92777	σ*
		⋮	⋮	⋮	⋮	⋮	112	5.92855	π*

[a]The optimized geometry of 1, 2, 4, 5-tetrachlorobenzene contains no imaginary frequencies.

Table 2.10: **The energies of transient negative ions and chloride ions (eV) observed in direct probe insertion electron monochromator mass spectrometer experiments for 1, 2, 3, 5-tetrachlorobenzene, and virtual molecular orbital eigenvalues (eV) of the 1, 2, 3, 5-tetrachlorobenzene optimized geometry[a] at the HF/6-31G*//HF/6-31G*, MP2/6-31G*//MP2/6-31G* and *B3LYP/D95//B3LYP/D95* levels.**

m/z	ε_{max}	MO	HF/6-31G*// HF/6-31G*		MP2/6-31G*// MP2/6-31G*		*MO*	*B3LYP/D95// B3LYP/D95*	
		54	0.09101	π*	0.08857	π*	*59*	*0.04182*	σ*
79, 214	0.1	55	0.09125	π*	0.08895	π*	*60*	*0.0903*	π*
		56	0.12864	σ*	0.1302	σ*	*61*	*0.14195*	σ*
		⋮	⋮	⋮	⋮	⋮	*62*	*0.15774*	σ*
		⋮	⋮	⋮	⋮	⋮	*63*	*0.16690*	σ*
180, 160	0.18, 0.2	57	0.19846	σ*	0.19929	σ*	*64*	*0.19192*	σ*
195	0.22	58	0.21336	σ*	0.2133	σ*	*65*	*0.23590*	σ*
35	0.25	59	0.23909	σ*	0.23733	σ*	*66*	*0.26235*	π*
		60	0.28771	σ*	0.28352	σ*	*67*	*0.27555*	σ*
		⋮	⋮	⋮	⋮	⋮	⋮	⋮	⋮
		154	2.99255	σ*	2.97137	σ*	*110*	*1.39403*	σ*
160	3	155	3.01671	σ*	2.99593	σ*	*111*	*5.92140*	σ*
		156	3.06785	σ*	3.05174	σ*	*112*	*5.92452*	π*
		⋮	⋮	⋮	⋮	⋮	⋮	⋮	⋮
		159	3.37041	π*	3.3536	π*	⋮	⋮	⋮
180, 215	3.8, 3.6	160	3.66057	σ*	3.62249	σ*	*113*	*5.95249*	π*
		161	4.40601	σ*	4.3963	σ*	*114*	*5.95522*	π*
		⋮	⋮	⋮	⋮	⋮	⋮	⋮	⋮
		169	4.80657	σ*	4.8048	σ*	⋮	⋮	⋮
35	5.07	170	5.05797	σ*	5.04685	σ*	*115*	*5.95819*	σ*
		⋮	⋮	⋮	⋮	⋮	*116*	*5.97569*	σ*

[a]The optimized geometry of 1, 2, 3, 5-tetrachlorobenzene contains no imaginary frequencies.

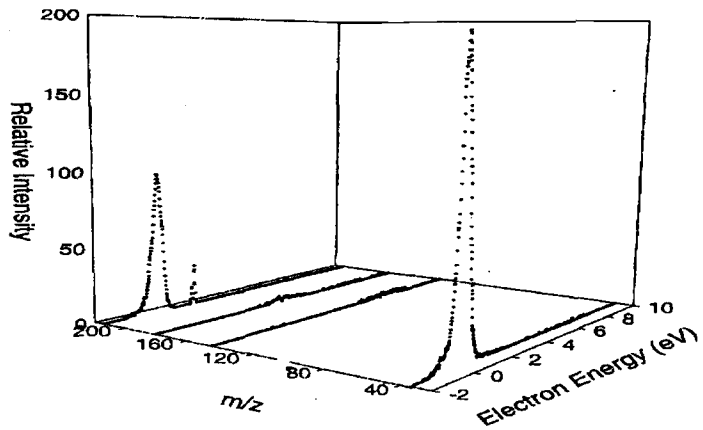

Figure 2.6: **Three-dimensional spectra of ion intensity vs. mass to charge (m/z) ratio vs. electron energy (eV) observed in DP/EM/MS experiments of 1, 2, 3, 4-tetrachlorobenzene (Note: the relative intensity ranges from 0 to 200).**

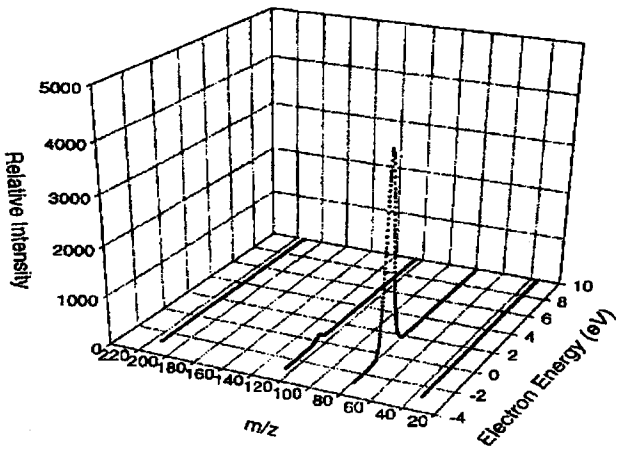

Figure 2.7: **Three-dimensional spectra of ion intensity vs. mass to charge ratio (m/z) vs. electron energy (eV) observed in DP/EM/MS experiments of 1, 2, 4, 5-tetrachlorobenzene (Note: the relative intensity ranges from 0 to 5000).**

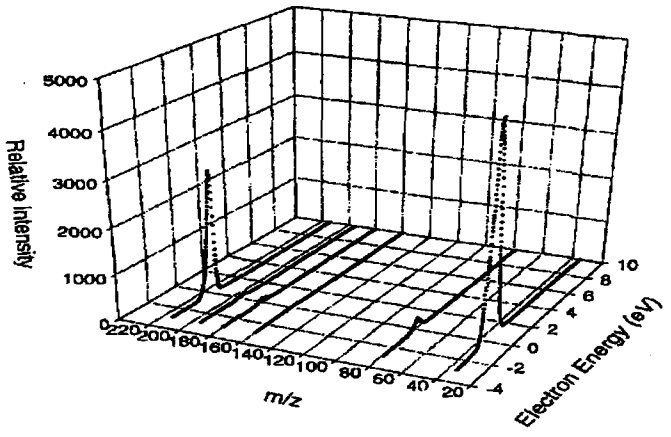

Figure 2.8: **Three-dimensional spectra of ion intensity vs. mass to charge ratio (m/z) vs. electron energy (eV) observed in DP/EM/MS experiments of 1, 2, 3, 5-tetrachlorobenzene (Note: the relative intensity ranges from 0 to 5000).**

between different electron capture pathways, a TNI of low intensity would most likely be the result, and the TNI for the $M^{-\cdot}$ is not very intense **Figure 2.9**. The LUMO + 2 eigenvalue at the HF/6-31G*//HF/6-31G* and MP2/6-31G*//MP2/6-31G* levels and the LUMO + 8 at the B3LYP/D95//B3LYP/D95 level are slightly below the energy of the Cl^-, therefore, the LUMO + 3 at the HF/6-31G*//HF/6-31G* and MP2/6-31G*//MP2/6-31G* levels and the LUMO + 9 at the B3LYP/D95//B3LYP/D95 level were chosen as the corresponding virtual orbitals for the Cl^- = 0.19 eV.

The three-dimensional representation of the TNIs observed in the DP/EM/MS experiments of 1, 3, 5-trichlorobenzene shows that the Cl^- is much more intense than the $M^{-\cdot}$, **Figure 2.10**. The energy of the 1, 3, 5-trichlorobenzene $M^{-\cdot}$ corresponds to virtual orbital eigenvalues: LUMO + 7 through LUMO + 9 at the HF/6-31G*//HF/6-31G* and MP2/6-31G*//MP2/6-31G* level, **Table 2.12**. The TNIs correspond to virtual molecular orbitals that are both σ^* and π^* orbitals. The $M^{-\cdot}$ formation is an resonance process where no bond cleavage occurs if 1) the molecule has a large number of degrees of freedom;[14,15] 2) pre-dissociation does not take place;[15,16] 3) and π^* and σ^* orbital mixing does not occur.[15,17-18] Electron capture by higher energy σ^* orbitals[19] would induce dissociative electron capture,[14] **Scheme 2.1**. Therefore, the eigenvalues of the 1, 3, 5-trichlorobenzene optimized geometry do not give a definitive answer into which type of orbital captures the electron to form the $M^{-\cdot}$. One way to distinguish if the electron is captured into a σ^* orbital verses a π^* orbital is to conduct TOF experiments to elucidate the lifetime of the TNIs of the molecular ions.[20-23]

Table 2.11: **The energies of transient negative ions and chloride ions (eV) observed in direct probe insertion electron monochromator mass spectrometer experiments for 1, 2, 3-trichlorobenzene, and virtual molecular orbital eigenvalues (eV) of the 1, 2, 3-trichlorobenzene optimized geometry[a] at the HF/6-31G*//HF/6-31G*, MP2/6-31G*// MP2/6-31G* and *B3LYP/D95//B3LYP/D95* levels.**

m/z	ε_{max}	MO	HF/6-31G*// HF/6-31G*		MP2/6-31G*// MP2/6-31G*		*MO*	*B3LYP/D95// B3LYP/D95*	
		46	0.10947	π*	0.10243	π*	⋮	⋮	⋮
		47	0.10506	π*	0.10268	π*	*53*	*0.13977*	σ*
78, 180	0.14, 0.15	48	0.1455	σ*	0.14718	σ*	*54*	*0.15230*	σ*
35	0.19	49	0.22318	σ*	0.22309	σ*	*55*	*0.20657*	σ*
		50	0.24095	σ*	0.23963	σ*	*56*	*0.21012*	σ*
		⋮	⋮	⋮	⋮	⋮	⋮	⋮	⋮
		153	5.06909	σ*	5.05759	σ*	⋮	⋮	⋮
		⋮	⋮	⋮	⋮	⋮	*108*	*6.06812*	σ*
35	6.6	⋮	⋮	⋮	⋮	⋮	*109*	*8.80015*	σ*
		⋮	⋮	⋮	⋮	⋮	*110*	*8.98210*	σ*

[a]The optimized geometry of 1, 2, 3-trichlorobenzene contains no imaginary frequencies

Table 2.12: **The energies of transient negative ions (eV) observed in direct probe insertion electron monochromator mass spectrometer experiments for 1, 3, 5-trichlorobenzene, and virtual molecular orbital eigenvalues (eV) of the 1, 3, 5-trichlorobenzene optimized geometry[a] at the HF/6-31G*//HF/6-31G*, MP2/6-31G*//MP2/6-31G* and *B3LYP/D95// B3LYP/D95* levels.**

m/z	ε_{max}	MO	HF/6-31G*// HF/6-31G*		MP2/6-31G*// MP2/6-31G*		*MO*	*B3LYP/D95// B3LYP/D95*	
		53	0.30292	σ*	0.29894	σ*	*60*	*0.28580*	*σ**
180	0.3	54	0.31044	π*	0.30867	π*	*61*	*0.33492*	*π**
		55	0.38654	σ*	0.38373	σ*	*62*	*0.33492*	*π**
		⋮	⋮	⋮	⋮	⋮	*⋮*	*⋮*	*⋮*
		66	0.61427	σ*	0.61426	π*	*78*	*0.60708*	*σ**
35	0.62	67	0.62508	π*	0.62518	π*	*79*	*0.66522*	*π**
		68	0.62508	π*	0.62518	π*	*80*	*0.67444*	*σ**
		⋮	⋮	⋮	⋮	⋮	*⋮*	*⋮*	*⋮*
		153	5.0637	σ*	5.05181	σ*	*⋮*	*⋮*	*⋮*
		⋮	⋮	⋮	⋮	⋮	*99*	*1.41473*	*σ**
35	5.28	⋮	⋮	⋮	⋮	⋮	*100*	*5.94521*	*π**
		⋮	⋮	⋮	⋮	⋮	*101*	*5.96226*	*π**

[a]The optimized geometry of 1, 3, 5-trichlorobenzene contains no imaginary frequencies.

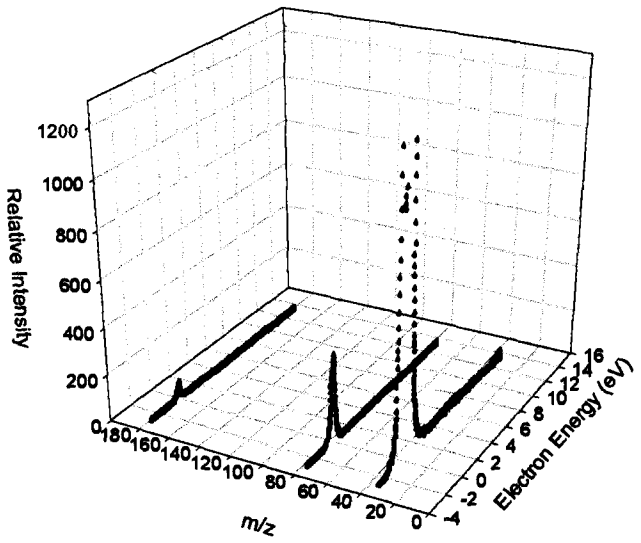

Figure 2.9: **Three-dimensional spectra of ion intensity vs. mass to charge (m/z) ratio vs. electron energy (eV) observed in DP/EM/MS experiments of 1, 2, 3-trichlorobenzene (Note: Relative intensity ranges from 0 to 1200).**

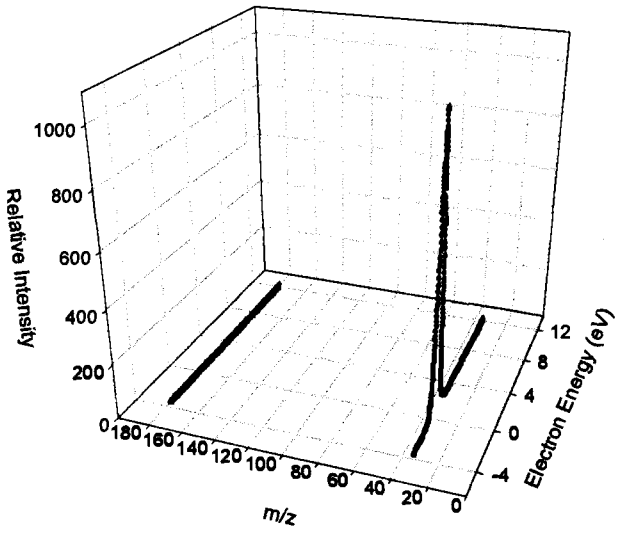

Figure 2.10: **Three-dimensional spectra of ion intensity vs. mass to charge (m/z) ratio vs. electron energy (eV) observed in DP/EM/MS experiments of 1, 3, 5-trichlorobenzene (Note: The relative intensity ranges from 0 to > 1000).**

Some researchers have calculated the energies of π^* negative ion resonance states with Koopmans' theorem. The Koopmans' theorem states that we can identify the ionization energy (in our case, electron attachment energy) with the energy of the orbital from which the electron is ejected (in the present study, the orbital that captures the electron) which is an approximation because it does not take into account the fact that the remaining electrons rearrange when ionization (electron attachment) occurs.[24] Staley and Strnad successfully used the linear regression equation from the correlation of the electron attachment energies (AE, i.e. energies of the transient negative ions) obtained from electron transmission spectroscopy (ETS) experiments with π^* virtual orbital eigenvalues calculated with a variety of *ab initio* methods and basis sets.[13] Deinzer and co-workers applied this method to polychlorinated dioxins studied on the EM/MS system. A strong correlation (R=0.9957) was found when the AEs of polychlorinated dioxins along with AEs of aromatic compounds taken from the literature were plotted against the π^* orbital eigenvalues calculated at the B3LYP/D95//B3LYP/D95 level.[25] A similar approach has been used for the polychlorinated benzenes studied in the DP/EM/MS experiments. Experimental attachment energies for the low energy TNIs and chloride ions of the polychlorinated benzenes have been correlated with π^* orbital eigenvalues from the HF/ 6-31G*//HF/6-31G*, MP2/6-31G*//MP2/6-31G* and B3LYP/D95//B3LYP/D95 calculations. Only the lower energy identifiable TNIs and chloride ions were used for several reasons. First, some of the unidentifiable TNIs may have been due to impurities and/or reactions occurring due to having too high a concentration of starting analyte vs. electrons in the DP/EM/MS experiments. Second, the Koopman's theorem should only be

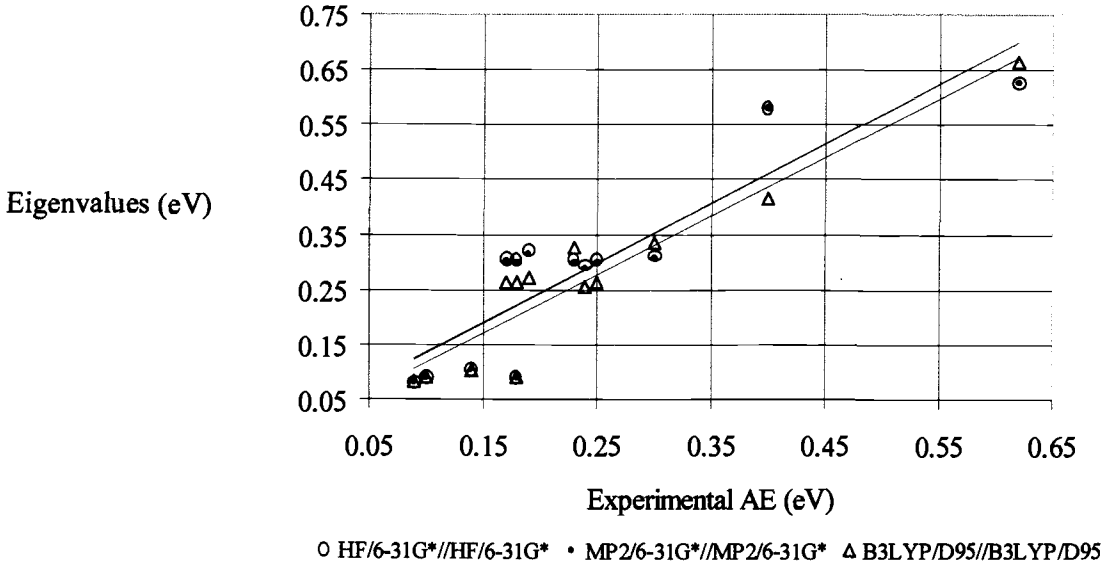

Figure 2.11: **Virtual molecular orbital eigenvalues (eV) calculated at the HF/ 6-31G*//HF/6-31G*, MP2/6-31G*//MP2/6-31G* and B3LYP/D95// B3LYP/D95 levels vs. the attachment energies (AE, eV) of the lower energy transient negative ions and chloride ions from DP/EM/MS experiments of polychlorinated benzenes.**

Table 2.13: **Experimental attachment energies (i. e. ε_{max}, eV) observed in DP/EM/MS experiments of polychlorinated benzenes and molecular orbital eigenvalues (eV) calculated at the HF/6-31G*//HF/6-31G*, MP2/6-31G*//MP2/6-31G* and B3LYP/D95//B3LYP/D95 levels.**

			Eigenvalues		
compound	**m/z**	ε_{max}	**HF/6-31G*// HF/6-31G***	**MP2/6-31G*// MP2/6-31G***	**B3LYP/D95// B3LYP/D95**
pentachlorobenzene	250	0.09	0.08162	0.07937	0.08349
	35	0.24	0.29306	0.28702	0.25542
1, 2, 3, 5-Tetrachlorobenzene	214	0.1	0.09125	0.08895	0.0903
	180	0.18	0.30363	0.29777	0.26235
	35	0.25	0.30363	0.29777	0.26235
1, 2, 3, 4-Tetrachlorobenzene	215	0.17	0.3066	0.30077	0.26329
	35	0.4	0.58165	0.58178	0.4148
1, 2, 4, 5-Tetrachlorobenzene	215	0.18	0.09108	0.08816	0.09083
	35	0.23	0.30379	0.29814	0.3256
1, 2, 3-Trichlorobenzene	180	0.14	0.10506	0.10243	0.10283
	35	0.19	0.32086	0.31505	0.27215
1, 3, 5-Trichlorobenzene	180	0.3	0.31044	0.30867	0.33492
	35	0.62	0.62508	0.62518	0.66522

Table 2.14: **Experimental attachment energies (i. e. ε_{max}, eV) observed in DP/EM/MS experiments of polychlorinated benzenes and calculated attachment energies at the HF/6-31G*//HF/6-31G*, MP2/6-31G*// MP2/6-31G* and B3LYP/D95//B3LYP/D95 levels.**

			Calculated Attachment Energies		
compound	**m/z**	ε_{max}	**HF/6-31G*// HF/6-31G***	**MP2/6-31G*// MP2/6-31G***	**B3LYP/D95// B3LYP/D95**
pentachlorobenzene	250	0.09	0.06	0.06	0.08
	35	0.24	0.20	0.20	0.22
1, 2, 3, 5-Tetrachlorobenzene	214	0.1	0.07	0.07	0.09
	180	0.18	0.14	0.14	0.16
	35	0.25	0.21	0.21	0.23
1, 2, 3, 4-Tetrachlorobenzene	215	0.17	0.13	0.13	0.15
	35	0.4	0.35	0.35	0.37
1, 2, 4, 5-Tetrachlorobenzene	215	0.18	0.14	0.14	0.16
	35	0.23	0.19	0.19	0.21
1, 2, 3-Trichlorobenzene	180	0.14	0.11	0.11	0.12
	35	0.19	0.15	0.15	0.17
1, 3, 5-Trichlorobenzene	180	0.3	0.26	0.25	0.27
	35	0.62	0.56	0.55	0.57

[b]Attachment energies calculated from the linear regression line AE = (eigenvalue + 0.0279)/1.0579 at the HF/6-31G*//HF/6-31G* level; AE = (eigenvalue + 0.0223)/1.0942 at the MP2/6-1G*//MP2/ 6-31G* level; and AE = (eigenvalue + 0.0084)/1.0724 at the B3LYP/D95//B3LYP/D95 level of Figure 2.17.

applied to those TNIs and chloride ions that are produced from ground state compounds capturing electrons into π^* orbitals.[13] Third, considerable mixing of higher energy virtual orbitals occurs making it difficult to tell which orbital is capturing the electron.[3,13,17-18] Therefore, only lower energy π^* virtual orbitals were chosen and only those π^* orbitals that have the highest p-orbital coefficients on both carbons and chlorines rather than carbons only, because carbon-chlorine bonds are broken in the majority of the dissociative electron capture processes discussed above. Since the electrons are captured in π^* orbitals, pre-dissociation or significant mixing of π^* and σ^* orbitals must occur so that the carbon-chlorine bond can cleave. When the AEs for the polychlorinated benzenes are plotted against the virtual orbital eigenvalues from the HF/6-31G*//HF/6-31G*, MP2/6-31G*// MP2/6-31G* and B3LYP/D95//B3LYP/D95 calculations, correlations are found with R-values = 0.892, 0.896 and 0.942, respectively, **Figure 2.11** and **Table 2.13**. AEs were calculated using the equations of the linear regression lines of HF/6-31G*//HF/6-31G*, MP2/6-31G*//MP2/6-31G* and B3LYP/D95//B3LYP/D95 levels, where the AEs = (orbital eigenvalue-constant)/x-coefficient, **equations 3.1**, **3.2** and **3.3**, respectively. The calculated AEs are relatively close to the experimental values at all three computational levels. In particular, it seems as though the B3LYP/D95//B3LYP/D95 models the orbitals

$$AE = \frac{eigenvalue + 0.0279}{1.0579} \qquad \textbf{Equation 2.1}$$

$$AE = \frac{eigenvalue + 0.0223}{1.0942} \qquad \textbf{Equation 2.2}$$

$$AE = \frac{eigenvalue + 0.0084}{1.0724} \qquad \textbf{Equation 2.3}$$

that capture the electrons more effectively than both the HF/6-31G*//HF/6-31G* and MP2/6-31G*//MP2/6-31G* levels, **Table 2.14**. These results are similar to those of Staley and Strnad. They found that computations at the HF/D95v//HF/6-31G and the HF/D95v/MP2/6-31G* levels produced calculated AEs that were much closer to experimental AEs than HF/6-31G//HF/6-31G level calculations.[13] Overall, a good correlation is found using the Koopmans' theorem for the lower energy TNIs and chloride ions of the polychlorinated benzenes studied on the EM/MS and the calculated AEs are relatively close to the DP/EM/MS experimental values.

Conclusion

The electron monochromator mass spectrometer is a powerful analytical tool that can be used to distinguish isomers of highly electronegative environmentally persistent compounds. This instrument has been used successfully to analyze and distinguish isomers of polyhalogenated benzenes. Therefore, in unknown samples, the presence of these compounds could be validated. In addition, one can tell how many isomers are present in a sample. The *ab initio* molecular orbital calculations provide insight into groups of molecular orbitals that may be capturing the electrons by directly comparing the energies of the TNIs and chloride ions and the eigenvalues of the optimized geometries of the neutral molecules calculated at the HF/6-31G*//HF/6-31G*, MP2/6-31G*//MP2/6-31G* and B3LYP/D95//B3LYP/D95 levels. That is, an electron that is captured into a σ^* orbital may lead to dissociative electron capture (i.e. TNIs that are very short-lived) and those electrons captured into π^* orbitals may result in both resonance electron capture and dissociative electron capture. The implementation of Koopman's theorem leads to a

correlation between the low energy π^* orbitals calculated at the HF/6-31G*//HF/6-31G*, MP2/6-31G*//MP2/6-31G* and B3LYP/D95//B3LYP/D95 levels plotted against the lower energy TNIs and chloride ions of the polychlorinated benzenes. The correlation results in calculated attachment energies that are very close to experimental values. In the future, more studies need to be performed to understand the electron capture mechanisms of the polychlorinated benzenes in the DP/EM/MS experiments. Time-of-flight experiments could be conducted to find the lifetimes of the TNIs.[20-23] These experimental lifetimes would provide insight into which orbitals are responsible for dissociative and resonance electron capture processes.

Acknowledgements

I would like to thank Max L. Deinzer for his lengthy and informative discussions, and allowing me to work with his group and their electron monochromator mass spectrometer system. I would also like to thank James Laramée and Paul Mazurkiewicz for their discussions and running my samples on the electron monochromator mass spectrometer system.

Support for this research by the Environmental Health Sciences, Oregon State University Chemistry Department and the N. L. Tarter fellowship is gratefully acknowledged.

References

1. Laramée, J. A..; Kocher, C. A.; Deinzer, M. L. *Analytical Chemistry* **1992,** *64,* 2316-2322.

2. Oster, T.; Kühn, A.; Illenberger, E. *Int. J. Mass Specctrom. Ion Proc.*, **1989**, *89*, 1-72.

3. Bulliard, C.; Allan, M.; Haselbach. E. *J. Phys. Chem.* **1994**, *98*, 11040-11045.

4. Hehre, W.J.; Radom, L.; Schleyer, P.v.R.; Pople, J.A. *Ab Initio Molecular Orbital Theory*; Wiley: New York, 1986.

5. *Spartan*, versions 4.1-5.0; Wavefunction, Inc.: Irvine, CA, 1993-1997.

6. *Gaussian 92*, Revision G.4, M. J. Frisch, G. W. Trucks, M. Head-Gordon, P. M. W. Gill, M. W. Wong, J. B. Foresman, B. G. Johnson, H. B. Schlegel, M. A. Robb, E. S. Replogle, R. Gomperts, J. L. Andres, K. Raghavachari, J. S. Binkley, C. Gonzalez, R. L. Martin, D. J. Fox, D. J. Defrees, J. Baker, J. J. P. Stewart, and J. A. Pople, Gaussian, Inc., Pittsburgh PA, 1992. *Gaussian 94*, Revisions C.2 and E.1, M. J. Frisch, G. W. Trucks, H. B. Schlegel, P. M. W. Gill, B. G. Johnson, M. A. Robb, J. R. Cheeseman, T. Keith, G. A. Petersson, J. A. Montgomery, K. Raghavachari, M. A. Al-Laham, V. G. Zakrzewski, J. V. Ortiz, J. B. Foresman, J. Cioslowski, B. B. Stefanov, A. Nanayakkara, M. Challacombe, C. Y. Peng, P. Y. Ayala, W. Chen, M. W. Wong, J. L. Andres, E. S. Replogle, R. Gomperts, R. L. Martin, D. J. Fox, J. S. Binkley, D. J. Defrees, J. Baker, J. P. Stewart, M. Head-Gordon, C. Gonzalez, and J. A. Pople, Gaussian, Inc., Pittsburgh PA, 1995.

7. Ditchfield, R.; Hehre, W.H.; Pople, J.A. *J. Chem. Phys.* **1971**, *54*, 724.

8. Hehre, W.H.; Ditchfield, R.; Pople, J.A. *J. Chem. Phys.* **1972**, *56*, 2257.

9. Hariharan, P.C.; Pople, J.A. *Mol. Phys.* **1974**, *27*, 209.

10. Gordon, M.S. *Chem. Phys. Lett.* **1980**, *76*, 163.

11. Hariharan, P.C.; Pople, J.A. *Theo. Chim. Acta.* **1973**, *28*, 213.

12. Forseman, J.B.; Frisch, Æ. *Exploring Chemistry with Electronic Methods*, 2nd Ed.; Gaussian, Inc.: Pittsburgh, PA, 1995-96.

13. Staley, S.W.; Strnad, J.T. *J. Phys. Chem.* **1994**, *98*, 116-121.

14. Laramée, J.A.; Mazurkiewicz, P.; Berkout, V.D.; Deinzer, M.L. *unpublished manuscript* 1996.

15. Dressler, R; Allan, M.; Haselbach, E. *Chimia,* **1985**, *39*, 385.

16. Clarke, D.D.; Coulson, C.A. *J. Chem. Soc. A*, **1969**, 169.

17. Stricklett, K.L.; Chu, S.C.; Burrow, P.D. *Chem. Phys. Lett.* **1986**, *131*, 279.

18. Olthoff, J.K.; Tossell, J.A.; Moore, J.H. *J. Chem. Phys.* **1985**, *83*, 5627.

19. Burrow, P.D.; Modelli, A.; Jordan, K.D. *Chem. Phys. Lett.* **1986**, *132*, 441.

20. *Time-of-Flight Mass Spectrometry*; Cotter, R.J., Ed.; ACS Symposium Series 549; American Chemical Society: Washington, DC, 1994.

21. White, F.A.; Wood, G.M. *Mass Spectrometry: Applications in Science and Engineering*; Wiley and Sons: New York, 1986.

22. Jennings, K.R.; Dolnikowski, G.G. *Methods in Enzymology*. **1990**, 193, 37-61.

23. Watson, T.T. *Introduction to Mass Spectrometry*, 3rd ed.; Lippincott-Raven: New York, 1997.

24. Atkins, P.W. *Physical Chemistry*, 4th Ed.; W.H. Freeman and Company: New York, 1990.

25. Berkout, V.D.; Mazurkiewicz, P.; Deinzer, M.L. *Anal. Chem.* in press, 1998.

Chapter 3: Computational Studies on the Fragmentation Pathways of Polychlorinated Benzene Radical Anions

Sharon Maley Herbelin and Peter K. Freeman*

Department of Chemistry
Oregon State University
Corvallis, OR 97331

Introduction

Researchers have been developing an understanding of the mechanisms involved in the photodehalogenation of polyhalogenated benzenes since many are prevalent environmental pollutants.[1,2-9] Results of photodehalogenation experiments on polyhalogenated benzenes reveal that an increase in quantum yield occurs when an electron transfer reagent is present.[1,4-5] The Freeman group has proposed that the products in photolysis experiments of polychlorinated benzenes in the presence of an electron transfer agent result from direct fission of the singlet, triplet and by cleavage of the radical anion that is produced from the transfer of an electron from the electron donor to the excited polyhaloarene, **Scheme 3.1**.[1,4] What is the fate of the radical anion? Does the radical anion cleave to form an aryl radical and chloride ion or form an aryl carbanion and chlorine atom? If we had the knowledge of the mode of bond fission combined with the regiochemistries of the products, we could thoroughly characterize the photodehalogenation process for any particular polyhaloarene undergoing reaction by the radical anion. Therefore, the Freeman and Deinzer research groups turned to gas chromatography electron capture chemical ionization mass spectrometry (GC/ECCI/MS) experiments to develop an understanding of the mode of fission.[1,10]

In 1986 the Freeman and Deinzer research groups studied the fragmentation pathways of polychlorinated benzenes using GC/ECCI/MS.[1] In a possibly oversimplified picture of the processes involved in the GC/ECCI/MS experiments the neutral molecule captures an electron that can go into a variety of different virtual molecular orbitals producing radical anions with differing energies and lifetimes. The radical anion could

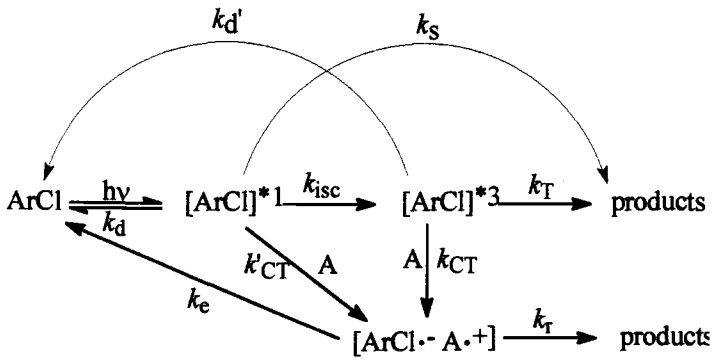

Scheme 3.1: **Kinetic scheme for product formation in the photolysis of a polychlorinated benzene in the presence of an electron donor (A).**

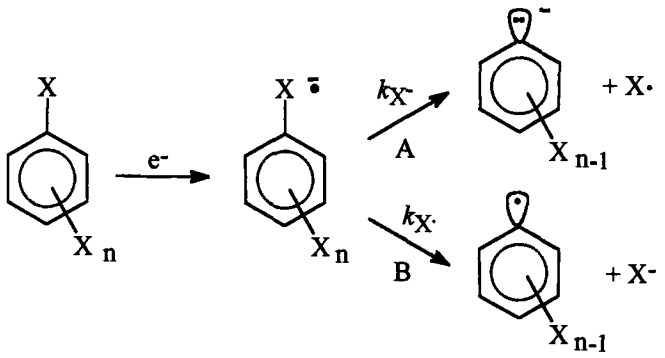

Scheme 3.2: Polyhalogenated benzenes radical anion cleavage pathways.

undergo cleavage to form the aryl radical and halide ion or the aryl carbanion and halogen atom, *pathways A* and *B*, respectively, **Scheme 3.2.** A Hammett relationship was found between the sum of the Hammett substitution constants ($\Sigma\sigma$) of the polyhalogenated benzenes and, from the results of the GC/ECCI/MS experiments, the log of the rate of chlorine atom formation over the rate of chloride ion formation [log ($k_{Cl\cdot}/k_{Cl^-}$)]. A Hammett plot of the log ($k_{Cl\cdot}/k_{Cl^-}$) vs. $\Sigma\sigma$ for the polychlorinated benzenes reveals that the radical anions of the trichlorobenzenes, tetrachlorobenzenes and pentachlorobenzene favored fission to form the aryl radical and the halide ion (dichlorobenzenes were not included), **Figure 3.1.** The favored cleavage pathway for the hexachlorobenzene radical anion is fission to form aryl carbanion and halogen atom. It was proposed that hexachlorobenzene favored bond fission to form the aryl carbanion and the chlorine atom because the chlorines on the phenyl ring can withdraw electron density stabilizing the anionic charge.[1]

Computations were run to investigate the polyhalogenated benzene radical anion cleavage pathways further and to find which methods and basis sets sufficiently modeled the results from the GC/ECCI/MS experiments, and the photochemical and non-photochemical experiments of the polyhalogenated benzenes in the presence of electron transfer reagents.

Computational Methods

Ab initio calculations[11] were carried out using the Spartan 4.0-5.0 molecular modeling and Gaussian 92/94 programs.[12,13] The AM1[14] and split valence 3-21G[15-16], 6-31G,[6-21] and the Dunning-Huzinaga *double zeta* (D95)[14,22] basis sets were employed. The restricted and restricted open shell Hartree-Fock (RHF and ROHF, respectively) methods

were used with the AM1 (RHF only), 3-21G and 6-31G* basis sets. The electron correlated Becke's three-parameter hybrid functional[23] combined with the Lee, Yang, and Parr (LYP) correlation functional, denoted B3LYP,[24] was used in the calculations using the 3-21G, 6-31G* and D95[14,22] basis sets. The optimized geometries from lower levels of theory were used as starting coordinates for higher-level geometry optimizations. The "/" separates the method from the basis set; and "//" separates the computational level of the energy from the level of the geometry optimization in the following example: B3LYP/D95//B3LYP/D95. Frequency calculations were executed to ensure that no imaginary frequencies were present in any of the optimized geometries, and, no imaginary frequencies were found for the optimized structures discussed, *vide infra.*[14] The zero-point vibrational energies calculated at the B3LYP/6-31G*//B3LYP/6-31G* and the HF/6-31G*//HF/6-31G* levels were scaled to 0.9613[14] and 0.9135,[14] respectively, and those calculated at the HF/AM1 and B3LYP/ 3-21G levels were not scaled.

Throughout this chapter, the changes in internal energy (ΔE_o) are calculated by subtracting the electronic energy plus the scaled zero point energy of the starting materials from the electronic energy plus the scaled zero point energy of the products.[14]

Results and Discussion

Geometry optimization, frequency and single point energy calculations were conducted on the polychlorinated benzenes studied in the GC/ECCI/MS experiments. Frequency calculations were conducted to ensure that all optimized structures contained no imaginary frequencies, and, no imaginary frequencies were present in any of the optimized

geometries discussed below. The electronic energies of the optimized geometries plus scaled zero point energies were used to calculate the changes in internal energy (ΔE_o).[13,14]

Geometry optimization and frequency calculations were conducted at the electron un-correlated HF/6-31G*//HF/6-31G* level to investigate if the most favorable cleavage pathways for pentachlorobenzene were well represented by the oversimplified picture discussed above, **Scheme 3.2**, or if the pentachlorobenzene radical anion underwent other modes of bond fission. The pentachlorobenzene radical anion could undergo cleavage to form chlorine atom and 2, 3, 5, 6-tetrachlorophenyl anion, *pathway A*, **Scheme 3.3**. The pentachlorobenzene radical anion may also undergo fission to form chloride ion and 2, 3, 5, 6-tetrachlorophenyl radical, *pathway B*, **Scheme 3.3**. The ΔE_o values for *pathways A* and *B* are calculated to be < 30 kcal/mol. The pentachlorobenzene radical anion may undergo other types of cleavages, **Scheme 3.3**. It may lose a chlorine molecule to form a 3, 4, 5-trichlorobenzyne radical anion, *pathway C*, **Scheme 3.3**. The ΔE_o value for the loss of chlorine molecule is 106.4 kcal/mol, a very high energy process which is unlikely to compete in the GC/ECCI/MS experiments, **Scheme 3.3**. The pentachlorobenzene radical anion is not the only species that could undergo bond fission. The 2, 3, 5, 6-tetrachlorophenyl anion could lose chloride ion to form 3, 4, 5-trichlorobenzyne that could capture an electron to form 3, 4, 5-trichlorobenzyne radical anion, *pathways D* and *G*, **Scheme 3.3**. The ΔE_o values for *pathways D* and *G* are 50.0 kcal/mol and 9.6 kcal/mol, respectively. The 2, 3, 5, 6-tetrachlorophenyl radical may cleave to form chlorine atom and 3, 4, 5-trichlorobenzyne that could also capture an electron to form the 3, 4, 5-trichlorobenzyne radical anion, *pathways E* and *G*, **Scheme 3.3**. The ΔE_o values for

pathways E and *G* are 71.7 kcal/mol and 9.6 kcal/mol, respectively. If a 2, 3, 5, 6-tetrachlorophenyl radical captures an electron to form the 2, 3, 5, 6-tetrachlorophenyl anion, the ΔE_o is 21.7 kcal/mol, *pathway F*, **Scheme 3.3**. Overall, the lowest energy cleavage pathway for pentachlorobenzene radical anion is chloride ion fission and the next lowest energy pathway is the loss of chlorine atom confirming that **Scheme 3.2** is not oversimplified, it contains the lowest energy cleavage pathways for the pentachlorobenzene radical anion. These HF/6-31G*//HF/6-31G* level calculations provide additional support for the results from the GC/ECCI/MS experiments where the favored mode of fission is to form chloride ion.[1]

Since the lowest energy pathways for bond fission for the pentachlorobenzene radical anion are cleavage to chloride ion and chlorine atom (*pathways A* and *B*, **Scheme 3.3**), geometry optimization and frequency calculations were conducted on *pathways A* and *B* for the remaining polychlorinated benzenes that were studied in the GC/ECCI/MS experiments.[1] In many cases, the geometry optimization and frequency calculations were run utilizing other methods and basis sets besides the HF/6-31G* so that the methods and basis sets could be found that most accurately model the GC/ECCI/MS experiments and the photochemical and the non-photochemical experiments of many of the polyhalogenated benzenes in the presence of electron transfer reagents.

Geometry optimization and frequency calculations were carried out for the trichlorobenzene isomers: 1, 3, 5-trichlorobenzene, 1, 2, 3-trichlorobenzene, 1, 2, 4-trichlorobenzene. The ΔE_o values for electron capture of 1, 3, 5-trichlorobenzene, 1, 2, 3-trichlorobenzene and 1, 2, 4-trichlorobenzene are slightly endothermic (2.7, 8.6, and 1.7

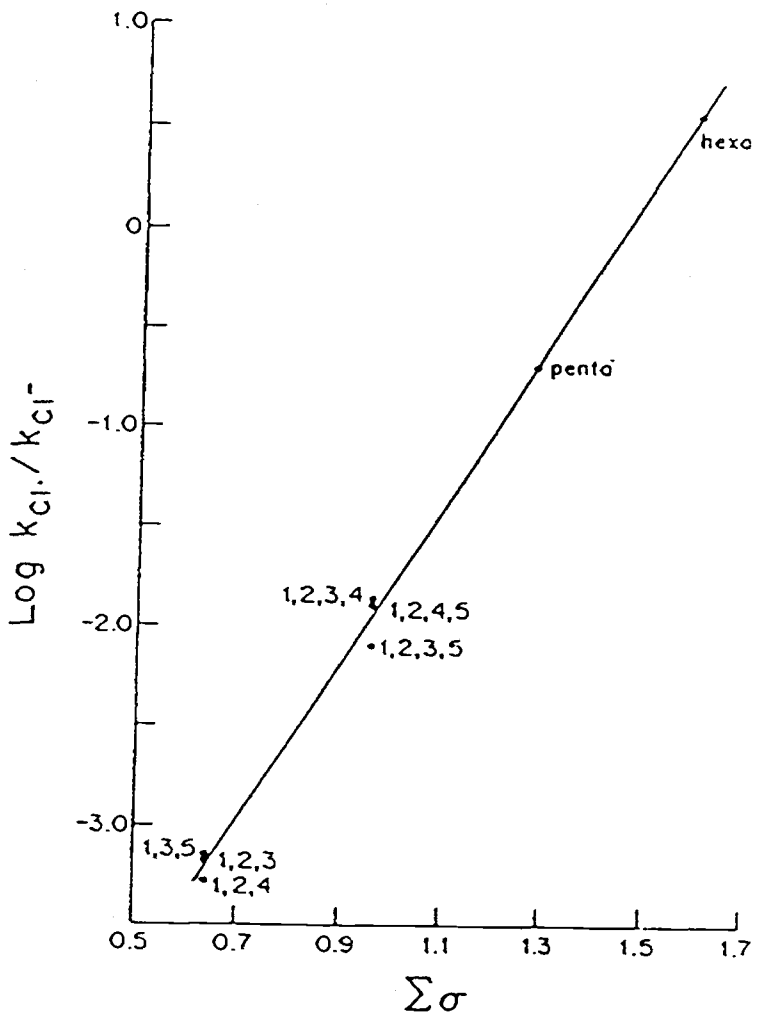

Figure 3.1: **Hammett plot of log (k_{Cl}/k_{Cl^-}) derived from GC/ECCI/MS experiments vs. $\Sigma\sigma$ for polychoroarene series.[1]**

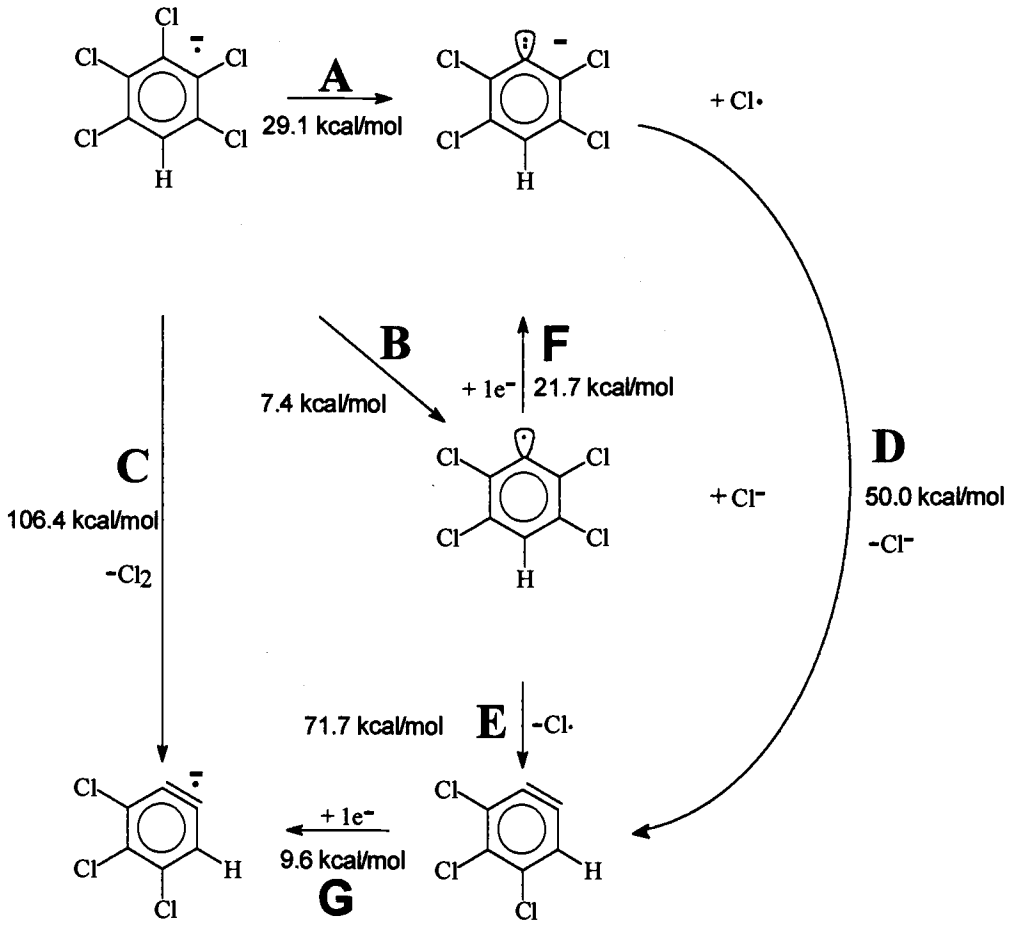

Scheme 3.3: **HF/6-31G*//HF/6-31G* ΔE_0 values in kcal/mol for pentachlorobenzene radical anion cleavage pathways.**

kcal/mol, respectively), **Schemes 3.4, 3.5** and **3.6**. The ΔE_o values for the 1, 3, 5-trichlorobenzene radical anion cleavage pathways revealed that fission to form chloride ion (*pathway B*) is 46.1 kcal/mol more favorable than fission to form chlorine atom, **Scheme 3.4**. The lower energy pathway for cleavage of either the chlorine at carbon number two or the chlorine at carbon number one for 1, 2, 3-trichlorobenzene radical anion is the loss of chloride ion at the HF/6-31G*//HF/6-31G* level by 35.1 and 43.6 kcal/mol, respectively, **Scheme 3.5**. The ΔE_o for the loss of chlorine at carbon number two from 1, 2, 3-trichlorobenzene is slightly favored over the loss of chlorine at carbon number one providing insight into which chlorine may have been lost to form chloride ion in the GC/ECCI/MS experiments.

Continuing, the lower energy pathway for cleavage of either the chlorine at carbon number four, carbon number two or carbon number one from 1, 2, 4-trichlorobenzene radical anion is fission to form chloride ion, *pathway B*, at the HF/6-31G*//HF/6-31G* level by 49.0, 40.5 and 41.9 kcal/mol, respectively, **Scheme 3.6**. A limitation of the HF/6-31G*// HF/6-31G* level calculations is that the energy difference between the two pathways, *A* and *B*, is exaggerated for the trichlorobenzene radical anions. One would not expect to see *pathway A* because the energy differences between the two pathways for the trichlorobenzene radical anions are > 40 kcal/mol but *pathway A* is observed in the GC/ECCI/MS experiments. Therefore, the computational results at the HF/6-31G*//HF/ 6-31G* level provide qualitative support for results from the GC/ECCI/MS experiments for all the trichlorobenzenes where *pathway B* is the favored process.[1]

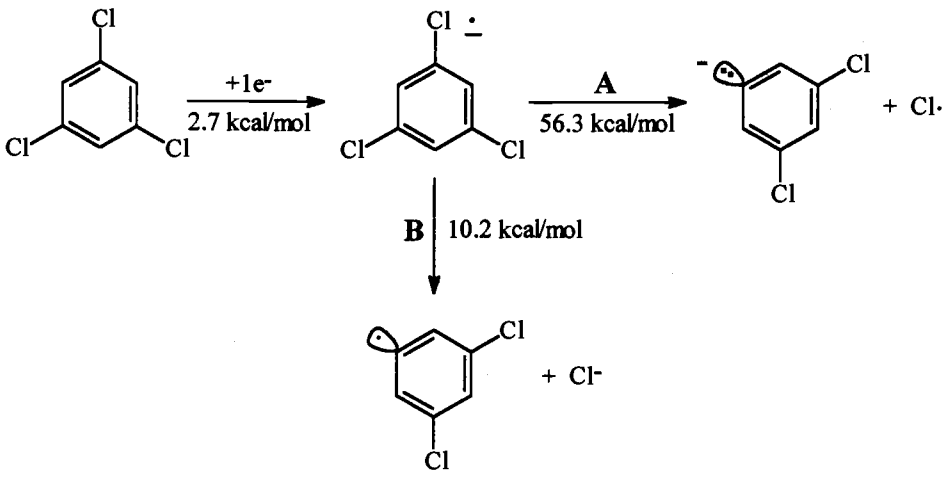

Scheme 3.4: **HF/6-31G*//HF/6-31G* ΔE_0 values in kcal/mol for the 1, 3, 5-trichlorobenzene radical anion cleavage pathways.**

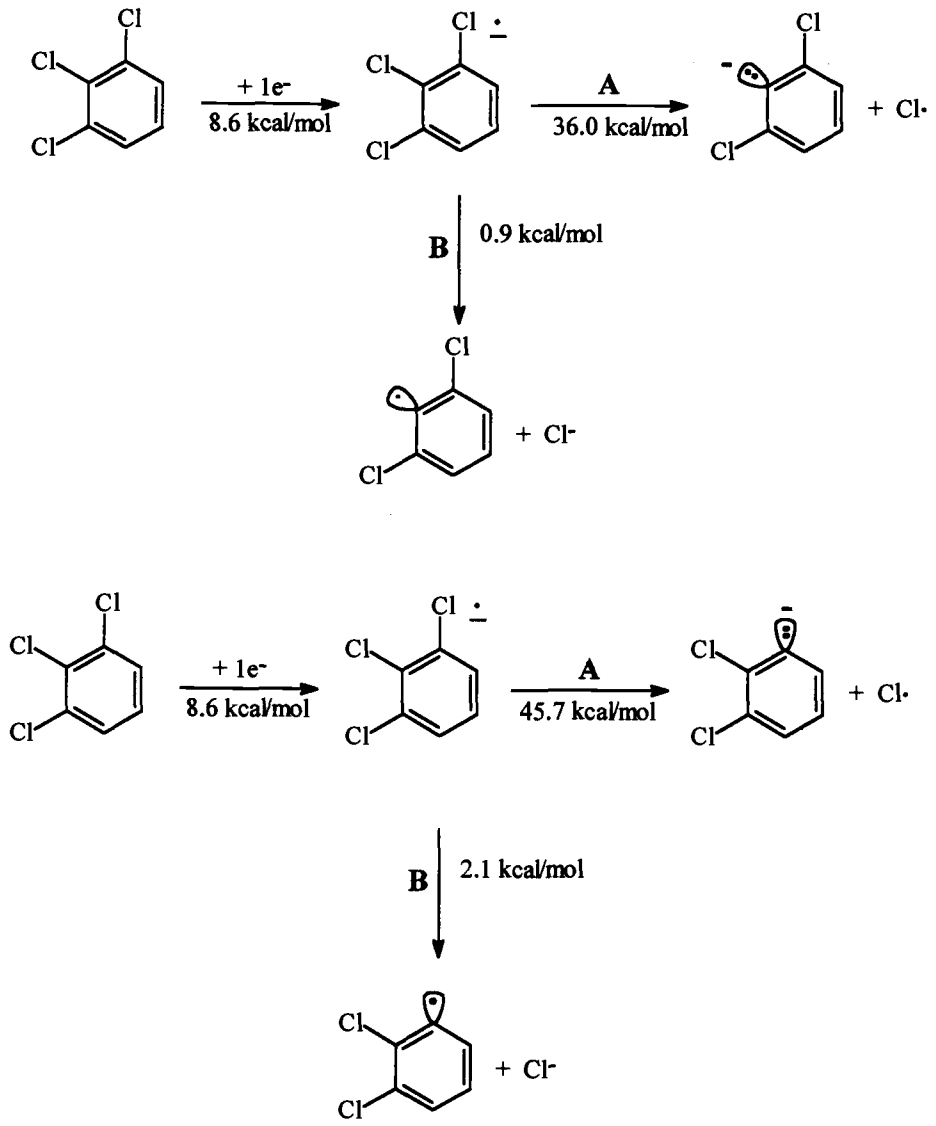

Scheme 3.5: **HF/6-31G*//HF/6-31G* ΔE_0 values in kcal/mol for 1, 2, 3-trichloro-benzene radical anion cleavage.**

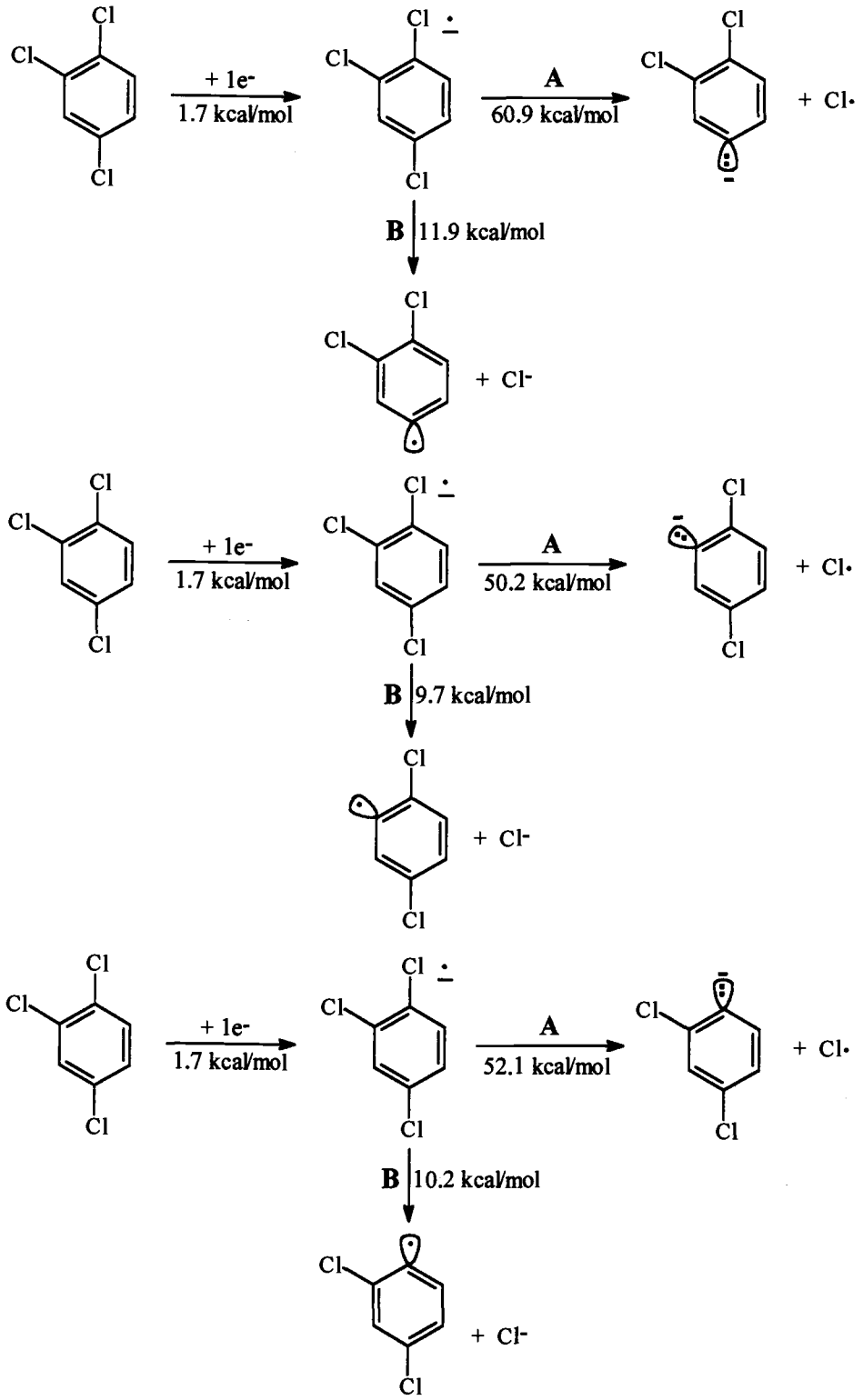

Scheme 3.6: **HF/6-31G*//HF/6-31G* ΔE_0 values in kcal/mol for 1, 2, 4-trichlorobenzene radical anion cleavage pathways.**

The ΔE_o for the loss of the chlorine at carbon number two from 1, 2, 4-trichlorobenzene radical anion is favored over the loss of chlorine at carbon number one or the chlorine at carbon number four revealing which chlorine may have been lost to form chloride ion in the GC/ECCI/MS experiments. In the photolysis of 1, 2, 4-trichlorobenzene in the presence of electron transfer reagent, triethyl amine and in the non-photochemical reaction of 1, 2, 4-trichlorobenzene in the presence of electron transfer reagent, lithium *p, p'*-di-*tert*-butylbiphenyl, it was proposed by Freeman and co-workers that the 1, 2, 4-trichlorobenzene radical anion underwent cleavage to form products and the order of chloride loss for these experiments is chloride loss at carbon number two > carbon number one > carbon number four (**Table 3.1**) which parallels the computational results for the loss of chloride ion.[1,6] The ΔE_o values for the differences in energy for the loss of chlorine at carbon number two, carbon number one and carbon number four do not explain the regiochemistry observed in the photochemical and non-photochemical experiments with precision. The ΔE_o values do reveal, however, a qualitative agreement with the experimental results. Since the relative ratio of products is temperature dependent in the photochemical and non-photochemical experiments, **Table 3.1**, the change in the sum of the electronic and thermal energies between the products and the reactants at 298.15 K and 318 K (25° C and 45° C, respectively) was used to estimate the differences in the energies of activation ($\Delta\Delta E = \Delta E_a$) for the two different pathways for chloride ion loss. The estimated ΔE_a values at the respective temperatures were inserted into the Arrhenius equation[25,26] to calculate the ratio of the rate constants of interest, **equation 3.1**. The relative ratios of product were calculated at the relevant temperatures, **Table 3.2**. The major product, 1, 4-dichlorobenzene is over-

$$\frac{k_{Cl^-}}{k'_{Cl^-}} = e^{-(\Delta E_a)/RT}$$ **Equation 3.1**

estimated and the minor product, 1, 2-dichlorobenzene is underestimated with respect to the photochemical and non-photochemical experiments. In sum, the incorporation of the ΔE_a from the HF/6-31G*//HF/6-31G* level calculations into the Arrhenius equation reveals that calculations at the HF/6-31G*//HF/6-31G* level are in qualitative agreement with the results of the photochemical and the non-photochemical experiments of 1, 2, 4-trichlorobenzene in the presence of electron transfer reagents.[6]

Geometry optimization and frequency calculations were run at the HF/6-31G*// HF/6-31G* level on the radical anion cleavage pathways of the tetrachlorobenzene isomers: 1, 2, 3, 4-tetrachlorobenzene, 1, 2, 4, 5-tetrachlorobenzene, and 1, 2, 3, 5-tetrachlorobenzene, **Schemes 3.7**, **3.8** and **3.9**. In addition, single point energy calculations at the B3LYP/6-31G* level on the HF/6-31G* optimized geometry were conducted on the 1, 2, 3, 5-tetrachlorobenzene radical anion cleavage pathways. The ΔE_o values are displayed in **Schemes 3.7**, **3.8**, and **Table 3.3**. The lower energy pathway for the fission of either the chlorine at carbon number two or carbon number one from 1, 2, 3, 4-tetrachlorobenzene radical anion is *pathway B* by 28.3 and 36.3 kcal/mol, respectively, **Scheme 3.7**. The HF/ 6-31G*//HF/6-31G* level calculations exaggerate the energy difference between the two pathways of 1, 2, 3, 4-tetrachlorobenzene radical anion. One would not expect to see

Table 3.1: Relative ratio of products from the 1, 2, 4-trichlorobenzene radical anion in various reaction conditions.

Reaction Conditions	Percent Ratio of Products 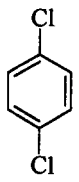	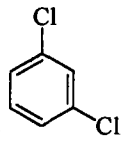	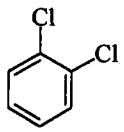
Photolysis with triethyl amine[a]	75.3 ± 0.25	18.2 ± 0.11	6.5 ± 0.35
Reaction with DBB at - 70°C[b]	87.7 ± 1.3	9.32 ± 0.97	2.97 ± 0.23
Extrapolated DBB results to 45°C[c]	75.3	13.7	9.89

[a]Photolysis of 0.05 M 1, 2, 4-trichlorobenzene in acetonitrile in the presence of 1.5 M triethyl amine 45°C.[1] [b]Reaction of 1, 2, 4-trichlorobenzene in tetrahydrofuran in the presence of lithium *p, p'*-di-*tert*-butylbiphenyl.[6] [c]The regiochemistries of the products were temperature dependent, therefore, the percent ratio of products at 45°C were extrapolated values from an Arrhenius plot of 1/temperature vs. log (rate of formation of 1, 4-dichlorobenzene/rate of formation of 1, 3-dichlorobenzene).[6]

Table 3.2: Relative ratio of products from the 1, 2, 4-trichlorobenzene radical anion from the calculations using the Arrhenius equation.

	Percent Ratio of Products[a]		
Temperature[b]	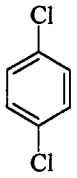	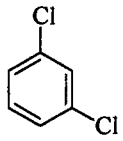	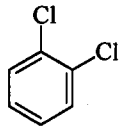
25	52.2	45.0	2.8
45	49.4	47.2	3.4

[a]The percent ratio of products was calculated from the results of the calculations using the Arrhenius equation. Estimated ΔE_a values were calculated from HF/6-31G*//HF/6-31G* level computations. [b]Temperature is in Celsius.

pathway A because the energy difference between the two pathways for the 1, 2, 3, 4-tetrachlorobenzene radical anion is greater than 5-6 kcal/mol, but *pathway A* is observed in the GC/ECCI/MS experiments. In sum, the computations at the HF/6-31G*//HF/6-31G* level qualitatively support the findings of the GC/ECCI/MS experiments.

The loss of the chloride at carbon number two is slightly favored over the loss of chloride at carbon number one indicating which chlorine may have been cleaved in the GC/ECCI/MS and these results parallel the results of photochemical experiments in the presence of an electron transfer reagent.[1,6,10,27] In photodehalogenation experiments of 1, 2, 3, 4-tetrachlorobenzene in the presence of triethyl amine it was suggested that the 1, 2, 3, 4-tetrachlorobenzene radical anion underwent cleavage to form products. The results of these photochemical experiments revealed that chloride at carbon number two is cleaved preferentially, **Table 3.4**. The estimated ΔE_a values at the HF/6-31G*//HF/6-31G* level at the pertinent temperatures were inserted into the Arrhenius equation,[25,26] which reveal that the percent product ratios are exaggerated with respect to the photochemical experiments, **Table 3.5**. Thus, the computations at the HF/6-31G*//HF/6-31G* level are in qualitative agreement with the results of the GC/ECCI/MS experiments and the results from 1, 2, 3, 4-tetrachlorobenzene photodehalogenation experiments in the presence of triethyl amine.[1]

The lower energy pathway for the loss of chlorine from 1, 2, 4, 5-tetrachlorobenzene radical anion is *pathway B* by 33.4 kcal/mol at the HF/6-31G*//HF/ 6-31G* level, **Scheme 3.8**. The HF/6-31G*//HF/6-31G* level calculations exaggerate the energy difference between the two pathways of 1, 2, 4, 5-tetrachlorobenzene radical anion. Once again, one

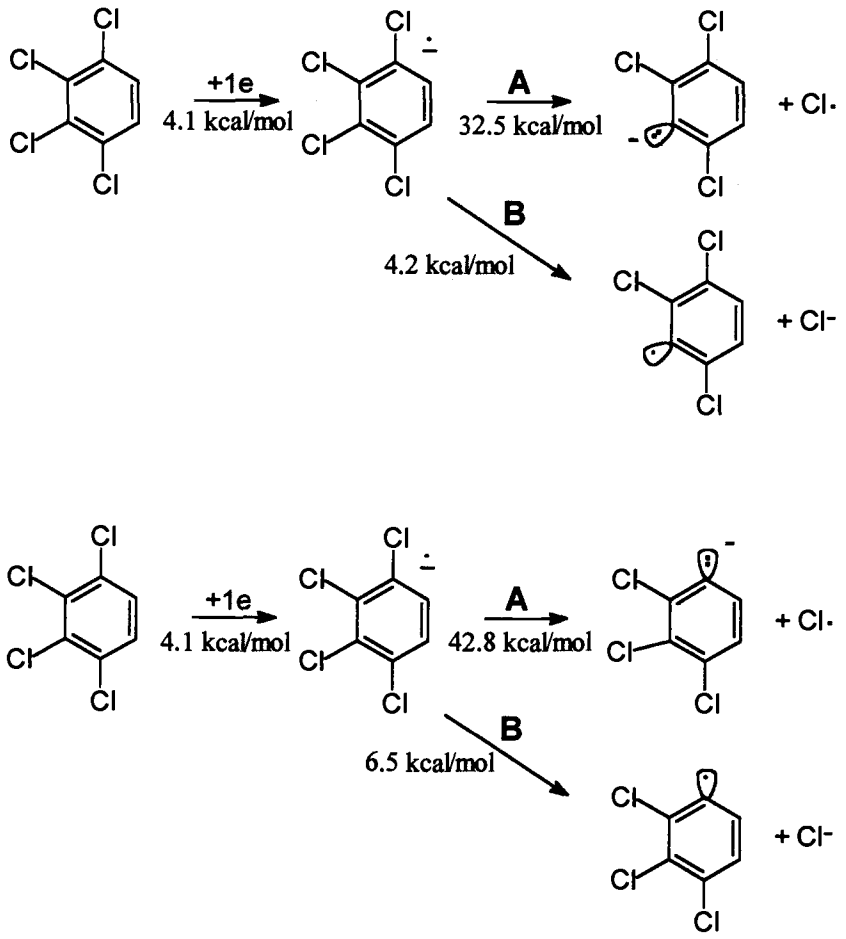

Scheme 3.7: **HF/6-31G*//HF/6-31G* ΔE_0 values in kcal/mol for 1, 2, 3, 4-tetrachlorobenzene radical anion cleavage pathways.**

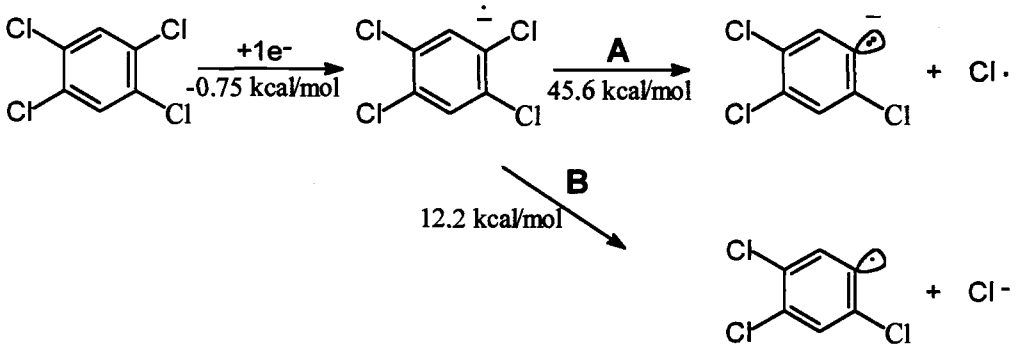

Scheme 3.8: **HF/6-31G*//HF/6-31G* ΔE_0 values in kcal/mol for 1, 2, 4, 5-tetrachlorobenzene radical anion cleavage pathways.**

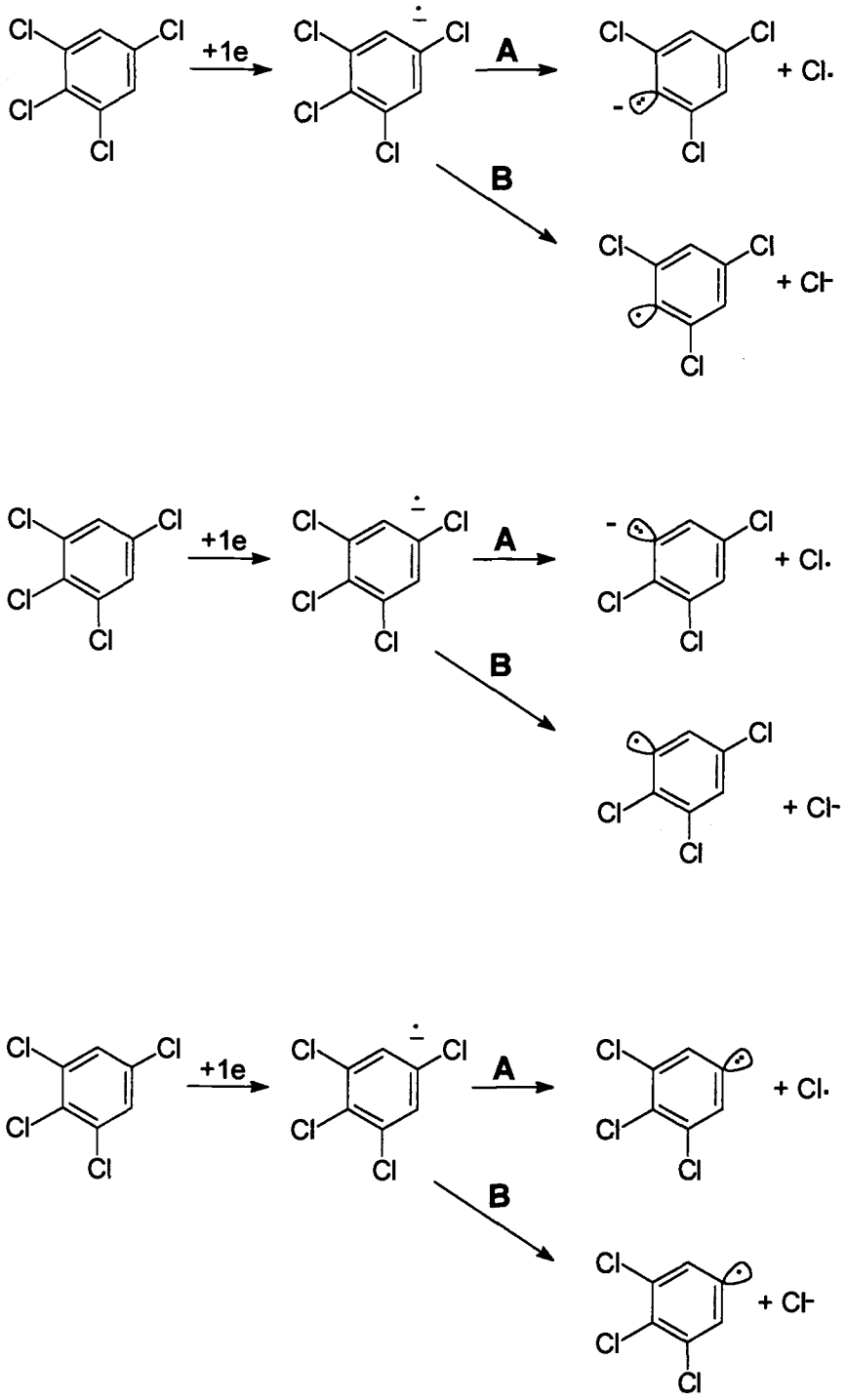

Scheme 3.9: **1, 2, 3, 5-tetrachlorobenzene radical anion cleavage pathways (energies of the pathways, Table 3.3).**

would not expect to see *pathway A* because the energy difference between the two pathways for the 1, 2, 4, 5-tetrachlorobenzene radical anion is greater than 5-6 kcal/ mol, but *pathway A* is observed in the GC/ECCI/MS experiments. Therefore, the computational results qualitatively support the findings of the GC/ECCI/MS experiments.

The lower energy pathway for the loss of chlorine at carbon number two, carbon number one or carbon number four from 1, 2, 3, 5-tetrachlorobenzene radical anion is *pathway B* by 27.0, 33.4 and 40.0 kcal/mol, respectively, at the HF/6-31G*//HF/6-31G* level, **Table 3.3** and **Scheme 3.9**. Once again, one would not expect to see *pathway A* because the energy differences between the two pathways for the tetrachlorobenzene radical anions are greater than 5-6 kcal/mol, but *pathway A* is observed in the GC/ECCI/MS experiments. The HF/6-31G*//HF/6-31G* level does not include electron correlation, therefore, it was proposed that if a method that included electron correlation were used, the energy difference between *pathway A* and *B* might be reduced for the 1, 2, 3, 5-tetra-chlorobenzene radical anion cleavage pathways. Therefore, single point energy calculations at the B3LYP/6-31G* level on the HF/6-31G* optimized geometries were completed. The B3LYP method was chosen because it takes into account electron correlation and it has been documented to take less computational time than other electron correlated methods such as the MP2 method.[14] In addition, the B3LYP method has been used successfully to model other types of aromatic systems including the vibrational spectra of chlorinated dioxins and nucleophilic substitution reactions of polyhalogenated benzenes and nitrobenzenes.[28,29] The B3LYP/6-31G*//HF/6-31G* level computations also show that *pathway B* is the lower energy pathway by 13, 19.2, and 27.1 kcal/mol for the same order of chlorine loss listed above, **Scheme 3.9** and **Table 3.3**. The energy difference involved in the loss of either

chlorine atom or chloride ion from the radical anion is much higher than the energy at the HF/6-31G*//HF/6-31G* level. Furthermore, the loss of either chloride at carbon number two or chloride at carbon number one is favored over the fission of the chloride at carbon number four providing insight into which chlorine(s) are most likely lost in the GC/ECCI/MS experiments.

In the photodehalogenation experiments of 1, 2, 3, 5-tetrachlorobenzene in the presence of triethyl amine, work in this laboratory suggested that the 1, 2, 3, 5-tetrachlorobenzene radical anion undergoes cleavage to form products. The results of the photochemical experiments indicate that chloride at carbon number one is cleaved preferentially, **Table 3.4**. Furthermore, the non-photochemical reaction of 1, 2, 3, 5-tetrachlorobenzene with lithium *p, p'*-di-*tert*-butylbiphenyl also showed that chlorine at carbon number one is lost preferentially, **Table 3.4**. The HF/6-31G*//HF/6-31G* level calculations revealed that the loss of the chloride at carbon number five is a higher energy process than the loss of the chloride at carbon number one and the chloride at carbon number two resulting in a lower yield (if any at all) of 1, 2, 3-trichlorobenzene produced in the photochemical and non-photochemical experiments, **Table 3.3**.[1,6] The ΔE_o values for the differences in energy for the loss of chloride at carbon number two and chloride at carbon number three does not explain the regiochemistries observed in photochemical experiments with exactness. The ΔE_o values do show, however, a qualitative agreement with the experimental results. If the estimated ΔE_a values are incorporated into the Arrhenius equation, we can get a better idea of how well the HF/6-31G*//HF/6-31G* level models the photochemical and non-photochemical experiments.[25,26] The Arrhenius calculations show

Table 3.3: **HF/6-31G*//HF/6-31G* and B3LYP/D95//HF/6-31G* ΔE_o values in kcal/mol for formation and cleavage pathways of the 1, 2, 3, 5-tetra-chlorobenzene radical anion.**

Method/Basis Set	Isomer	Radical Anion	*A*	*B*
HF/6-31G*//HF/6-31G*[a]		4.4		
HF/6-31G*//HF/6-31G*[a]	1, 3, 5-Trichlorobenzene		32.1	5.1
HF/6-31G*//HF/6-31G*[a]	1, 2, 4-Trichlorobenzene		39.2	5.8
HF/6-31G*//HF/6-31G*[a]	1, 2, 3-Trichlorobenzene		48.6	8.6
B3LYP/6-31G*//HF/6-31G*[b]		-8.7		
B3LYP/6-31G*/HF/6-31G*[b]	1, 3, 5-Trichlorobenzene		48.8	35.8
B3LYP/6-31G*//HF/6-31G*[b]	1, 2, 4-Trichlorobenzene		54.7	35.5
B3LYP/6-31G*//HF/6-31G*[b]	1, 2, 3-Trichlorobenzene		65.7	38.6

[a] ΔE_o values = $[(E_{products} + ZPE) - (E_{starting\ material} + ZPE)]$ in kcal/mol at the HF/6-31G*//HF/6-31G* level.[14] See **Scheme 3.9** for 1, 2, 3, 5-tetrachlorobenzene radical anion cleavage pathways. [b] ΔE_o values = $[(E_{products} + ZPE) - (E_{starting\ material} + ZPE)]$ in kcal/mol where the E values are from the single point energy calculation at the B3LYP/6-31G* and the scaled zero point energy (ZPE) is taken from the frequency calculation at the HF/6-31G* level.[14] See **Scheme 3.9** for 1, 2, 3, 5-tetra-chlorobenzene radical anion cleavage pathways.

Table 3.4: **Relative ratio of products from the 1, 2, 3, 4-tetrachlorobenzene and the 1, 2, 3, 5-tetrachlorobenzene radical anions in various reaction conditions.**

	Percentage Ratio of Products		
Tetrachlorobenzene	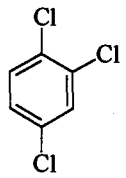	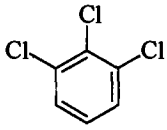	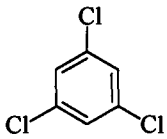
1, 2, 3, 4-Tetrachlorobenzene[a]	80.12 ± 2.7	19.8 ± 2.7	0.0
1, 2, 3, 5-Tetrachlorobenzene[a]	75.45 ± 1.4	5.78 ± 0.61	18.77 ± 1.0
1, 2, 3, 5-Tetrachlorobenzene[b]	97.1 ± 0.63	0.0	2.90 ± 0.50

[a]Photolysis of 0.05 M of individual tetrachlorobenzenes in acetonitrile with 1.5 M triethyl amine.[1]
[b]Reaction of 1, 2, 3, 5-tetrachlorobenzene in tetrahydrofuran at -65°C in the presence of lithium *p*, *p*'-di-*tert*-butylbiphenyl. The regiochemistry of the products were not temperature dependent.[6]

Table 3.5: Percent composition of products of 1, 2, 3, 4-tetrachlorobenzene and 1, 2, 3, 5-tetrachlorobenzene radical anion cleavage pathways from the calculations using the Arrhenius equation.

		Percentage Ratio of Products[a]		
Tetrachlorobenzene	**T[b]**	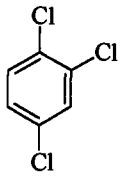	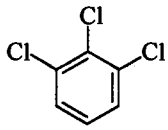	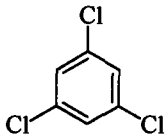
1, 2, 3, 4-Tetrachlorobenzene	25	97.9	2.1	—
	45	97.4	2.6	—
1, 2, 3, 5-Tetrachlorobenzene	25	35.1	0.1	64.8
	45	30.3	0.4	69.3

[a]The percent ratios of products were calculated from the results of the calculations using the Arrhenius equation and are corrected for statistical advantages. Estimated ΔE_a values were calculated from HF/6-31G*//HF/6-31G* level computations. [b]Temperature is in Celsius.

that statistically corrected percent ratios of the products are the exact opposite of the regiochemistry observed in the photochemical and non-photochemical experiments, **Table 3.5**. In sum, the HF/6-31G*//HF/6-31G* and B3LYP/6-31G*//HF/6-31G* levels qualitatively support the GC/ECCI/MS experiments. The B3LYP/6-31G*//HF/6-31G* level ΔE_o values for the differences in energy for the loss of chloride from carbon number two, number one and carbon number five do not explain the regiochemistry observed in the photochemical and non-photochemical experiments,[1,6] although, the ΔE_o values are in qualitative agreement with the experimental results. The ΔE_o values at the HF/6-31G*// HF/6-31G* level for the differences in energy for the loss chloride ion are misleading because the lowest energy pathway does not lead to the formation of the major product that was observed in the photochemical and non-photochemical experiments.

Geometry optimization and frequency calculations were performed at the HF/ 6-31G*//HF/6-31G* level on the pentachlorobenzene radical anion cleavage pathways. The results indicate that p*athway B* is the lower energy pathway for the formation of 2, 3, 5, 6-tetrachlorophenyl, 2, 3, 4, 6-tetrachlorophenyl or 2, 3, 4, 5-tetrachlorophenyl radicals, **Scheme 3.10** and **Table 3.6**. The computational studies at the HF/6-31G*// HF/6-31G* level for the pentachlorobenzene radical anion cleavage pathways to form the 2, 3, 5, 6-tetrachlorophenyl anion and the 2, 3, 5, 6-tetrachlorophenyl radical have been discussed previously (**Scheme 3.3**), and p*athway B* is found to be lower in energy by 21.7 kcal/mol at the HF/6-31G*//HF/6-31G* level, **Schemes 3.3** and **3.10,** and **Table 3.6**. The formation of 2, 3, 4, 6-tetrachlorophenyl and 2, 3, 4, 5-tetrachlorophenyl radicals are 21.9 kcal/mol and 27.9 kcal/mol, respectively, lower in energy than the formation of

2, 3, 4, 6-tetrachloro-phenyl and 2, 3, 4, 5-tetrachlorophenyl anions at the HF/6-31G*// HF/6-31G* level. The HF/6-31G*//HF/6-31G* level calculations exaggerate the energy differences between the *A* and *B* pathways for the pentachlorobenzene radical anion. One would not expect to see *pathway A* because the energy differences between the two pathways for the pentachlorobenzene radical anion are 21.9 and 28.1 kcal/mol, respectively, but *pathway A* is observed in the GC/ECCI/MS experiments. Therefore, the computational results at this level qualitatively support what is found in the GC/ECCI/MS experiments where *pathway B* is the favored cleavage pathway for the pentachlorobenzene radical anion.[1]

B3LYP/6-31G*//B3LYP/6-31G* level geometry optimization and frequency calculations were executed and revealed that *pathway B* is favored over *pathway A* by 13.8 kcal/mol, 15.4 kcal/mol and 22.2 kcal/mol, respectively, for the formation of 2, 3, 5, 6-tetra-chlorophenyl radical, 2, 3, 4, 6-tetrachlorophenyl radical and 2, 3, 4, 5-tetrachlorophenyl radical, **Table 3.6**. The energy differences between *pathway A* and *B* for the B3LYP/ 6-31G*//B3LYP/6-31G* level calculations are less than the HF/6-31G*//HF/6-31G* level, although, the energy differences are still exaggerated. In addition single point energy calculations were run at the B3LYP/D95 level on the B3LYP/6-31G* level optimized geometries. The D95 basis set was chosen because it has been found to provide the diffuseness and flexibility needed to qualitatively model temporary negative ion states which are formed upon capture of an electron by a molecule.[22] The B3LYP/D95//B3LYP/6-31G* ΔE_o values (including the scaled zero point energies of the B3LYP/6-31G* frequency calculations) revealed that *pathway A* is preferred by 4.9 and 3.0 kcal/mol, respectively, for

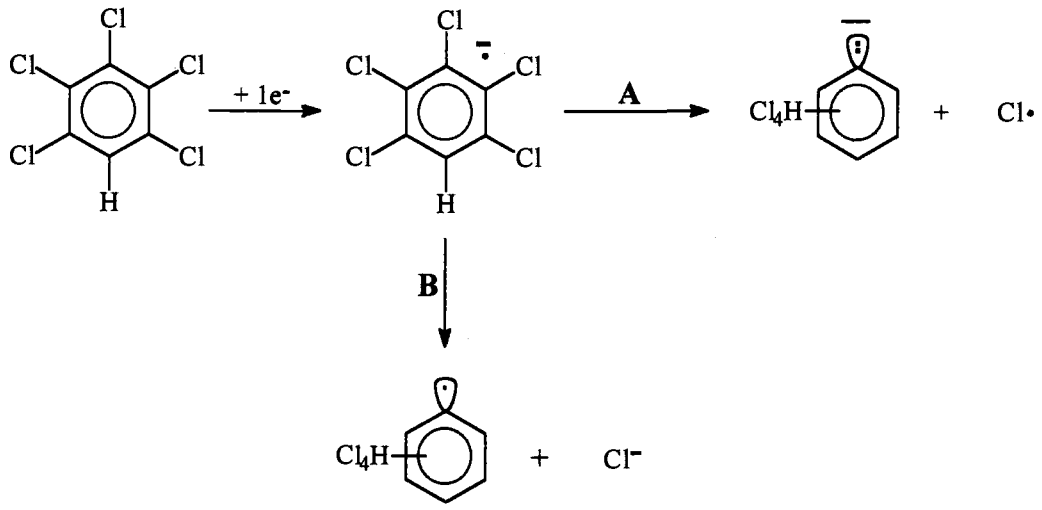

Scheme 3.10: **Pentachlorobenzene radical anion cleavage pathways for the loss of chlorine at carbon number one, chlorine at carbon number two or chlorine at carbon number three (energies of the pathways, Table 3.6).**

Table 3.6: **HF/6-31G*//HF/6-31G*, B3LYP/6-31G*//B3LYP/6-31G*, and B3LYP/D95//B3LYP/6-31G* ΔE_o values in kcal/mol for formation and cleavage pathways of the pentachlorobenzene radical anion for the loss of either the chlorine at carbon number three, carbon number two or carbon number one.**

Method/Basis Set	Isomer[a]	Radical Anion	*A*	*B*
HF/6-31G*// HF/6-31G*[a]		-0.32		
HF/6-31G*// HF/6-31G*[a]	1, 2, 4, 5-tetrachlorobenzene		29.1	7.4
HF/6-31G*// HF/6-31G*[a]	1, 2, 3, 5-tetrachlorobenzene		30.5	8.6
HF/6-31G*// HF/6-31G*[a]	1, 2, 3, 4-tetrachlorobenzene		38.6	10.5
B3LYP/6-31G*// B3LYP/6-31G*[b]		-2.08		
B3LYP/6-31G*// B3LYP/6-31G*[b]	1, 2, 4, 5-tetrachlorobenzene		43.8	30.0
B3LYP/6-31G*// B3LYP/6-31G*[b]	1, 2, 3, 5-tetrachlorobenzene		46.6	31.2
B3LYP/6-31G*// B3LYP/6-31G*[b]	1, 2, 3, 4-tetrachlorobenzene		54.5	32.3
B3LYP/D95// B3LYP/6-31G*[c]		-32.2		
B3LYP/D95// B3LYP/6-31G*[c]	1, 2, 4, 5-tetrachlorobenzene		35.5	40.4
B3LYP/D95// B3LYP/6-31G*[c]	1, 2, 3, 5-tetrachlorobenzene		38.8	41.8
B3LYP/D95// B3LYP/6-31G*[c]	1, 2, 3, 4-tetrachlorobenzene		47.4	43.2

[a] ΔE_o values = $[(E_{products} + ZPE) - (E_{starting\ material} + ZPE)]$ in kcal/mol at the HF/6-31G*//HF/6-31G* level.[14] See **Scheme 3.10** for pentachlorobenzene radical anion cleavage pathways. [b] ΔE_o values = $[(E_{products} + ZPE) - (E_{starting\ material} + ZPE)]$ in kcal/mol at the B3LYP/6-31G*//B3LYP/6-31G* level.[14] See **Scheme 3.10** for pentachlorobenzene radical anion cleavage pathways.[14] [c] ΔE_o values = $[(E_{products} + ZPE) - (E_{starting\ material} + ZPE)]$ in kcal/mol at the B3LYP/D95//B3LYP/6-31G* level.[14] See **Scheme 3.10** for pentachlorobenzene radical anion cleavage pathways.

the formation of 1, 2, 4, 5-tetrachlorobenzene and 1, 2, 3, 5-tetrachlorobenzene isomers, **Table 3.6**. These computational results are the opposite of what was found in the GC/ECCI/MS experiments, however, *pathway B* is favored by 4.2 kcal/mol for the 1, 2, 3, 4-tetrachlorobenzene isomer supporting the results of the GC/ECCI/MS experiments, although 1, 2, 3, 4-tetrachlorobenzene formation is the least competitive pathway. The energy difference between *pathway A* and *B* is much smaller (< 5 kcal/mol) than previous studies, and the energy differences tilt in the correct direction for major product formation. Therefore, the HF/6-31G*//HF/6-31G* and B3LYP/6-31G*//B3LYP/6-31G* calculations are in qualitative agreement with the results of the GC/ECCI/MS experiments[1] and the B3LYP/D95//B3LYP/6-31G* over corrects by a small amount.

The HF/6-31G*//HF/6-31G* and the B3LYP/6-31G*//B3LYP/6-31G* calculations have provided insight into which chlorine of the pentachlorobenzene radical anion may have been cleaved preferentially in the GC/ECCI/MS experiments. The pentachlorobenzene radical anion cleaves to form chloride ion and the ΔE_o values reveal that the order of chloride loss is chloride at carbon number three > carbon number two > carbon number one (i.e. the formation of the 2, 3, 5, 6-tetrachlorophenyl radical is lower in energy than 2, 3, 4, 6-tetrachlorophenyl radical formation which in turn is lower in energy than 2, 3, 4, 5-tetrachlorophenyl radical). The GC/ECCI/MS experiments did not reveal which chlorine is cleaved, only that the most favorable radical anion cleavage pathway is *pathway B*. In the photolysis of pentachlorobenzene in the presence of electron transfer agent triethyl amine and non-photochemical electron transfer using lithium *p, p'*-di-*tert*-butylbiphenyl it was proposed that the pentachlorobenzene radical anion underwent fission to form the products and the order of chloride loss in these experiments is chloride at carbon number

three > chloride at carbon number two > chloride at carbon number one, **Table 3.7**, which parallels the computational results. The estimated ΔE_a values at 298.15 K and 318 K were entered into the Arrhenius equation.[25,26] The percent composition of the major and minor products are overestimated at the HF/6-31G*//HF/6-31G* and B3LYP/6-31G*//B3LYP/6-31G* levels, although, qualitatively, the experimental results are nicely supported, **Table 3.8**.

Computations were run to investigate the hexachlorobenzene radical anion cleavage pathways. In the GC/ECCI/MS experiments the favored pathway for hexachlorobenzene radical anion is *pathway A*, cleavage to form pentachlorobenzene anion and chlorine atom. Although, HF/6-31G*//HF/6-31G* and B3LYP/6-31G*//B3LYP/6-31G* level calculations both suggest that *pathway B* is the favored pathway by 16.9 and 10.0 kcal/mol, respectively, **Scheme 3.11** and **Table 3.9**. The energy differences between *pathway A* and *pathway B* are less than analogous radical anion cleavage pathways discussed above. Therefore, it was postulated that if the calculations were conducted using an electron correlated method and, in particular, a basis set that may model negative ions more effectively than those discussed thus far, the energies of the hexachlorobenzene radical anion pathways may become smaller and the *A* versus *B* choice may even switch. Single point energy calculations were run at the B3LYP/D95 level on the B3LYP/6-31G* level optimized geometries. The B3LYP/D95//B3LYP/6-31G* ΔE_o values (including the scaled zero point energies of the B3LYP/6-31G* frequency calculations) reveal that *pathway A* is favored over *pathway B* by

Table 3.7: Relative ratio of products from the pentachlorobenzene radical anion in various reaction conditions.

Reaction Conditions	Percent Ratio of Products		
	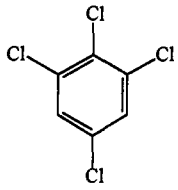	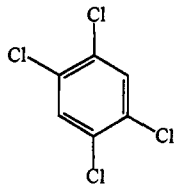	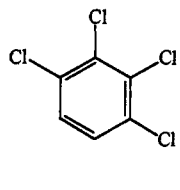
Reaction with DBB at -68 °C[a]	3.34 ± 0.43	95.7 ± 0.5	0.96 ± 0.09
Photolysis with triethyl amine[b]	25.32 ± 0.47	66.21 ± 0.46	8.47 ± 0.06
Extrapolated DBB results to 45 °C[c]	25.9	62.5	6.67

[a]Reaction of pentachlorobenzene in tetrahydrofuran in the presence of lithium *p, p'*-di-*tert*-butylbiphenyl.[6] [b]Photolysis of 0.05 M pentachlorobenzene in acetonitrile in the presence of 1.5 M triethyl amine 40 °C.[1] [c]The regiochemistries of the products were temperature dependent, therefore, the percent ratio of products at 45 °C were extrapolated values from an Arrhenius plot of 1/temperature vs. log (rate of formation of 1, 2, 4, 5-tetrachlorobenzene/rate of formation of 1,2, 3, 5-tetrachlorobenzene).[6]

Table 3.8 : The percent composition of products of the pentachlorobenzene radical anion cleavage pathways from the calculations using the Arrhenius equation.

		Percent Ratio of Products[a]		
Method and Basis Set	**T[b]**	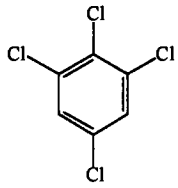	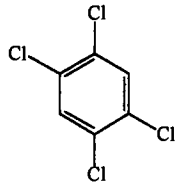	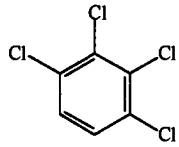
HF/6-31G*// HF6-31G*	25	28.0	70.9	1.1
	45	31.4	67.1	1.5
B3LYP/6-31G*// B3LYP/6-31G*	25	26.0	69.5	4.5
	45	10.8	87.2	2.0

[a]The percent ratios of products were calculated from the results of the calculations using the Arrhenius equation and are corrected for statistical advantages. [b]Temperature is in Celsius.

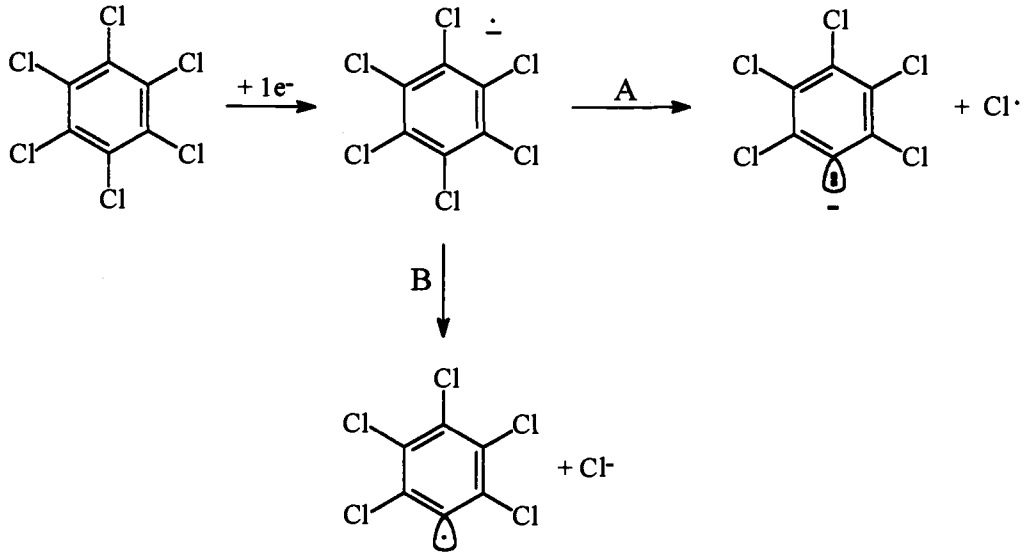

Scheme 3.11: Hexachlorobenzene radical anion cleavage pathways (energies of the pathways, Table 3.9).

Table 3.9: HF/6-31G*//HF/6-31G*, B3LYP/6-31G*//B3LYP/6-31G*, and B3LYP/D95//B3LYP/6-31G* ΔE_o values in kcal/mol for formation and cleavage pathways of the hexachlorobenzene radical anion.

Method/Basis Set	Radical Anion	*A*	*B*
HF/6-31G*//HF/6-31G*[a]	-3.12		
HF/6-31G//HF/6-31G**[a]		26.96	10.02
B3LYP/6-31G*//B3LYP/6-31G*[b]	-21.5		
B3LYP/6-31G*//B3LYP/6-31G*[b]		43.3	33.3
B3LYP/D95//B3LYP/6-31G*[c]	-41.7		
B3LYP/D95//B3LYP/6-31G*[c]		41.2	50.4

[a] ΔE_o values = $[(E_{products} + ZPE) - (E_{starting\ material} + ZPE)]$ in kcal/mol at the HF/6-31G*//HF/6-31G* level.[14] See **Scheme 3.11** for hexachlorobenzene radical anion cleavage pathways. [b] ΔE_o values = $[(E_{products} + ZPE) - (E_{starting\ material} + ZPE)]$ in kcal/mol at the B3LYP/6-31G*//B3LYP/6-31G* level.[14] See **Scheme 3.11** for hexachlorobenzene radical anion cleavage pathways. [c] ΔE_o values = $[(E_{products} + ZPE) - (E_{starting\ material} + ZPE)]$ in kcal/mol where the E is taken from the B3LYP/D95 single point energy of the B3LYP/6-31G* optimized geometry, and the scaled zero point energy (ZPE) is from the frequency calculation at the B3LYP/631G* level.[14] See **Scheme 3.11** for hexachlorobenzene radical anion cleavage pathways.

9.2 kcal/mol, **Table 3.9.** The energy difference between *pathway A* and *B* is smaller than previous studies with the exception of the B3LYP/D95//B3LYP/6-31G* calculations on the pentachlorobenzene radical anion fragmentation, although, it is still exaggerated. Therefore, the single point energy calculation provides the best method to model the processes involved in the GC/ECCI/MS experiments for the hexachlorobenzene radical anion cleavage pathways, because the B3LYP method includes electron correlation and the D95 basis set provides the diffuseness and flexibility needed to sufficiently model the negative ions.[22]

Conclusion

Computational chemistry studies were undertaken to investigate the polyhalogenated benzene radical anion cleavage pathways further and to find methods and basis sets that were adequate to model the results from the GC/ECCI/MS experiments, and photochemical and non-photochemical experiments in the presence of electron transfer reagents.[1,6] HF/ 6-31G*//HF/6-31G* and B3LYP/6-31G* level calculations were sufficient to qualitatively model the mode of fragmentation for trichlorobenzenes, tetrachlorobenzenes and pentachlorobenzene radical anions, although, the energy difference between pathways *A* and *B* are exaggerated. The regiochemistry of the percent product ratios from the calculations using the Arrhenius equation[25,26] produces results that are the exact opposite of the percent product ratios observed in the photochemical and non-photochemical experiments of 1, 2, 3, 5-tetrachlorobenzene in the presence of electron transfer reagents, however, the results qualitatively support the electron transfer photochemistry of 1, 2, 4-trichlorobenzene, 1, 2, 3, 4-tetrachlorobenzene and pentachlorobenzene, and the non-photochemical electron

transfer reactions of 1, 2, 4-trichlorobenzene and pentachlorobenzene at the respective temperatures of the reactions.[1,6] The ΔE_a values that were used in the Arrhenius equation are estimations of the relative rates. In the future, the relative rates of the radical anion cleavage pathways can be calculated from the computed relative transition states. The ΔE_o values for HF/6-31G*//HF/6-31G* and B3LYP/6-31G*//B3LYP/6-31G* level calculations of the hexachlorobenzene radical anion revealed that *pathway B* not *pathway A* is the lower in energy, the opposite of what was found in the GC/ECCI/MS experiments. In contrast, a B3LYP/D95//B3LYP/6-31G* calculation revealed that *pathway A* is more favorable in the hexachlorobenzene radical anion cleavage pathways. The B3LYP/D95//B3LYP/6-31G* calculations provide the best method to model the hexachlorobenzene radical anion cleavage pathways because the D95 basis set provides the diffuseness and flexibility required to model the negative ions.[22] Overall, the computations that were run, qualitatively support the results from the GC/ECCI/MS experiments, and the photochemical and non-photochemical experiments of many of the polyhalogenated benzenes in the presence of electron transfer reagents. Furthermore, insight was provided into which chlorines are cleaved preferentially and which methods and basis sets are most appropriate to model radical anion cleavage pathways of polychlorinated benzenes.

References

1. Freeman, P.K.; Srinivasa, R.; Campbell, J.-A.; Deinzer, M.L. *J. Am. Chem. Soc.*, **1986**, *108*, 5531-5536.

2. Crosby, D. G.; Hamadmad, N. *J. Agr. Food Chem.* **1971**, *19*, 1171-1174.

3. Crosby, D. F. Moilanen, K. W.; Wong, A. S. *Eviron. Health Perspect.* **1973**, *5*, 259-266.

4. Freeman, P. K.; Ramnath, N. *J. Org. Chem.* **1988**, *53*, 148-152.

5. Freeman, P. K.; Ramnath, N.; Richardson, A. D. *J. Org. Chem.* **1991**, *56*, 3643-3646.

6. Freeman, P. K.; Ramnath, N. *J. Org. Chem.* **1991**, *56*, 3646-3651.

7. Freeman, P. K.; Jang, J-S.; Haugen, C.M. *Tetrahedron* **1996**, *52*, 8397-8406.

8. Bunce, N.L.; Hayes, P.J.; Lemke, M.E. *Can. J. Chem.* **1983**, *61*, 1103-1104.

9. Åkermark, B.; Baeckström, P.; Westlin, U.E.; Göthe, R.; Wachtmesiter, C. *Acta Chem. Scand. B.* **1976**, *30*, 49-52.

10. Harrison, A.G. *Chemical Ionization Mass Spectrometry*, 2nd Ed.; American Chemical Society: Washington, DC, 1997.

11. Hehre, W.J.; Radom, L.; Schleyer, P.v.R.; Pople, J.A. *Ab Initio Molecular Orbital Theory*; Wiley: New York, 1986.

12. *Spartan*, versions 4.1-5.0; Wavefunction, Inc.: Irvine, CA, 1993-1997.

13. *Gaussian 92*, Revision G.4, M. J. Frisch, G. W. Trucks, M. Head-Gordon, P. M. W. Gill, M. W. Wong, J. B. Foresman, B. G. Johnson, H. B. Schlegel, M. A. Robb, E. S. Replogle, R. Gomperts, J. L. Andres, K. Raghavachari, J. S. Binkley, C. Gonzalez, R. L. Martin, D. J. Fox, D. J. Defrees, J. Baker, J. J. P. Stewart, and J. A. Pople, Gaussian, Inc., Pittsburgh PA, 1992. *Gaussian 94*, Revisions C.2 and E.1, M. J. Frisch, G. W. Trucks, H. B. Schlegel, P. M. W. Gill, B. G. Johnson, M. A. Robb, J. R. Cheeseman, T. Keith, G. A. Petersson, J. A. Montgomery, K. Raghavachari, M. A. Al-Laham, V. G. Zakrzewski, J. V. Ortiz, J. B. Foresman, J. Cioslowski, B. B. Stefanov, A. Nanayakkara, M. Challacombe, C. Y. Peng, P. Y. Ayala, W. Chen, M. W. Wong, J. L. Andres, E. S. Replogle, R. Gomperts, R. L. Martin, D. J. Fox, J. S. Binkley, D. J. Defrees, J. Baker, J. P. Stewart, M. Head-Gordon, C. Gonzalez, and J. A. Pople, Gaussian, Inc., Pittsburgh PA, 1995.

14. Forseman, J.B.; Frisch, Æ. *Exploring Chemistry with Electronic Methods*, 2nd Ed.; Gaussian, Inc.: Pittsburgh, PA, 1995-96.

15. Binkley, J.S.; Pople, J.A.; Hehre, W.J. *J. Am. Chem. Soc.* **1980**, *102*, 939.

16. Dobbs, K.D.; Hehre, W.J. *J. Comp. Chem.* **1987**, *8*, 880.

17. Ditchfield, R.; Hehre, W.H.; Pople, J.A. *J. Chem. Phys.* **1971**, *54*, 724.

18. Hehre, W.H.; Ditchfield, R.; Pople, J.A. *J. Chem. Phys.* **1972**, *56*, 2257.

19. Hariharan, P.C.; Pople, J.A. *Mol. Phys.* **1974**, *27*, 209.

20. Gordon, M.S. *Chem. Phys. Lett.* **1980**, *76*, 163.

21. Hariharan, P.C.; Pople, J.A. *Theo. Chim. Acta.* **1973**, *28*, 213.

22. Staley, S.W.; Strnad, J.T. *J. Phys. Chem.* **1994**, *98*, 116-121.

23. Becke, A.D. *J. Chem. Phys.* **1993**, *98*, 5648.

24. Lee, C.; Yang, W.; Parr, R.G. *Phys. Rev. B.* **1988**, *37*, 785.

25. Lowry, T.H.; Richardson, K.S. *Mechanism and Theory in Organic Chemistry*, 3rd ed.; Harper & Row, Publishers: New York, 1987.

26. Carey, F.A.; Sunberg, R.J. *Advanced Organic Chemistry Part A: Structure and Mechanisms*, 3rd ed.; Plenum Press, NY, 1990.

27. Barofsky, D.F.; Deinzer, M.L. *Mass Spectrometry of Organic Molecules (AC637/CH537)*, Fall **1992**, Class Notes, Oregon State University.

28. Raunhut, G.; Pulay, P. *J. Am. Chem. Soc.*, **1995**, 117, 4167-4172.

29. Glukhovtsev, M. N.; Bach, R.D.; Laiter, S. *J. Org. Chem.* **1997**, 62, 4036-4046.

Chapter 4: Electron Capture Chemical Ionization Mass Spectrometric Analysis of Polyhalogenated Benzenes

Sharon Maley Herbelin and Peter K. Freeman*

Department of Chemistry
Oregon State University
Corvallis, OR 97331

Introduction

Electron Capture Chemical ionization mass spectrometry (ECCI/MS)[1] is a very powerful analytical tool to study molecules with high electron affinity (EA) such as polyhalogenated benzenes that can stabilize the negative charge. The samples can be introduced into a mass spectrometer via a gas chromatograph interface (GC/MS) or direct probe insertion (DP/MS). ECCI is considered a soft ionization technique because ionization occurs by interaction of neutral molecules with nearly thermal energy electrons and/or with negatively charged reagent ions when stable anions can be formed from the buffer gas. This soft ionization technique allows for structural and fragmentation information to be retained which involves two primary ionic processes: a) resonance electron capture to form a molecular radical anion, and/or b) and c) dissociative electron capture which produces fragment ions with the charge residing on either of the two fragments, **eq. 4.1**. These two processes require quite different energies 0.1 and 0-15 eV, respectively. Resonance electron capture requires collisional stabilization to prevent auto-

$$a)\ AB + e^- \longrightarrow AB^{-\cdot}$$
$$b)\ AB + e^- \longrightarrow A^- + B^{\cdot}$$
$$c)\ AB + e^- \longrightarrow A^{\cdot} + B^-$$

Equation 4.1

detachment.[2] This stabilization involves interaction between the radical anion and the buffer gas (such as He or CH_4) which absorbs excess energy. A molecule undergoing resonance electron capture must have an EA $\geq$ 2.5 eV to prevent competition from autodetachment, **eq. 4.2**. A variety of other ion-molecule reactions can take place in the

$$AB^{-\cdot} \longrightarrow AB + e^{-} \qquad \textbf{Equation 4.2}$$

ionization chamber such as d) proton transfer from a neutral molecule to an anion, e) charge exchange and f) nucleophilic addition, **eq. 4.3**.[3]

$$\begin{aligned} &d)\ AB + X^{-} \longrightarrow (AB-H)^{-} + XH \\ &e)\ AB + X^{-} \longrightarrow AB^{-} + X \quad where \quad EA(AB) \rangle EA(X) \\ &f)\ AB + X^{-} \longrightarrow ABX^{-} \end{aligned} \qquad \textbf{Equation 4.3}$$

As long as the EA of a molecule is above 2.5 eV, one would expect to see negative ions such as the molecular ion, polyhalophenyl anions and halide ions. The ions that are formed can be distinguished from each other by their mass to charge ratio (m/z) and natural abundance of isotopes, Br^{79}: Br^{81} is 100:97.3, and Cl^{35}: Cl^{37} is 100:32.0. A distinct isotopic pattern is observed that easily identifies the number of halogens present and allows for simple identification of polyhalogenated benzene ions.[4] Which type of reactions are involved in the ECCI of polychlorinated and polybrominated benzenes? Do resonance and dissociative electron capture processes take place? Will any of the ion-molecule reactions be observed? ECCI/MS studies were conducted to elucidate which ionic processes would be observed for the polyhalogenated benzenes.

In 1996 the Freeman and Deinzer research groups studied the fragmentation pathways of polychlorinated benzenes using GC/ECCI/MS.[6] It was proposed that the neutral molecule captures an electron that can go into a variety of different virtual molecular orbitals producing radical anions with differing energies and lifetimes. The radical anion

could undergo cleavage to form the aryl radical and halide ion or the aryl carbanion and halogen atom. A Hammett relationship was found between the sum of the Hammett substitution constants ($\Sigma\sigma$) of the polychlorinated benzenes, and, from the results of the GC/ECCI/MS experiments, the log of the rate of chlorine atom formation over the rate of chloride ion formation [log ($k_{Cl\cdot}/k_{Cl^-}$)]. A Hammett plot of the log ($k_{Cl\cdot}/k_{Cl^-}$) vs. $\Sigma\sigma$ for the polychlorinated benzenes reveals that the radical anions of the trichlorobenzenes, tetrachlorobenzenes and pentachlorobenzene favored fission to form the aryl radical and the halide ion (dichlorobenzenes were not included). The favored cleavage pathway for the hexachlorobenzene radical anion is fission to form aryl carbanion and halogen atom. It was proposed that hexachlorobenzene favored bond fission to form the aryl carbanion and the chlorine atom because the chlorines on the phenyl ring can withdraw electron density stabilizing the anionic charge.[4] A similar study on the polybrominated benzenes was conducted in 1997 by Couch and Freeman. A Hammett plot of the log ($k_{Br\cdot}/k_{Br^-}$) vs. $\Sigma\sigma$ for the polybrominated benzenes shows that the tribromobenzenes, tetrabromobenzenes, pentabromobenzene, and hexabromobenzene preferentially cleave to form the aryl radical and halide ion (the dibromobenzenes were not included).[5] Interestingly, it was also discovered in the 1997 study that the dibromobenzenes and the tribromobenzenes not only cleaved to form aryl radicals, bromide ions, aryl carbanions and bromine atoms but also underwent "bromine addition" to form molecular ion plus bromide ion.[5] How could "bromine addition" occur? Is it simply nucleophilic addition of a bromide ion to a neutral molecule with subsequent loss of hydride?[5] This would be a very high energy process. What is actually happening in these "bromine addition" reactions? Further GC/ECCI/MS

and DP/ECCI/MS experiments were undertaken along with computational studies to probe the mechanisms of the "bromine addition" reactions.

Experimental Methods

Chemicals

The chemicals were obtained from commercial sources. 1, 2, 3-trichlorobenzene, 1, 2-dibromobenzene, 1, 3-dibromobenzene, 1, 4-dibromobenzene, 1, 3, 5-tribromo-benzene, 1, 2, 3-tribromobenzene, and 1, 2, 4-tribromobenzene were obtained from Aldrich Chemical Co. 1, 4-Dibromobenzene, 1, 2, 4-tribromobenzene were used directly from the manufactures' bottle. 1, 2, 3-Trichlorobenzene and 1, 2, 4-tribromobenzene were crystallized one time each from ethanol. All other compounds were purified by preparative gas chromatography using a Varian 3700 Gas Chromatograph equipped with a thermal conductivity detector. The Varian 3700 gas chromatograph was equipped with a 4′ × 1/8″-10% OV-101 on chromosorb and a 4′ × 1/8″-Chromosorb W on 80/100 solid support reference column. All compounds were found to be > 99 % pure by analysis on a Varian 3300 and/or a Varian 3400 gas chromatograph equipped with flame ionization detector, and a Varian 3400 gas chromatograph interfaced with a Finnegan 4023 mass spectrometer operating in electron capture chemical ionization mode.

The mass spectrometry experiments of the polyhalogenated benzenes were conducted on a Finnegan 4023 mass spectrometer operating in electron capture chemical ionization mode. The samples were introduced by direct probe insertion or by a Varian

3400 gas chromatograph interfaced to the mass spectrometer with source temperatures of 120° C or 140°C. A sample DP/ECCI mass spectrum for each compound can be found in **Appendix A.**

Computations

Ab initio calculations[6] were carried out using the Spartan 4.0-5.0 molecular modeling and Gaussian 92/94 programs.[7,8] The AM1[9] and split valence 3-21G,[10-11] and 6-311+G(2d,p)[9,12] basis sets were employed. The electron un-correlated restricted and restricted open shell Hartree-Fock (RHF and ROHF, respectively) methods were used with the AM1 (RHF only) and 3-21G basis set. The electron correlated Becke's three-parameter hybrid functional[13] combined with the Lee, Yang, and Parr (LYP) correlation functional, denoted B3LYP,[14] was used with the 6-311+G(2d,p)[9,12] basis set. The optimized geometries from lower levels of theory were used as starting coordinates for higher-level geometry optimizations. The "/" separates the method from the basis set; and "//" separates the computational level of the energy from the level of the geometry optimization in the following example: B3LYP/D95//B3LYP/D95. Frequency calculations were executed to ensure that no imaginary frequencies were present in any of the optimized geometries, and, no imaginary frequencies were found for the optimized structures discussed *vide infra*.[9]

The split valence basis set 6-311+G(2d,p)[9,12] was incorporated to run B3LYP/ 6-311+G(2d,p)//HF/3-21G calculations. The single point energy calculations were run so that more accurate energies could be obtained for the compounds of interest. Many of the calculations did not finish successfully. The Gaussian 94 program contains a variety of different keywords and options one can incorporate in handling difficult cases (i. e. molecules with odd geometries and/or many electrons). The options and keywords

available in the Gaussian 94 program were exhaustively pursued and, still, many of the single point energy calculations did not complete. Therefore, the changes in internal energies are listed in subsequent paragraphs and schemes for those pathways that had all molecules involved in the reaction successfully finish at the B3LYP/6-311+G(2d,p)// HF/3-21G level.

Throughout this chapter, the changes in internal energy (ΔE_o) are calculated by subtracting the electronic energy plus the zero point energy of the starting materials from the electronic energy plus the zero point energy of the products at B3LYP/6-311+G(2d,p)// HF/3-21G level. At the HF/AM1//HF/AM1 level the heat of formation includes the zero point energy, thus, the changes in internal energy are calculated by subtracting the heat of formation of the products minus the heat of formation of the starting materials.[9]

Results and Discussion

GC/ECCI/MS experiments of dibromobenzenes and tribromobenzenes were repeated[5] and no "bromine addition" adducts were observed for any of the dibromobenzenes or tribromobenzenes. Since the GC/ECCI/MS experiments did not reveal any "bromine addition" ions, DP/ECCI/MS experiments were conducted. In the DP/ECCI/MS experiments "bromine addition" adducts ($[M+Br]^-$) were found for 1, 2-dibromobenzene, 1, 3-dibromobenzene, 1, 4-dibromobenzene, 1, 2, 3-tribromobenzene, 1, 2, 4-tribromobenzene, and 1, 3, 5-tribromobenzene, **Tables 4.1** and **4.2** (an example spectrum for each compound can be found in **Appendix A**). In many instances the $[M+Br]^-$ is more intense than the molecular ion of the neutral molecule ($M^{-\cdot}$). In many cases more than one "bromine addition" reaction occurred to form ions with two or three bromines

added. In particular, 1, 3, 5-tribromobenzene revealed a m/z value corresponding to the addition of three bromines with subsequent loss of three hydrogens. The theoretical isotopic pattern of this hexabromobenzene adduct was calculated using the ISOPRO[15] program and is not an exact match to the actual isotopic pattern found in the mass spectrum. The isotopic pattern may be skewed due to too high a scan rate and the presence of large number of bromine atoms. The DP/ECCI/MS experiments reveal m/z values and isotopic patterns for nucleophilic addition of bromide ions to neutral molecules of 1, 2-dibromobenzene, 1, 4-dibromobenzene, 1, 2, 4-tribromobenzene and 1, 2, 3-tribromobenzene. Computations conducted at the HF/AM1//HF/AM1 level of theory suggest that bromide addition to the dibromobenzenes and tribromobenzenes is an exothermic process. The changes in internal energy, ΔE_o, at the HF/AM1//HF/AM1 level are -14.3, -14.9 (*-10.6* at the *B3LYP/6-311+G(2d,p)//HF/3-21G* level), -22.2, and -19.8 kcal/mol for bromide ion addition to carbon number two of 1, 4-dibromobenzene, carbon number four of 1, 2-dibromobenzene, carbon number five of 1, 2, 4-tribromobenzene, and carbon number five of 1, 2, 3-tribromobenzene respectively, *pathways A*, *B*, *C* and *D*, **Schemes 4.1** and **4.2**. Computations on 1, 2, 4-tribromobenzene capturing chloride ion were not conducted but the reaction is assumed to be an exothermic process since the above examples do release energy. The ions for bromide addition to 1, 3-dibromobenzene and 1, 3, 5-tribromobenzene are not present in the DP/ECCI mass spectrum even though the ΔE_o values at the HF/AM1//HF/AM1 level are exothermic for bromide ion addition to carbon number four of 1, 3-dibromobenzene and carbon number two of 1, 3, 5-tribromobenzene (-12.7 and -24.2 kcal/mol, respectively). The 1, 3-dibromobenzene and 1, 3, 5-tribromobenzene mass spectra do contain m/z values and isotopic patterns that correspond to a neutral molecule

Table 4.1: **Mass/charge (m/z) values and relative ion intensities observed in spectra of DP/ECCI/MS experiments of 1, 2-dibromobenzene, 1, 3-dibromobenzene and 1, 4-dibromobenzene.**

		1, 2-Dibromobenzene
Run		**Relative Ion Intensities**
1		$Br^- > (M+Br)^- > (M-Br)^- > (M-H)^-$
2		$Br^- > (M-H)^- > (M-Br)^-$
3*		$Br^- > (M+Br)^- > (M-H)^- \approx M^{-\cdot} \approx (M-Br)^- \approx (M+2Br-2H)^-$ trace
4		$Br^- > (M+Br)^- > (M-H)^-$
5		$Br^- > (M-H)^-$
		1, 3-Dibromobenzene
Run		**Relative Ion Intensities**
1*		$Br^- > (M+2Br-2H)^- > (M+Br-2H)^- > (M-H)^-$
2		$Br^- > (M-H)^-$
3		$Br^- > (M-H)^-$
		1, 4-Dibromobenzene
Run		**Relative Ion Intensities**
1*	Beginning*	$Br^- > (M+Br)^- > (M-H)^-$
	End	$Br^- > (M+Br)^- > (M-H)^- > (M+2Br-2H)^-$
2		$Br^- > (M+Br)^- > (M-H)^-$
3		$Br^- > (M-H)^-$

*Spectra can be found in **Appendix A.**

Table 4.2: **Mass/charge (m/z) values and relative ion intensities observed in spectra of DP/ECCI/MS experiments of 1, 2, 4-tribromobenzene, 1, 2, 3-tribromobenzene and 1, 3, 5-tribromobenzene.**

		1, 2, 4-Tribromobenzene
Run		**Relative Ion Intensities†**
1*		$Br^- > M^{-\cdot} > (M+Br)^- > (M+Br-H)^{-\cdot}$
2		$Br^- > (M+Br)^- > M^{-\cdot} > (M+Br-H)^{-\cdot}$
3		$Br^- > (M+Br)^- > M^{-\cdot} > (M+Br-H)^{-\cdot} > (M-Br+2H)^-$ (trace)
		1, 2, 3-Tribromobenzene
Run		**Relative Ion Intensities†**
1	Beginning	$Br^- > (M+Br)^- > M^{-\cdot}$
	End	$Br^- > (M+Br)^- > M^{-\cdot} > (M-Br+H)^{-\cdot}$
2*	Beginning *	$Br^- > (M+Br)^- > M^{-\cdot}$
	End	$Br^- > (M+Br)^- > M^{-\cdot} > (M-2Br+H)^{-\cdot}$
		1, 3, 5-Tribromobenzene
Run		**Relative Ion Intensities**
1*	Beginning	$Br^- > M^{-\cdot} > (M+3Br-3H)^{-\cdot}$
	End*	$Br^- > M+3Br-3H)^{-\cdot} > M^{-\cdot} > ((M+2Br-3H)^-$
2	Beginning	$Br^- > M^{-\cdot} > (M+3Br-3H)^{-\cdot}$ (trace)
	End	$Br^- > (M+3Br-3H)^{-\cdot} > M^{-\cdot} > (M+2Br-3H)^- > (M-2Br+2H)^{-\cdot}$
3	Beginning	$Br^- > M^{-\cdot} > (M+3Br-3H)^{-\cdot}$ (trace)
	End	$Br^- > (M+3Br-3H)^{-\cdot} > M^{-\cdot} > (M+2Br-3H)^- > (M-Br+H)^{-\cdot} \approx (M-2Br+2H)^{-\cdot}$ (trace)

†Mass range was not set high enough to observe $(M + 2Br)^-$ and so forth. *Spectra can be found in **Appendix A.**

plus bromide ion(s) minus hydrogen(s). Are these ions coming about from loss of hydride ion with subsequent electron capture? The ΔE_o values at the HF/AM1//HF/AM1 level are 126.7 (*120* at the *B3LYP/6-311+G(2d,p)//HF/3-21G* level) and 136.6 kcal/mol for the loss of hydride from carbon number six of 3, 4, 6-tribromo-2, 4-cyclohexadienyl carbanion and carbon number six of 1, 3, 5, 6-tetrabromo-2, 4-cyclohexadienyl carbanion, *pathways E and F*, **Scheme 4.1**. Thus, the hydride loss reaction is unlikely to occur in the DP/ECCI/MS experiments.

In a previous GC/ECCI/MS experiment methylene bromide was added to the ionization chamber to increase the concentration of bromide ion. No increase of ions due to "bromine addition" reactions was observed.[5] This is surprising because methylene bromide should be a ready source of bromide ion. It was postulated that the addition of methylene bromide may not have resulted in "bromine addition" because the electron energy may have increased resulting in more fragmentation of parent and product ions.[5] Even though the isotopic patterns and m/z values provide evidence for nucleophilic addition of bromide ion to 1, 2-dibromobenzene; 1, 4-dibromobenzene; 1, 2, 4-tribromobenzene; and 1, 2, 3-tribromobenzene, the nucleophilic addition mechanism alone does not explain the addition of two and three bromines to 1, 2-dibromobenzene; 1, 3-dibromobenzene; 1, 4-dibromobenzene; and 1, 3, 5-tribromobenzene. Furthermore, the nucleophilic addition mechanism does not explain the formation of ions from the addition or loss of hydrogen(s) from the dibromobenzenes and tribromobenzenes. Therefore, further inquiry is needed to understand the mechanisms involved in the DP/ECCI/MS experiments.

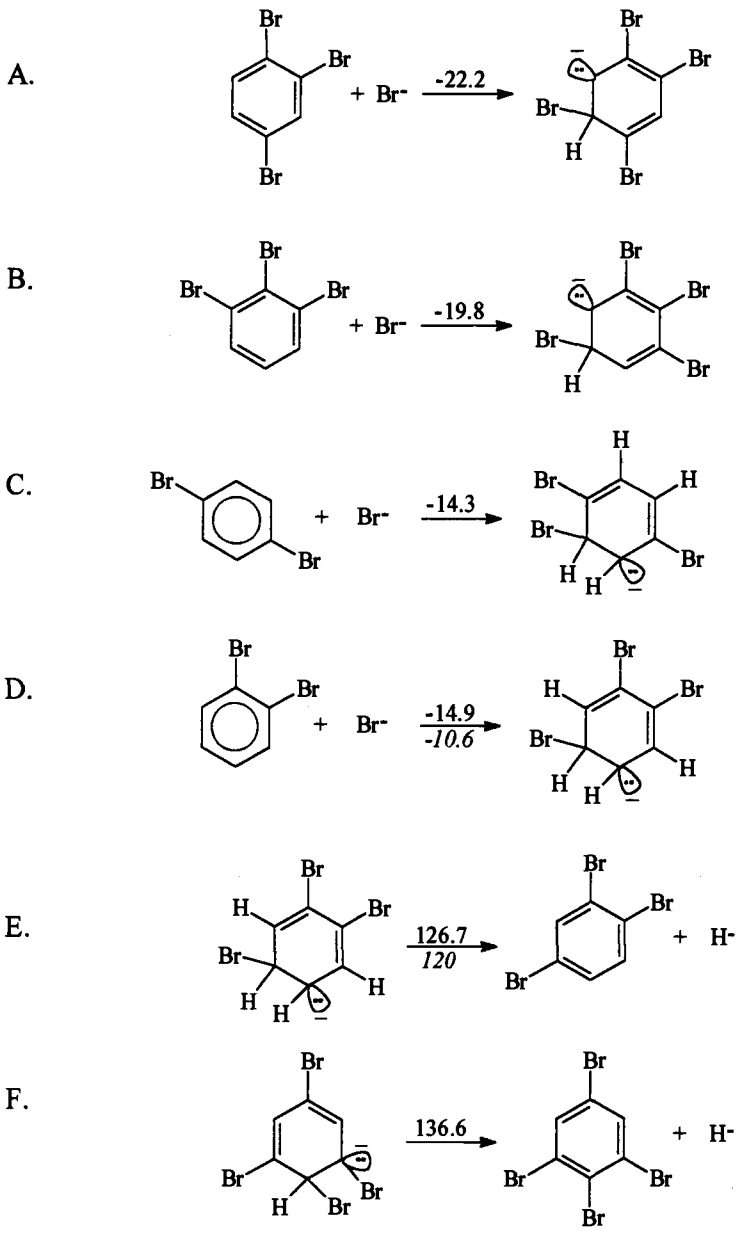

Scheme 4.1: **HF/AM1//HF/AM1 level changes in internal energy in kcal/mol of the addition of bromide ion to A) 1, 4-dibromobenzene, B) 1, 2-dibromobenzene (and at the *B3LYP/6-311+G(2d,p)//HF/3-21G* level), C) 1, 2, 4-tribromobenzene, and D) 1, 2, 3-tribromobenzene. The changes in internal energy for hydride loss from bromine addition adducts to form E) 1, 2, 4-tribromobenzene at the HF/AM1//HF/AM1 and *B3LYP/6-311+G(2d,p)//HF/3-21G* levels, and F) 1, 2, 3, 5-tetrabromobenzene at the HF/AM1//HF/AM1 level.**

Could polybrominated benzene impurities be present in small amounts and be responsible for the ions formed from the apparent addition of one to three bromines? The dibromobenzenes and tribromobenzenes were found to be > 99% pure by GC and GC/ECCI/MS. To ensure small amounts of impurities were not responsible for the ions with the addition of two and three bromines, DP/ECCI/MS experiments were conducted mixing 1, 2, 3-trichlorobenzene and 1, 2, 3-tribromobenzene. Resonance electron capture resulting in the formation of the molecular ion was found for 1, 2, 3-trichlorobenzene and 1, 2, 3-tribromobenzene. Dissociative electron capture process where cleavage to form chloride or bromide ions occurs are also present in the spectra, **Table 4.3** (see **Appendix A** for an example spectrum). In addition, cross "bromine addition" and "chlorine addition" occurred resulting in the observation of ions from addition of one chlorine and/or one bromine with loss of hydrogen(s) in many cases. Ions from the addition of two to three bromines minus two to three hydrogens are present in the second and third runs of the DP/ECCI/MS experiments and are not very intense, **Table 4.3**. Since the "bromine and/or chlorine addition" ions seem to be a "real" occurrence, some questions need to be answered. What might be happening mechanistically in the ionization chamber? How could more than one halogen become attached to the parent molecules? Computational experiments were undertaken to investigate mechanisms that may explain the observation of ions resulting from "halogen addition" reactions in the DP/ECCI/MS experiments.

Initially, a literature search was conducted to see if other researchers had observed 'halogen addition" in ECCI/MS experiments. Nucleophilic addition has been observed in ECCI/MS experiments,[1,3] although, nucleophilic addition alone does not explain how more than one halogen is added to the aromatic ring because once a halogen is attached, the halogenated aryl carbanion could only lose hydride ion (which is a high energy process at

the HF/AM1//HF/AM1 level, **Scheme 4.1**) or revert back to the starting material. No references for addition of more than one halogen to the aromatic ring were found for ECCI/MS experiments. Bunnett and co-workers did observe "bromine addition" in solution along with dehalogenation, and a "halogen dance" where the parent halogenated benzene isomerized. These researchers observed addition of only one bromine or chlorine to an aromatic system, however, the mechanisms that they proposed may explain how more than one halide could be added to an aromatic ring in the DP/ECCI/MS experiments.[16]

Bunnett and co-workers discovered in a reaction of 1, 2, 4-tribromobenzene with potassium anilide in ammonia (or with potassium *tert*-butoxide in hexamethlyphosphoric triamide) that bromine addition occurred to form 1, 2, 4, 5-tetrabromobenzene and 1, 2, 3, 5-tetrabromobenzene. The researchers also observed 1, 3, 5-tribromobenzene and 1, 4-dibromobenzene in the reactions of 1, 2, 4-tribromobenzene. No "chlorine addition" or "halogen dance" products were found when trichlorobenzenes were allowed to react with a strong base. Only, *t*-butoxy polychlorophenyl ethers and polychlorophenols were present. 1, 2, 3, 5-Tetrachlorobenzene and 1, 2, 4, 5-tetrachlorobenzene both underwent halogen addition to form pentachlorobenzene in similar conditions discussed above.[8] Bunnett and co-workers considered many different mechanisms to explain the "halogen dance" and the "halogen addition" products that were observed in these reactions. A radical mechanism was ruled out as all tests for radicals were negative. An "aryne" mechanism was also postulated because "arynes" are known to form in strongly basic conditions. This mechanism was ruled out because when reactions were loaded with a halide salt (which should allow for the incorporation of a foreign halide), the reaction products were not changed.[17] Aryl carbanions would be more likely to abstract a hydrogen from the solvent than lose a halide ion to form an aryne. A 1, 2-halogen shift was ruled out

Table 4.3: **Mass/charge (m/z) values and relative ion intensities observed in the spectra from DP/ECCI/MS experiments of a mixture of 1, 2, 3-trichlorobenzene (M) and 1, 2, 3-tribromobenzene (*m*) mixture.**

Run #	m/z Observed in the Beginning of the TIC Peak
#1	$Br^- > Cl^- > (M+Cl)^- > (M+Br-2H)^- > m^{-\cdot} > (m+Cl)^- > (m+Br)^- > (M-H)^-$
#2*	$Br^- > Cl^- > (M+Br-2H)^- > (M+Cl)^- > (m+Br)^- > (m+Cl)^- > m^{-\cdot} > (M-H)^-$
#3	$Br^- > Cl^- > (M+Br-2H)^- > (m+Br)^- > m^{-\cdot} > (m+Cl)^- > (M+Cl)^- > (M-H)^-$ trace
	m/z Observed in the Middle of the TIC Peak
#1	$Br^- > (m+Br)^- > m^{-\cdot} > Cl^- > (M+Br-2H)^- > (M+Cl)^- > (m+Cl)^- > (m-Br)^-$ trace
#2	$Br^- > Cl^- > (m+Br)^- > (M+Br-2H)^- > (M+Cl)^- > m^{-\cdot} > (m+Cl)^- > (M-H)^- \approx (m-Br)^-$ trace
#3	$Br^- > Cl^- > (M+Cl)^- > (M+Br-2H)^-)^- > (m+Cl)^- > (m+Br)^- > m^{-\cdot} > (M-H)^- \approx (m-Br)^-$ trace
	m/z Observed in the End of the TIC Peak
#1	$Br^- > m^{-\cdot} > (m+Br)^- > (m-Br)^-$ trace
#2	$Br^- > (m+Br)^- > m^{-\cdot} > Cl^- > (M+Br-2H)^- > (m+Cl)^- \approx (m-Br)^-$ trace
#3	$Br^- > Cl^- > m^{-\cdot} > (m+Br)^- > (M+Cl)^- > (M+Br-2H)^- > (m-Br)^- \approx (m+3Br-3H)^- \approx (m+Cl)^- \approx (m+2Br-3H)^-$ trace

*Spectra can be found in **Appendix A.**

because 1, 3, 5-tribromobenzene did not revert back to 1, 2, 4-tribromobenzene except if a small amount of a tetrabromobenzene was present. Plus, it was found that 1, 2, 3-tribromobenzene readily underwent a "halogen dance" to 1, 3, 5-tribromobenzene if tetrabromobenzenes were formed during the reaction. Bunnett and co-workers did discover that when deuterated 1, 2, 4-tribromobenzene was allowed to react with potassium anilide in ammonia, all the deuteriums were replaced with hydrogens. It was proposed that aryl carbanions were produced and reprotonated repeatedly. The mechanisms mentioned thus far do not explain disproportionation and "halide addition" reactions. Therefore, Bunnett and co-workers proposed a "positive halogen transfer" mechanism because a) it explained disproportionation and "halogen addition" and b) it explained why tetrabromobenzenes had to be present for 1, 2, 4-tribromobenzene and 1, 2, 3-tribromobenzene to undergo a "halogen dance."[18]

Bunnett and coworkers proposed "6-halogen" (*2n halogen*) mechanisms and "7-halogen" (*2n + 1 halogen*) mechanisms for "positive halogen transfer" and "halogen dance" reactions. It was found that halogens and hydrogens that are ortho to two other halogens were transferred preferentially in these "halogen transfer" reactions over halogens that are ortho to one other halogen or ortho to no halogens because these ortho halogens and hydrogens were found to be more "electrophilic." In the "6-halogen" mechanism a dibromophenyl anion would attack a neutral tetrabromobenzene and pull off a positive halogen leaving a tribromophenyl anion and a neutral tribromobenzene, *pathway A*, **Scheme 4.2**. In the "7-halogen" mechanism a tribromophenyl anion attacks a neutral tetrabromobenzene to abstract a positive halogen leaving a tribromophenyl anion and a neutral tetrabromobenzene, *pathway B*, **Scheme 4.2**. Bunnett and co-workers realized that

the "7-halogen" mechanism was much more plausible than the "6-halogen" mechanism because the tribromobenzenes did not undergo positive halogen transfers unless a tetrabromobenzene was present.[18]

Could the "positive halogen transfer" reactions be occurring in the DP/ECCI/MS experiments? Or could an aryne species be formed with subsequent halogen addition? The aryne mechanism is highly unlikely because when methylene bromide was added to the source no increase in ions due to "bromine addition" were observed in previous experiments conducted by Couch and Freeman.[5] Computations at the HF/AM1//HF/AM1 level reveal that the formation of 4-bromobenzyne from 1, 4-dibromobenzene and 2, 5-dibromophenyl anion is a high energy process with the ΔE_o value = 77.3 kcal/mol, *pathway C*, **Scheme 4.2**. No other computations on other polybrominated benzenes were conducted since endothermicity for this example is so great.

The DP/ECCI/MS experiments of the 1, 2, 3-trichlorobenzene and 1, 2, 3-tribromobenzene mixture revealed that "bromine addition" and "chlorine addition" reactions took place forming ions with one or more halogens attached to the starting materials and in some instances hydrogen loss took place, **Table 4.3**. The m/z value for the addition of bromide ion to 1, 2, 3-trichlorobenzene corresponds to 1, 2, 3-trichlorobenzene plus bromide ion minus two hydrogens, whereas, the m/z value and isotopic patterns of bromide ion addition or chloride ion addition to 1, 2, 3-tribromobenzene, and the chloride addition to 1, 2, 3-trichlorobenzene corresponds to the respective trihalogenated benzene with no loss of hydrogen. We are unsure why this is the case, where one halogenated benzene loses hydrogen and others do not. The m/z value for the molecular ion for 1, 2, 3-trichlorobenzene seems to be one mass unit less resulting in 1, 2, 3-trichlorobenzene minus hydrogen. Dissociative electron capture processes are also observed where cleavage

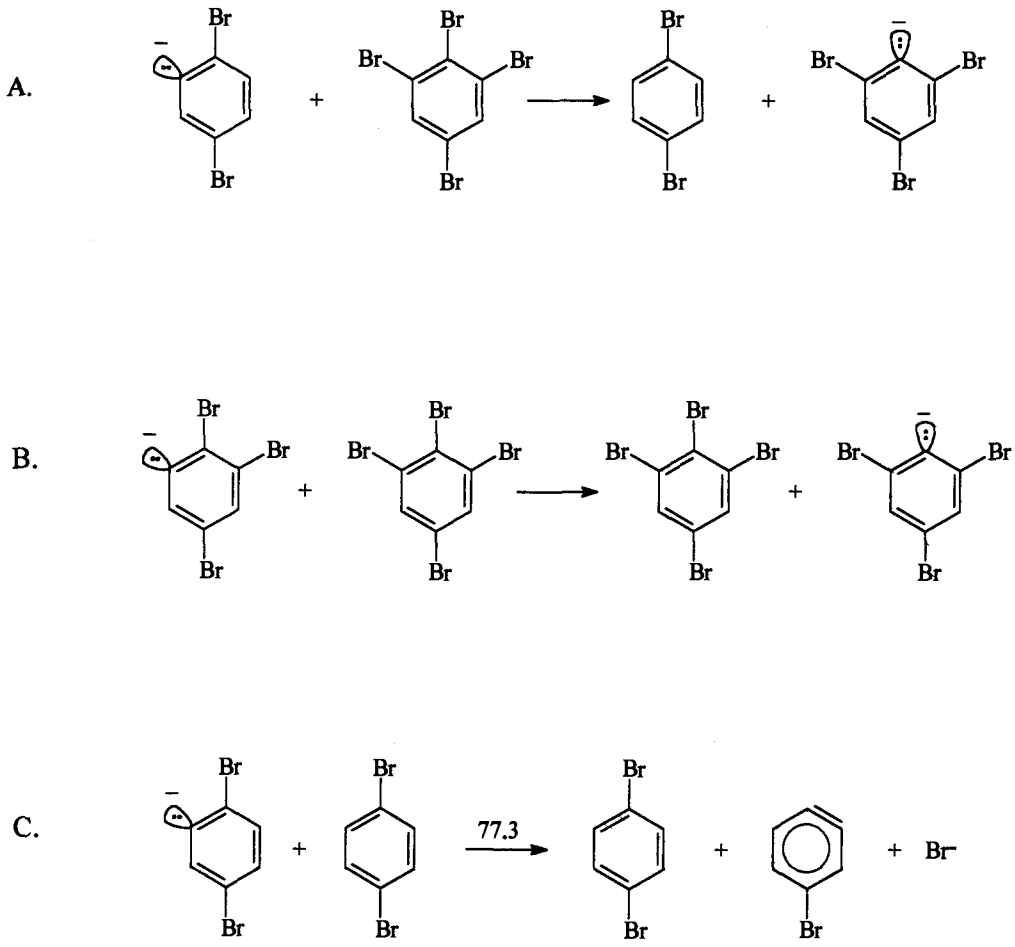

Scheme 4.2: **A) "6-Halogen" mechanism proposed by Bunnett and co-workers and B) "7-halogen" mechanism proposed by Bunnett and co-workers.[10] C) The change in internal energy in kcal/mol at the HF/AM1// HF/AM1 level for formation of 4-bromobenzyne.**

occurs with the charge residing on either fragment. Both chloride and bromide ions are seen in the spectra. Plus, small amounts of 1, 2, 3-tribromobenzene minus bromine are seen. In the very last experiment at the end of the TIC (total ion chromatogram) ions are present for 1, 2, 3-tribromobenzene plus two bromines minus three hydrogens, and 1, 2, 3-tribromobenzene plus three bromines minus three hydrogens. Some of the ions in these DP/ECCI/MS experiments are typical reactions that have been found to occur in ECCI/MS experiments such as those presented in **equations 4.1**, **4.2** and **4.3**. Certain ions that are formed can not be explained by these common reactions. Therefore, the unusual adducts observed in the DP/ECCI/MS experiments may possibly be explained by the mechanisms proposed by Bunnett and co- workers.[16-18]

Computational experiments were conducted on "positive halogen" and hydrogen abstraction pathways for the compounds studied in the DP/ECCI/MS experiments. "Positive halogen transfer" may explain the "halogen addition" in the ECCI/MS experiments. If this mechanism is applicable, aryl carbanions need to be formed to start the "chain" mechanism. It has been found from the Hammond Plot from previous GC/ECCI/MS experiments that the polybrominated benzenes prefer to cleave to form aryl radical and the halide ion. The ΔE_o values at the HF/AM1//HF/AM1 show that the lower energy pathway for cleavage of the dibromobenzene and tribromobenzene radical anions is fragmentation to form aryl radical and halide ion (except for 1, 4-dibromobenzene). The energy differences between the ΔE_o values for the three tribromobenzene isomer radical anion cleavage pathways for bromine fission are 13.3 and *35.2* kcal/mol for 1, 3, 5-tribromobenzene, 11.5 and *25.4* kcal/mol, 13.6 and *31.9* kcal/mol for 1, 2, 3-tribromobenzene, 14.6 and *39.8* kcal/mol and 12.4 kcal/mol for 1, 2, 4-tribromobenzene, 20.7 and *40.2* kcal/mol for 1, 2-dibromobenzene, 21.9 and *46.6* kcal/mol for 1, 3-dibromo-

benzene, and -29.7 and *41.7* kcal/mol for 1, 4-dibromobenzene at the HF/AM1//HF/AM1 and *B3LYP/6-311+G(2d,p)//HF/3-21G* levels, respectively, **Schemes 4.3**, **4.4**, and **4.5**. The computations overestimate the energy differences between the formation of the halide ion and the halogen radical because polybrominated aryl carbanions are observed in these DP/ECCI mass spectra. The lower energy pathway for 1, 4-dibromobenzene is to cleave to form bromine atom, which is the exact opposite of what is found in the ECCI/MS experiments at the HF/AM1//HF/AM1 level, although the B3LYP/6-311+G(2d,p)//HF/3-21G level calculations result in ΔE_o values that mirror experimental results. The B3LYP/6-311+G(2d,p)//HF/3-21G does a better job of modeling this radical anion cleavage pathway because it takes into account electron correlation. Overall, the computations show that the radical anion cleavage pathways for tribromobenzenes and dibromobenzenes favor the formation of bromide ion, which is one of the possible initiation steps for the "chain" mechanism, **Schemes 4.3**, **4.4**, and **4.5**.

Computations at the HF/AM1//HF/AM1 level were continued to elucidate other mechanisms that may be involved in the formation of aryl carbanions. An aryl carbanion may be formed directly from the cleavage of the radical anion or a bromide ion may be formed (discussed above). The bromide ion may abstract a hydrogen from 1, 2, 3-tribromobenzene or 1, 3, 5-tribromobenzene to form hydrogen bromide plus 3, 4, 5-tribromophenyl or 2, 4, 6-tribromophenyl carbanion, *pathways A* and *B*, **Scheme 4.6**. A bromide or chloride ion may abstract hydrogen from a neutral molecule of 1, 2, 3-trichlorobenzene to form hydrogen chloride and 3, 4, 5-trichlorophenyl anion, *pathways C* and *D*, **Scheme 4.6**. The ΔE_o values for the hydrogen abstraction are 22.1 and *53.6*, 18.5 and *42.3*, 24.5 and 10.4, respectively, at the HF/AM1//HF/AM1 *and B3LYP/6-311+G(2d,p)//HF/3-21G* levels. Another example of carbanion formation is the formation of 3, 4, 5-trichlorophenyl

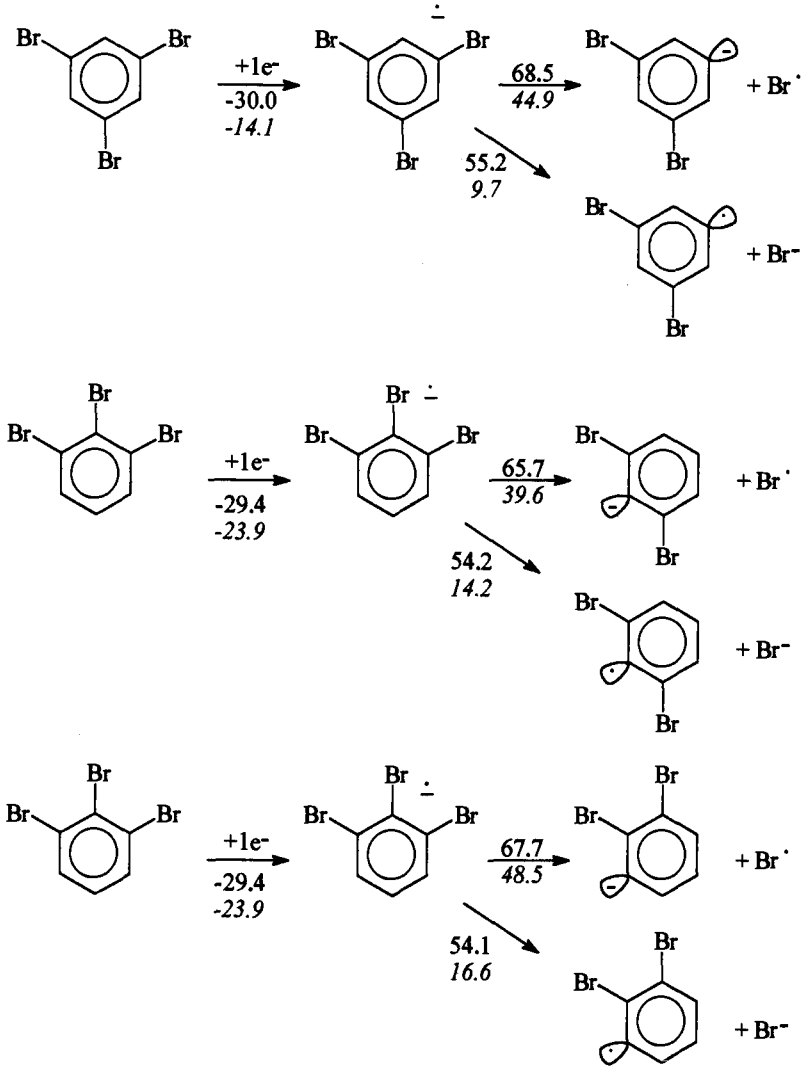

Scheme 4.3: **The changes in internal energy in kcal/mol at the HF/AM1//HF/AM1 and *B3LYP/6-311+G(2d,p)//HF/3-21G* levels for the 1, 3, 5-tribromobenzene and 1, 2, 3-tribromobenzene radical anion cleavage pathways.**

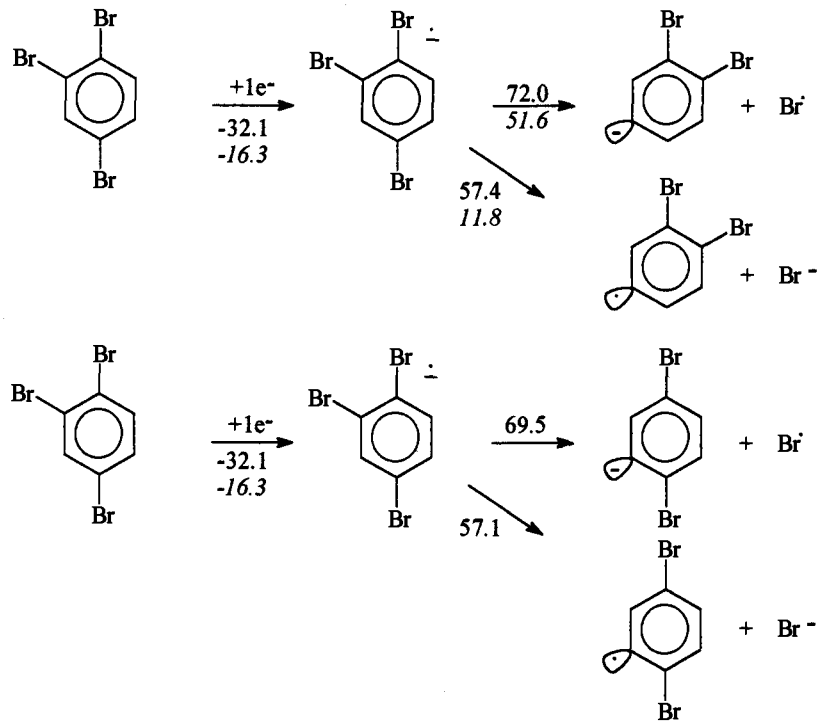

Scheme 4.4: **The changes in internal energy in kcal/mol at the HF/AM1//HF/AM1 and *B3LYP/6-311+G(2d,p)//HF/3-21G* levels for 1, 2, 4-tribromo-benzene radical anion cleavage pathways.**

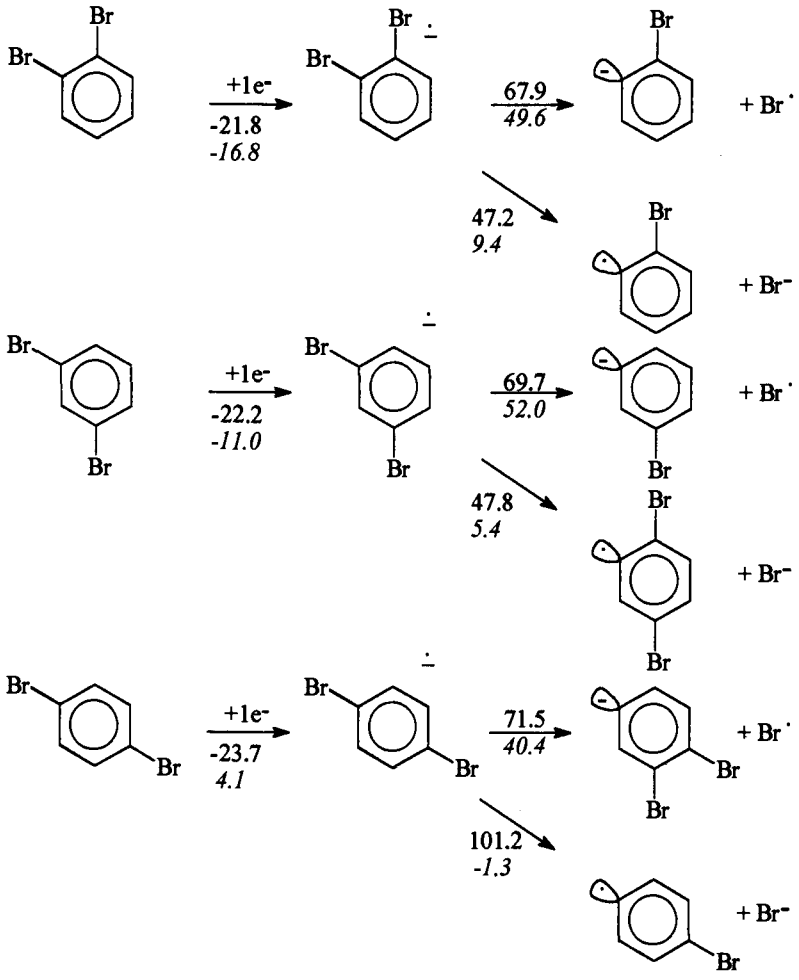

Scheme 4.5: **The changes in internal energy in kcal/mol at the HF/AM1//HF/AM1 and *B3LYP/6-311+G(2d,p)//HF/3-21G* levels for the 1, 2-dibromobenzene, 1, 3-dibromobenzene and 1, 4-dibromobenzene radical anion cleavage pathways.**

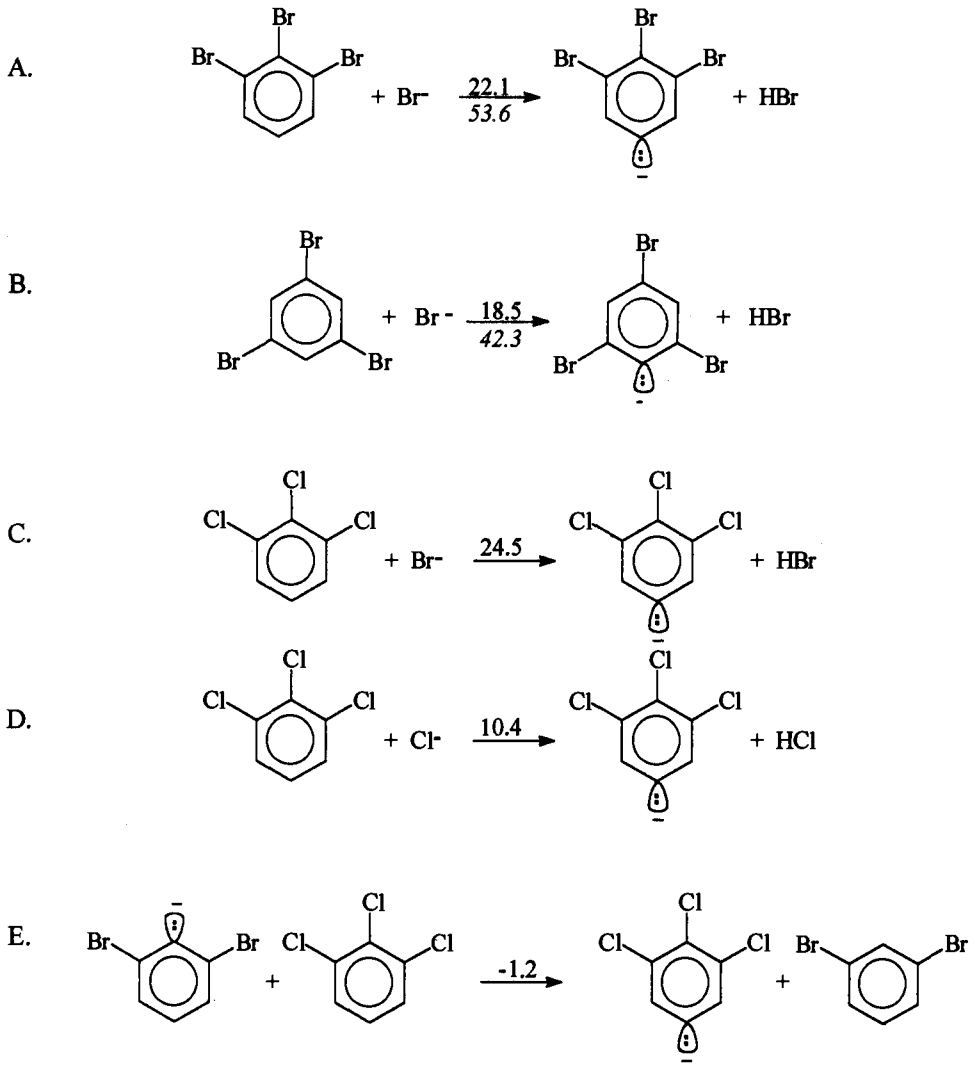

Scheme 4.6: **The changes in internal energy in kcal/mol at the HF/AM1//HF/AM1 and *B3LYP/6-311+G(2d,p)//HF/3-21G* levels for A, B, and C) hydrogen abstraction by bromide ion, D) hydrogen abstraction by chloride ion, and E) 2, 6-dibromophenyl anion abstracting hydrogen from 1, 2, 3-trichlorobenzene.**

anion, which may come about from abstraction of hydrogen from 1, 2, 3-trichlorobenzene by 2, 6-dibromophenyl anion. This reaction is favorable with ΔE_o value = -1.2 kcal/mol at the HF/AM1//HF/AM1 level, *pathway E*, **Scheme 4.6**. In the ECCI/MS experiments, this latter process is more than likely taking place since it is a more energetically favorable process than former pathways.

Computations were performed on "positive halogen" mechanisms for both the mixture of 1, 2, 3-trichlorobenzene and 1, 2, 3-tribromobenzene, and the polybrominated benzenes themselves. We do not know which hydrogens, bromines or chlorines are transferred, therefore, for the purpose of the following discussion, one example pathway has been chosen for each of the dibromobenzenes, tribromobenzenes and 1, 2, 3-trichlorobenzene. In general, it has been found that once the initial aryl carbanion is formed, the subsequent steps to form halide addition adducts are favorable. That is, the hydrogen abstraction steps are exothermic and the "positive halogen transfer" steps are endothermic. We will begin our discussion by looking at the mechanism that may be involved in the formation of 2, 3, 4-trichloro-6-bromophenyl anion in the DP/ECCI/MS experiments of the mixture of 1, 2, 3-trichlorobenzene and 1, 2, 3-tribromobenzene. The HF/AM1//HF/AM1 calculations reveal that the reaction of 3, 4, 5-trichlorophenyl anion with 1, 2, 3-tribromobenzene to form 1, 2, 3-trichloro-5-bromobenzene and 2, 6-dibromophenyl ion is slightly endothermic (ΔE_o value = 1.1 kcal/mol). Subsequently, 1, 2, 3-trichloro-5-bromobenzene may react with 2, 6-dibromophenyl ion to form 1, 3-dibromobenzene and 2, 3, 4-trichloro-6-bromophenyl anion, **Scheme 4.7**. The ΔE_o value is equal to –9.6 and *-13.7* kcal/mol at the HF/AM1//HF/AM1 and *B3LYP/6-311+G(2d,p)//HF/3-21G* levels.

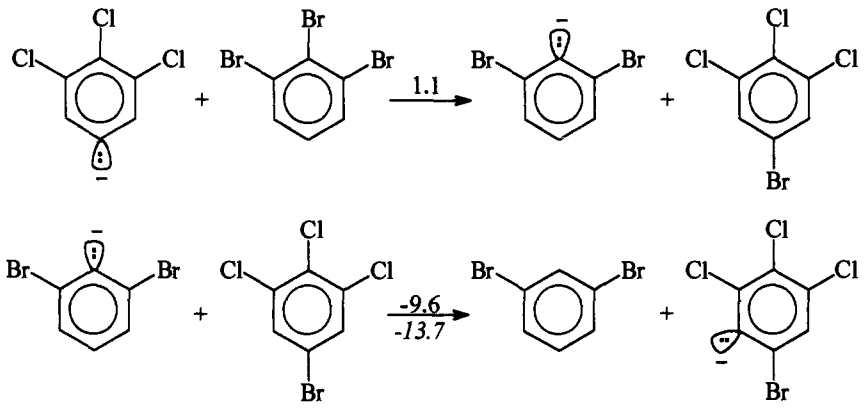

Scheme 4.7: **The changes in internal energy in kcal/mol at the HF/AM1//HF/AM1 and *B3LYP/6-311+G(2d,p)//HF/3-21G* levels 3, 4, 5-trichlorophenyl anion abstracting a "positive bromine" from 1, 2, 3-trichlorobenzene followed by deprotonation.**

Continuing, 1, 2, 3-tribromobenzene underwent a series of "halogen addition" and proton transfer reactions to ultimately form the hexabromobenzene radical anion in the DP/ECCI/MS experiments of the mixture of 1, 2, 3-trichlorobenzene and 1, 2, 3-tribromobenzene. Once 3, 4, 5-tribromophenyl anion is formed by abstraction of hydrogen by bromide ion (ΔE_o value = 22.1 and *53.6* kcal/mol at the HF/AM1//HF/AM1 and *B3LYP/6-311+G(2d,p)//HF/3-21G* levels), **Scheme 4.6**, and/or the 2, 6-dibromophenyl anion taking hydrogen from 1, 2, 3-tribromobenzene (ΔE_o value = -3.4 kcal/mol at the HF/AM1//HF/AM1 level), step #2, **Scheme 4.8**, it can attack 1, 2, 3-tribromobenzene abstracting a "positive bromine", step #3, **Scheme 4.8**. Step #3 of **Scheme 4.8** has an ΔE_o value = 3.6 kcal/mol at the HF/AM1//HF/AM1 level. 1, 2, 3, 5-Tetrabromobenzene may continue the chain mechanism and participate in step #4 where 2, 6-dibromophenyl anion may abstract hydrogen to form 1, 3-dibromobenzene and 2, 3, 4, 6-tetrabromophenyl anion, **Scheme 4.8**. Step #4 has an ΔE_o value = -12.4 kcal/mol at the HF/AM1//HF/AM1 level. Step #5 of **Scheme 4.8** involves capture of positive bromine from 1, 2, 3-tribromobenzene by 2, 3, 4, 6-tetrabromophenyl anion and is an endothermic process with a ΔE_o value = 13.0 and *13.7* kcal/mol at the HF/AM1//HF/AM1 and *B3LYP/6-311+G(2d,p)// HF/3-21G* levels. 2, 6-Dibromophenyl anion may abstract hydrogen from pentabromobenzene resulting in 1, 3-dibromobenzene and pentabromophenyl anion, which is observed in the mass spectrum, step #6, **Scheme 4.8**. Step #6 has a ΔE_o value = -17.3 and *-16.5* kcal/mol mol at the HF/AM1//HF/AM1 and *B3LYP/6-311+G(2d,p)//HF/3-21G*

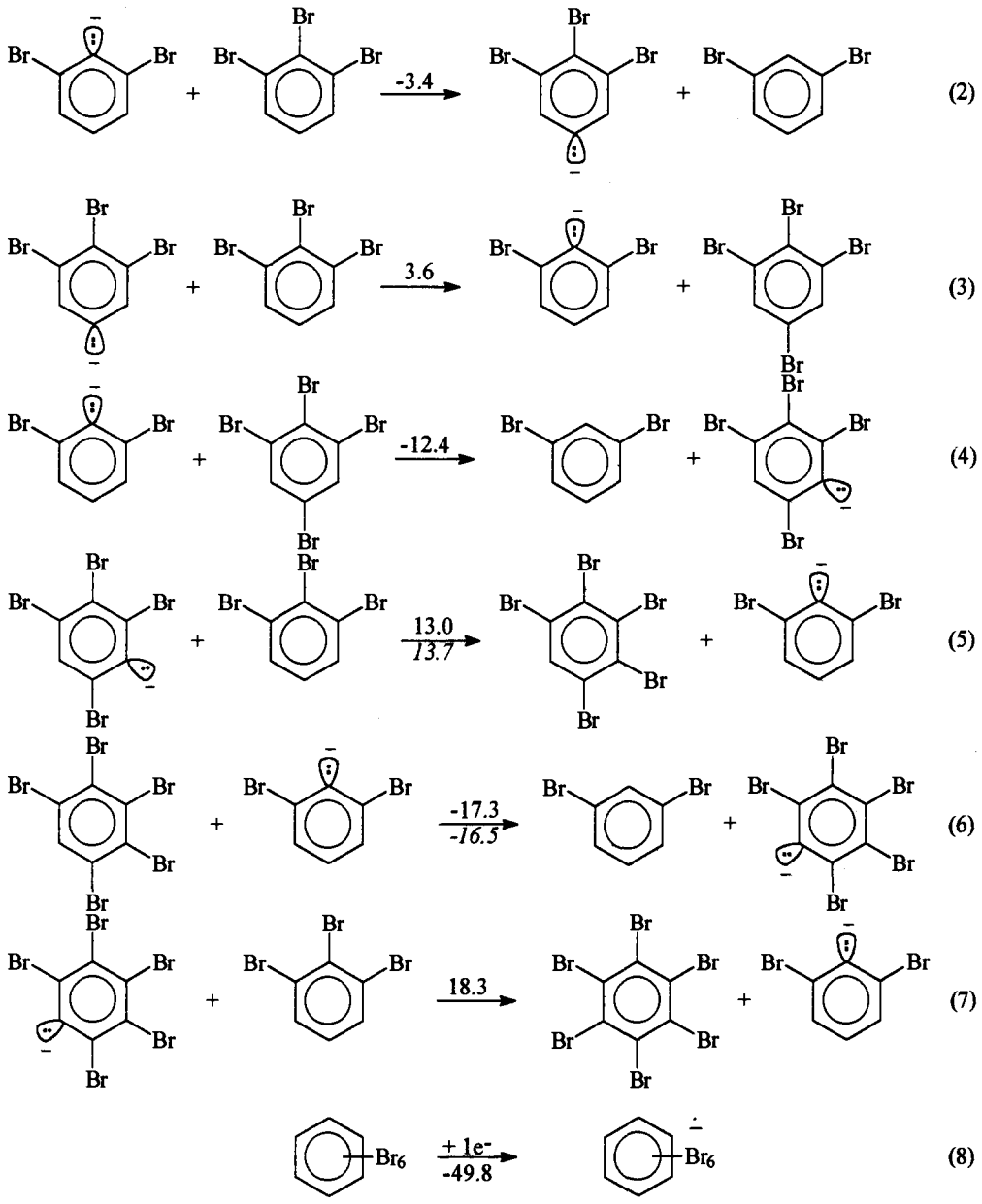

Scheme 4.8: **The changes in internal energy in kcal/mol at the HF/AM1//HF/AM1 and *B3LYP/6-311+G(2d,p)//HF/3-21G* levels for the formation of 1, 3-dibromobenzene and bromine addition adducts of 1, 2, 3-tribromobenzene.**

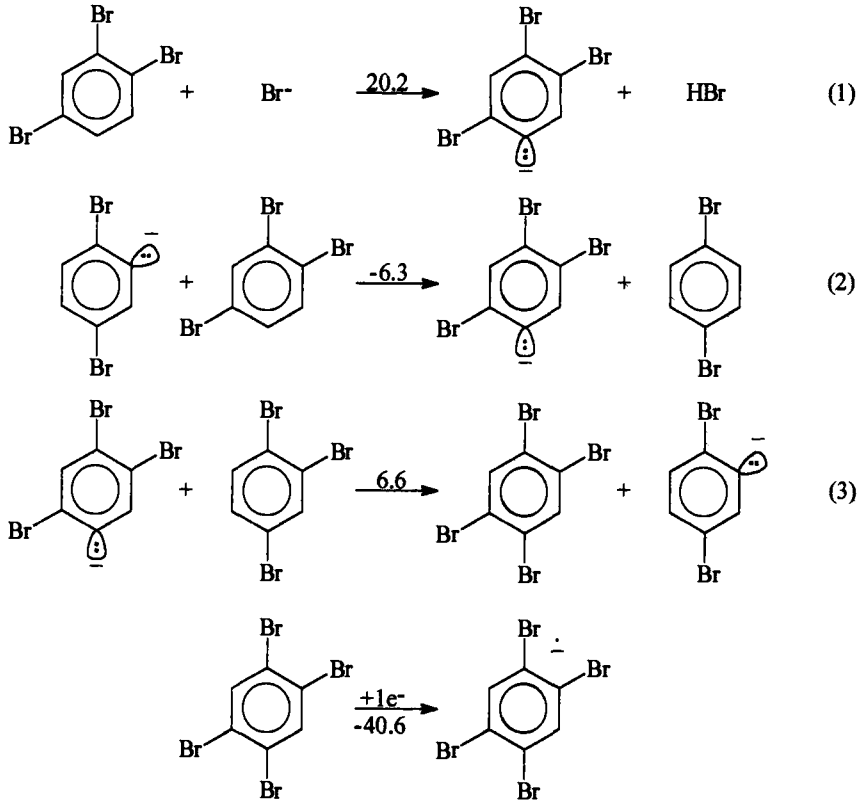

Scheme 4.9: **The changes in internal energy in kcal/mol at the HF/AM1//HF/AM1 level for the formation of bromine addition adducts of 1, 2, 4-tri-bromobenzene.**

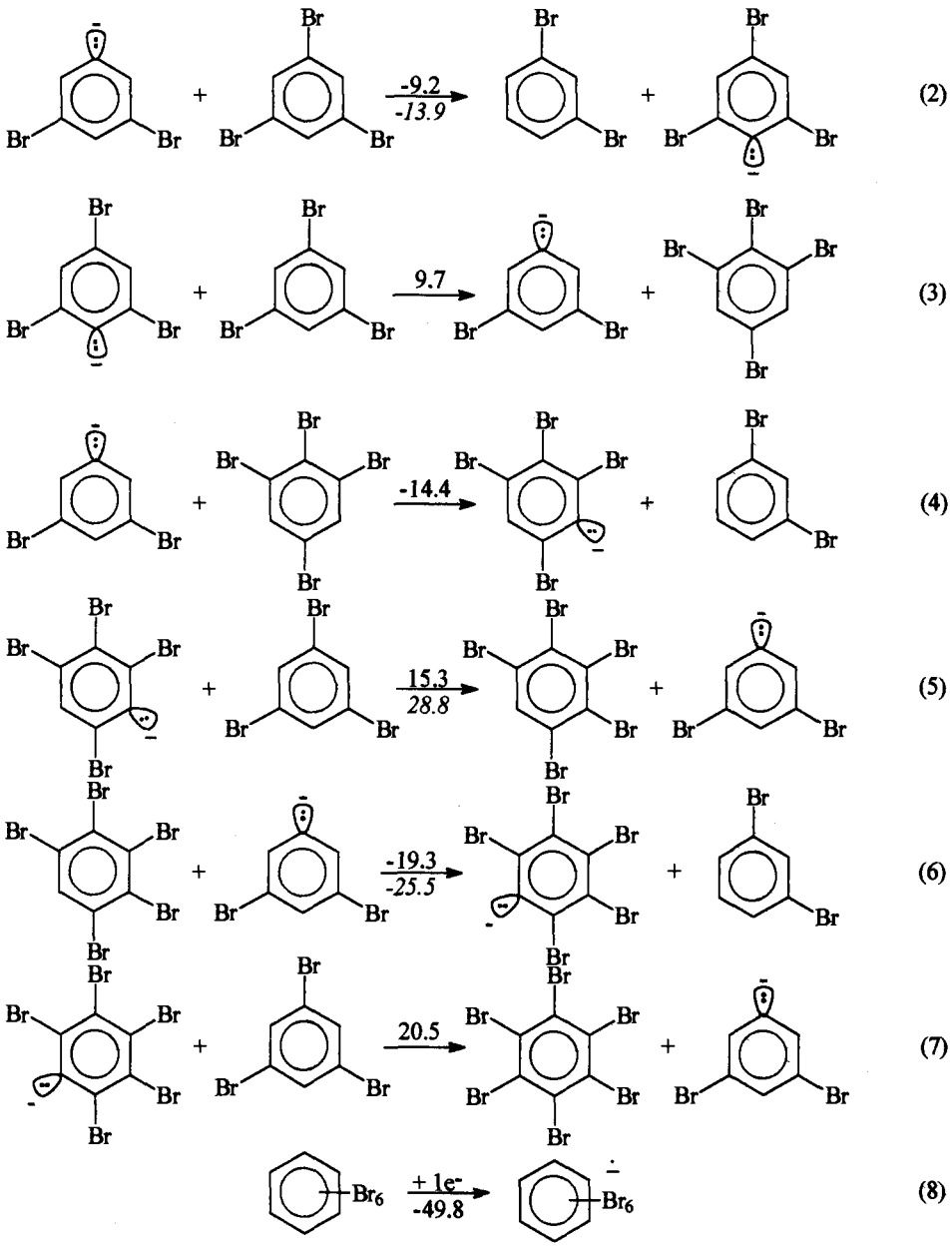

Scheme 4.10: The changes in internal energy in kcal/mol at the HF/AM1//HF/AM1 and *B3LYP/6-311+G(2d,p)//HF/3-21G* levels for the formation of bromine addition adducts of 1, 3, 5-tribromobenzene.

levels. One more "positive halogen transfer" may take place to form hexabromobenzene, step #7, **Scheme 4.8**. Electron capture by hexabromobenzene will result in the formation of hexabromobenzene radical anion, step #8, which is present in the ECCI mass spectrum. The last two steps have ΔE_o values = 18.3 and –49.8 kcal/mol, respectively, at the HF/AM1//HF/AM1 level. Thus, the computations show that the starting 3, 4, 5-tribromophenyl anion can readily undergo a series of "positive bromine transfers" and hydrogen abstractions to form the hexabromobenzene radical anion.

In the DP/ECCI/MS experiments of 1, 2, 3-tribromobenzene itself, starting material plus bromide ion (**Scheme 4.1**) and starting material minus bromine plus hydrogen were observed in the spectra (i.e. formation of a dibromobenzene radical anion). 1, 3-Dibromobenzene is formed in steps #2, #4 and #6 of **Scheme 4.8**. Thus, the mechanism proposed by Bunnett and co-workers also explains how the starting material minus bromine plus hydrogen may form in the DP/ECCI/MS experiments. Once the dibromobenzene is formed in steps #2, #4 and #6, it can capture an electron to form the radical anion. The capture of an electron by the dibromobenzenes is an exothermic process at both the HF/AM1//HF/AM1 and *B3LYP/6-311+G(2d,p)//HF/3-21G* levels (except 1, 4-dibromobenzene is endothermic at the *B3LYP/6-311+G(2d,p)//HF/3-21G* level), **Scheme 4.5**. Ions formed from continued "bromine addition" and hydrogen transfers were not observed because the mass range was not set high enough to detect these ions.

In the DP/ECCI mass spectra of 1, 2, 4-tribromobenzene m/z values and isotopic patterns for tetrabromobenzenes were present. As an example, 1, 2, 4, 5-tetrabromobenzene may have arisen from steps #1 through #3 in **Scheme 4.9**. Steps #1 through #3 have ΔE_o values = 20.2, -6.3 and 6.6 kcal/mol at the HF/AM1//HF/AM1 level. Then, 1, 2, 4, 5-tetrabromobenzene may capture an electron to form the radical anion. This

electron capture process is exothermic with a ΔE_o value = -40.6 kcal/mol at the HF/AM1//HF/AM1 level. Ions with more bromines added to the starting material may have been formed, although, once again, the mass range was not set high enough to detect these ions.

In the DP/ECCI/MS experiments of 1, 3, 5-tribromobenzene, ions were observed for the addition of one to three bromines to the starting material. The chain mechanism may be propagated by the 2, 4, 6-tribromophenyl anion. The 2, 4, 6-tribromophenyl anion may have come about from the reaction of bromide ion with 1, 3, 5-tribromobenzene (**Scheme 4.6**) and/or 3, 5-dibromophenyl anion abstracting hydrogen from 1, 3, 5-tribromobenzene, step #2, **Scheme 4.10**. The latter step is more likely since it is an exothermic process with a ΔE_o value = -9.2 and –13.9 at the HF/AM1//HF/AM1 and *B3LYP/6-311+G(2d,p)//HF/3-21G* levels. The chain mechanism can be carried through to termination that involves the formation of the hexabromobenzene radical anion. Once again, the hydrogen abstraction steps are exothermic releasing up to ~ 20 kcal/mol and the "bromine addition" reactions are endothermic resulting in the use of up to ~ 20 kcal/mol at the HF/AM1//HF/AM1 level, steps #2 through #8, **Scheme 4.10**. Overall, the "positive halogen transfers" and hydrogen abstraction mechanisms proposed by Bunnett and co-workers provide an explanation for the results of the DP/ECCI/MS experiments of the tribromobenzenes.

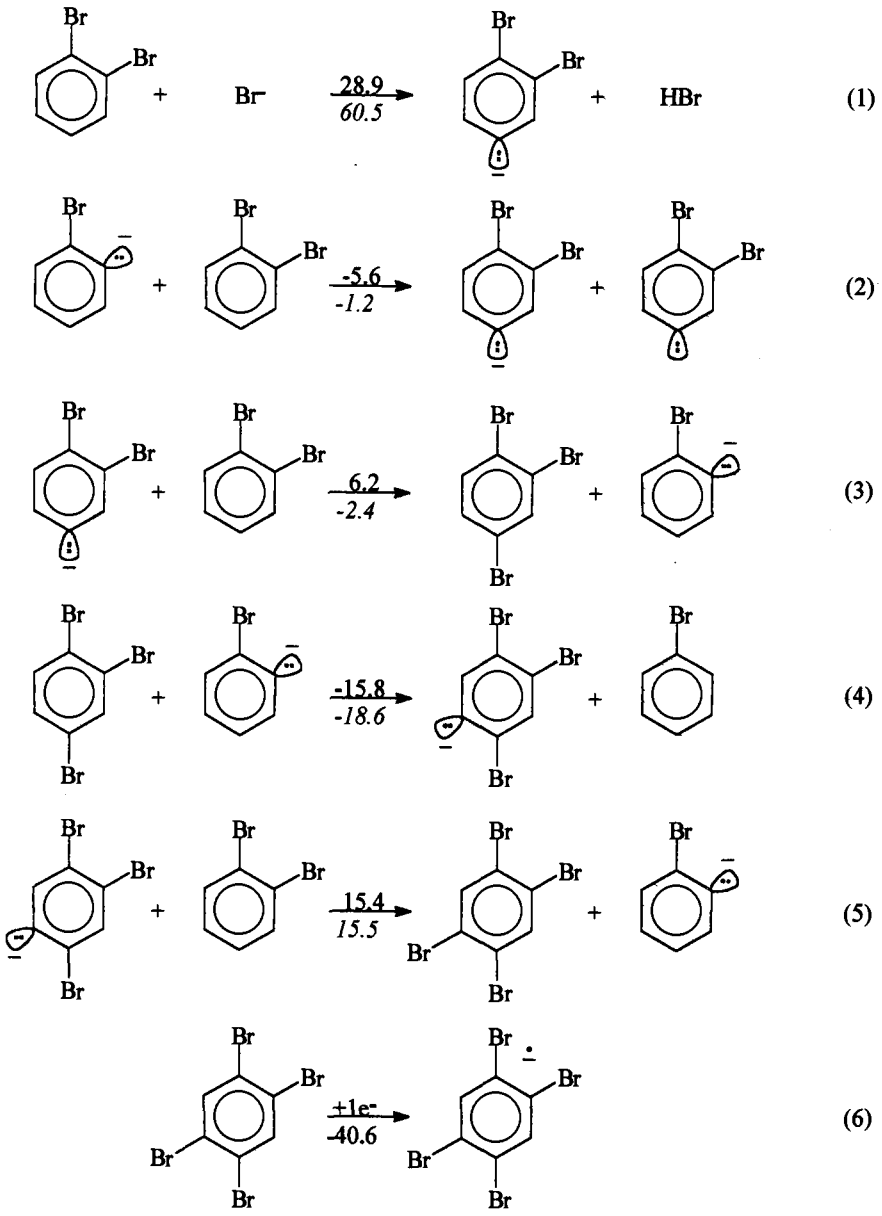

Scheme 4.11: The changes in internal energy in kcal/mol at the HF/AM1//HF/AM1 and *B3LYP/6-311+G(2d,p)//HF/3-21G* levels for the formation of bromine addition adducts of 1, 2-dibromobenzene.

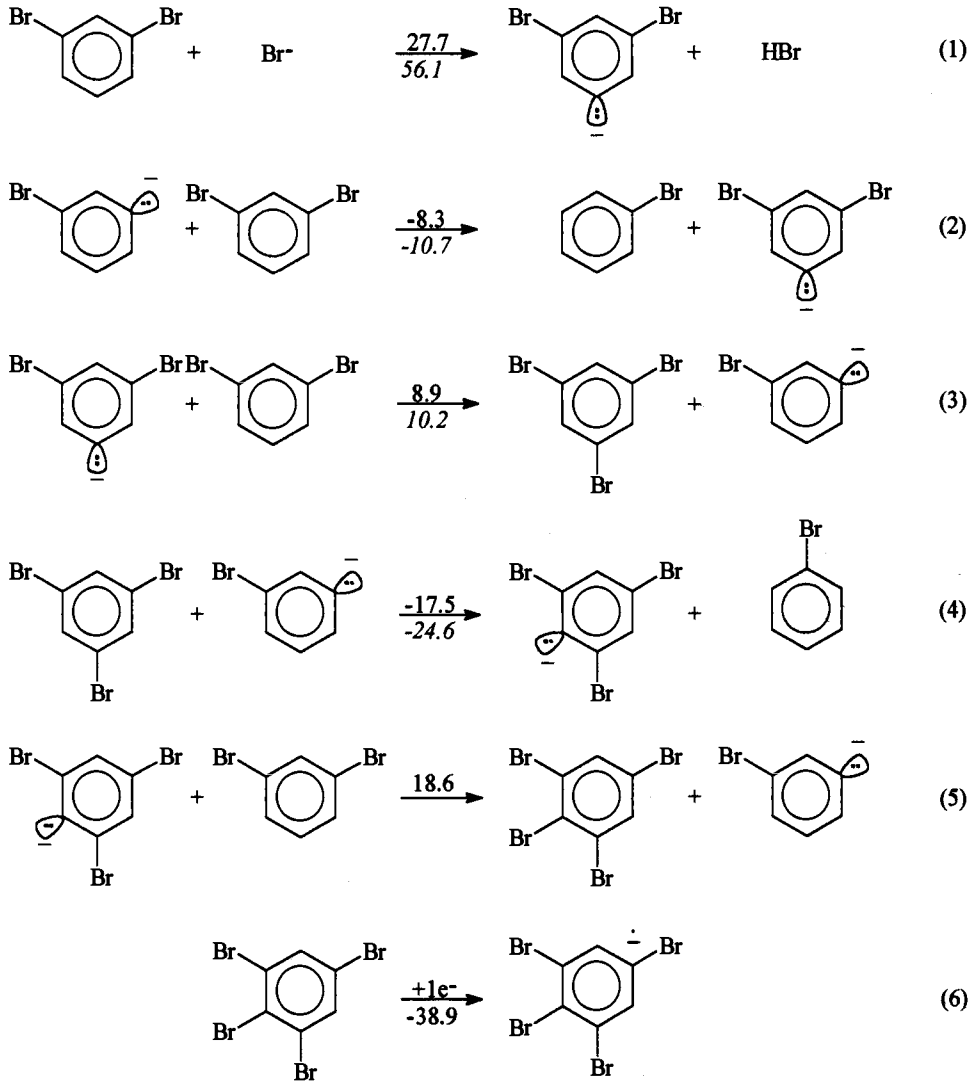

Scheme 4.12: **The changes in internal energy in kcal/mol at the HF/AM1//HF/AM1 and *B3LYP/6-311+G(2d,p)//HF/3-21G* levels for the formation of bromine addition adducts of 1, 3-dibromobenzene.**

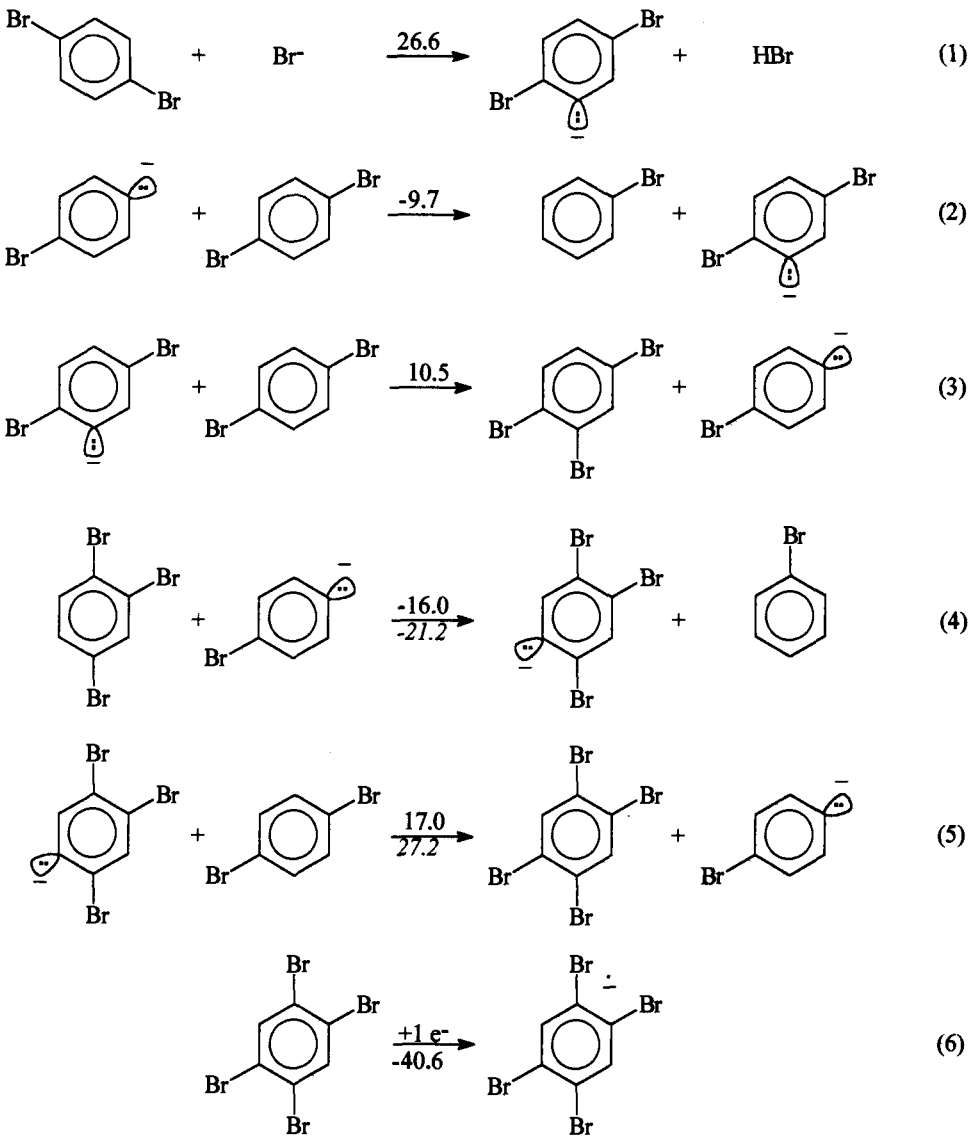

Scheme 4.13: The changes in internal energy in kcal/mol at the HF/AM1//HF/AM1 and *B3LYP/6-311+G(2d,p)//HF/3-21G* levels for the formation of bromine addition adducts of 1, 4-dibromobenzene.

A series of "positive halogen transfers" and hydrogen abstractions may take place to form ions with one to two bromines added to the dibromobenzene starting materials, **Schemes 4.11**, **4.12** and **4.13**. Once the aryl carbanions are formed by steps #1 or #2 (**Schemes 4.11** through **4.13**), some of the aryl carbanions live long enough to be detected. Other aryl carbanions can participate in the propagation steps of the bromine addition mechanism to ultimately form the tetrabromobenzene radical anions that are found in the mass spectrum. The hydrogen abstraction steps are exothermic (except for hydrogen abstraction by bromide ion) releasing up to ~18 and ~ *25* kcal/mol and the bromine transfer steps are endothermic and use up to ~19 and ~*27* kcal/mol at the HF/AM1//HF/AM1 level and the *B3LYP/6-311+G(2d,p)//HF/3-21G* levels.

Conclusion

Overall, it seems that the bromine and chlorine addition adducts are not due to impurities in the sample. The results of the DP/ECCI/MS experiments reveal that typical reactions (**equations 4.1-4.3**), plus, atypical reactions involving sequential "positive halogen transfers" and hydrogen abstractions to form ions with one to three bromines added to the starting material are occurring in the ionization chamber. Thus, the mechanism for halogen addition and isomerization put forth by Bunnett and co-workers provides insight into the mechanisms that may be involved in the formation of the unusual ions found in the DP/ECCI/MS spectra.

Acknowledgements

I would like to thank Don Griffin for contributing his time and expertise on the ECCI/MS system, and for his informative discussions.

Support for this research by the Environmental Health Sciences, Oregon State University Chemistry Department and the N. L. Tarter fellowship is gratefully acknowledged.

References

1. Harrison, A.G. *Chemical Ionization Mass Spectrometry*, 2nd Ed.; American Chemical Society: Washington, DC, 1997.

2. Laramée, J. A.; Kocher, C. A.; Deinzer, M. L. *Analytical Chemistry* **1992,** *64,* 2316-2322.

3. Barofsky, D.F.; Deinzer, M.L. *Mass Spectrometry of Organic Molecules (AC637/CH537)*, Fall **1992**, Class Notes, Oregon State University.

4. Freeman, P.K.; Srinivasa, R.; Campbell, J.-A.; Deinzer, M.L. *J. Am. Chem. Soc.*, **1986**, *108*, 5531-5536.

5. Couch, T.L. Ph.D. Thesis, Oregon State University, Corvallis, OR, 1997.

6. Hehre, W.J.; Radom, L.; Schleyer, P.v.R.; Pople, J.A. *Ab Initio Molecular Orbital Theory*; Wiley: New York, 1986.

7. *Spartan*, versions 4.1-5.0; Wavefunction, Inc.: Irvine, CA, 1993-1997.

8. *Gaussian 92*, Revision G.4, M. J. Frisch, G. W. Trucks, M. Head-Gordon, P. M. W. Gill, M. W. Wong, J. B. Foresman, B. G. Johnson, H. B. Schlegel, M. A. Robb, E. S. Replogle, R. Gomperts, J. L. Andres, K. Raghavachari, J. S. Binkley, C. Gonzalez, R. L. Martin, D. J. Fox, D. J. Defrees, J. Baker, J. J. P. Stewart, and J. A. Pople, Gaussian, Inc., Pittsburgh PA, 1992. *Gaussian 94*, Revisions C.2 and E.1, M. J. Frisch, G. W. Trucks, H. B. Schlegel, P. M. W. Gill, B. G. Johnson, M. A. Robb, J. R. Cheeseman, T. Keith, G. A. Petersson, J. A. Montgomery, K. Raghavachari, M. A. Al-Laham, V. G. Zakrzewski, J. V. Ortiz, J. B. Foresman, J. Cioslowski, B. B. Stefanov, A. Nanayakkara, M. Challacombe, C. Y. Peng, P. Y. Ayala, W. Chen, M. W. Wong, J. L. Andres, E. S. Replogle, R. Gomperts, R. L. Martin, D. J. Fox, J. S. Binkley, D. J. Defrees, J. Baker, J. P. Stewart, M. Head-Gordon, C. Gonzalez, and J. A. Pople, Gaussian, Inc., Pittsburgh PA, 1995.

9. Forseman, J.B.; Frisch, Æ. *Exploring Chemistry with Electronic Methods*, 2nd Ed.; Gaussian, Inc.: Pittsburgh, PA, 1995-96.

10. Binkley, J.S.; Pople, J.A.; Hehre, W.J. *J. Am. Chem. Soc.* **1980**, *102*, 939.

11. Dobbs, K.D.; Hehre, W.J. *J. Comp. Chem.* **1987**, *8*, 880.

12. Staley, S.W.; Strnad, J.T. *J. Phys. Chem.* **1994**, *98*, 116-121.

13. Becke, A.D. *J. Chem. Phys.* **1993**, *98*, 5648.

14. Lee, C.; Yang, W.; Parr, R.G. *Phys. Rev. B.* **1988**, *37*, 785.

15. *ISOPRO - Isotopic Abundance Simulator,* version 2.0; M.W. Senko: Department of Chemistry, Cornell University, Ithaca, NY.

16. Mach, M.H.; Bunnett, J.F. *J. Org. Chem.*, **1980**, *45*, 4660-4666.

17. Bunnett, J.F.; Moyer, Jr., C.E. *J. Am. Chem. Soc.*, **1971**, 93, 1183-1205.

18. Bunnett, J.F. *Acc. Chem. Res.* **1972**, *5*, 139-147.

Chapter 5: The Photochemistry of Polychlorinated benzenes. Are π-Chloropolychlorobenzenes Intermediates?

Sharon Maley Herbelin and Peter K. Freeman*

Department of Chemistry
Oregon State University
Corvallis, OR 97331

Introduction

Researchers have been developing an understanding of the mechanisms involved in the photodehalogenation of polyhalogenated benzenes since many are prevalent environmental pollutants.[1-9] In 1973 Lemal and co-workers[10] assumed that in the photolysis of chlorobenzene in cyclohexane at 253.7 nm a 1:1 mixture of hydrochloric acid (HCl) and benzene, and a very small amount of chlorocyclohexane should be formed, because once a chlorine atom is formed it should abstract a hydrogen much more rapidly than phenyl radical. The results of the experiments were quite different; the researchers found 90% benzene and 35% HCl along with 53% chlorocyclohexane and 1% phenylcyclohexane, **Scheme 5.1** and **Table 5.1**. Lemal and co-workers were puzzled because it seemed as though the phenyl radicals were abstracting hydrogen from cyclohexane faster than the chlorine atom. The results were difficult to digest because it has been found that chlorine atom attacks cyclohexane 10,000 faster than phenyl radical. Therefore, Lemal and co-workers proposed that a novel biradical, a π-chlorobenzene intermediate, is formed and is responsible for the enhanced selectivity of chlorine atoms. The π-chlorobenzene intermediate abstracts hydrogen from the solvent to produce cyclohexyl radical and a benzene-chlorine atom complex. This complex may react with the cyclohexyl radical to form chlorocyclohexane and benzene or cyclohexyl radical and benzene-chlorine atom complex may escape the solvent cage and react with solvent molecules or other radicals present in solution, **Scheme 5.2**. Overall, the π-chloro-benzene intermediate explains how the phenyl radical could abstract hydrogen from cyclohexane faster than chlorine atom resulting in lower yields of HCl.[10]

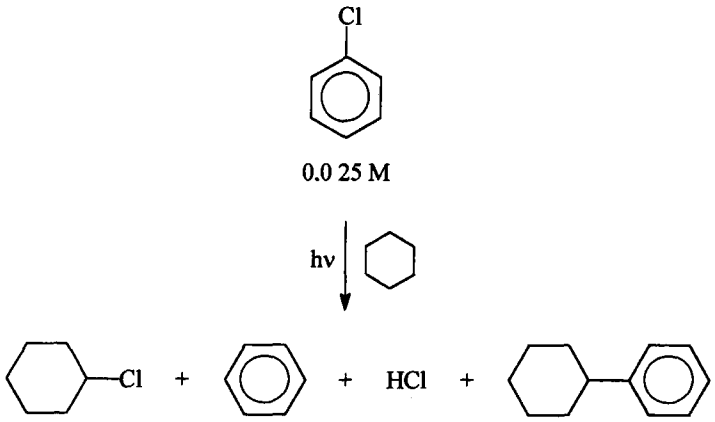

Scheme 5.1: Photolysis products of chlorobenzene in cyclohexane at 253.7 nm.

Table 5.1: Products from photolysis of 0.025 M chlorobenzene in cyclohexane.

Product[a]	Percent Yield of Product
Chlorocyclohexane	~ 53
Benzene	~ 90
HCl	~ 35
Phenylcyclohexane	~ 1
Bicyclohexyl	~ 11

[a]All yields are referred to the starting chlorobenzene concentration.[10]

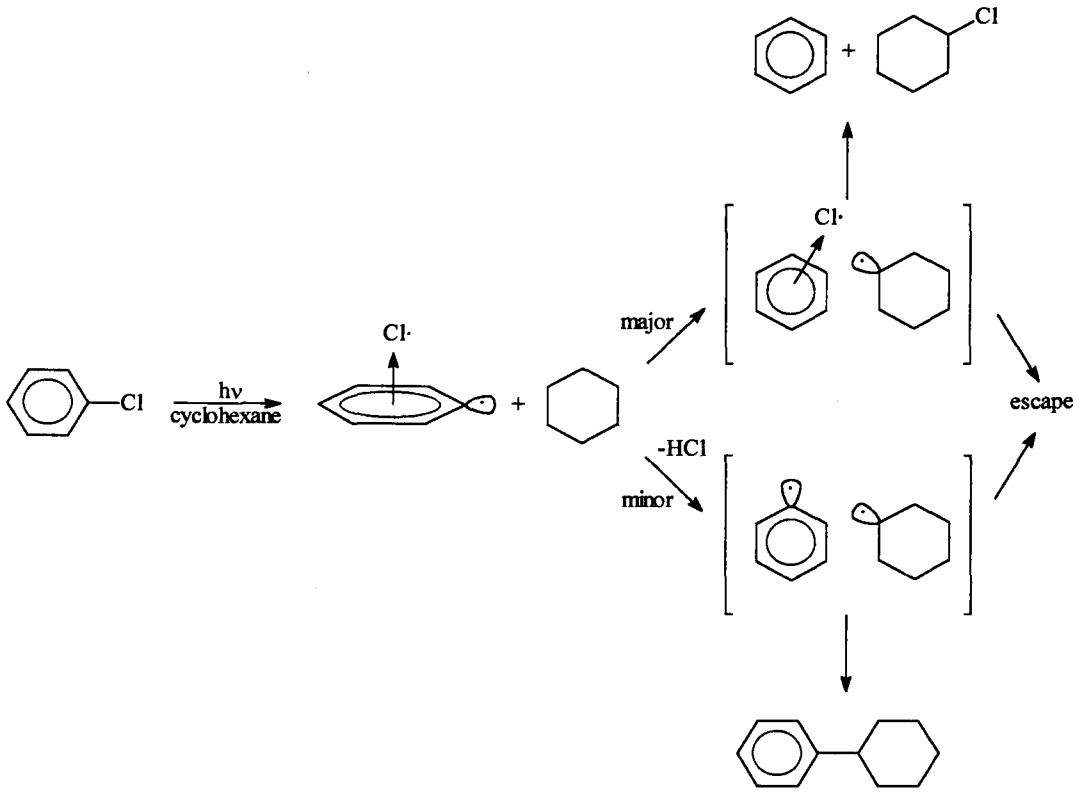

Scheme 5.2: **Mechanistic scheme of chlorobenzene photolysis in cyclohexane at 253.7 nm that includes the involvement of π-chlorobenzene intermediate proposed by Lemal and co-workers.[10]**

In 1977 Arnold and Wong became interested in the unusual π-chlorobenzene intermediate proposed by Lemal and co-workers[10] because they thought it might be applicable to syntheses.[11] Arnold and co-workers irradiated a dilute solution of chlorobenzene in cyclohexane and obtained major products similar to Lemal and co-workers: benzene, chlorocyclohexane, HCl and bicyclohexyl, **Table 5.2**. The only difference in percent products formed with respect to the starting material (chlorobenzene) between Lemal and Arnold's results is the yield of bicyclohexyl which is 42% rather than 11%.[10,11] Arnold and co-worker ran other reactions to assess the importance of the presence of HCl in the formation of chlorocyclohexane. Experiments were run where argon gas was bubbled through a sample of chlorobenzene during the photolysis in cyclohexane. This purged sample was photolyzed simultaneously with a sample that was not purged with argon. In the sample that was bubbled with argon during the photolysis, the yield of chlorocyclohexane dropped by one half compared to the unpurged sample, **Table 5.3**. Furthermore, a reaction that involved adding excess cyclohexene to the photolysis solution of chlorobenzene in cyclohexane resulted in a significantly higher yield of chlorocyclohexane and no HCl, **Table 5.3**. In a photolysis of cyclohexene and HCl no addition occurred to form chlorocyclohexane until a small amount of benzene was added to the reaction mixture. The researchers proposed that the major pathway to form products in the photolysis of chlorobenzene in cyclohexane involved a more traditional reaction mechanism that entails a photosensitized addition of HCl to cyclohexene. It was put forth that cyclohexene is formed from the reaction of phenyl radical and chlorine atom with cyclohexane with subsequent disproportionation of cyclohexyl radicals to form cyclohexane and cyclohexene, **Scheme 5.3**. Arnold and Wong also ran photolysis of *o*-chloropropylbenzene in neopentane, because neopentane cannot readily disproportionate;

consequently, if neopentyl chloride was formed, it would be formed via a π-chloropropylbenzene intermediate rather than photosensitized HCl addition to a double bond. A small amount of neopentyl chloride (< 5%) was formed along with a trace amount of 2, 2, 5, 5-tetramethylhexane. Therefore, Arnold and co-workers concluded that a mechanism involving a π-chloropropylbenzene intermediate was responsible for < 5% of the reaction products, **Scheme 5.3**.[11]

Even though the amount of products from the photolysis of chloropropylbenzene in cyclohexane arose from the π-chlorobenzene intermediate is small, it is still a notable pathway. What is the nature of the π-chlorobenzene intermediate? Would the chlorine atom be centered over the middle of the phenyl ring or associated with the radical site or another carbon in an isomeric chlorobenzene type intermediate? Could other poly-chlorinated benzenes form π-polychlorobenzene intermediates? Computational experiments were undertaken to delve into the nature of π-chlorobenzene and π-hexa-chlorobenzene intermediates. Photochemical experiments were conducted to see if any of the products of a photolysis of hexachlorobenzene in cyclohexane and a solvent that does not readily disproportionate, tetramethylsilane arise from a π-hexachlorobenzene intermediate.

Computational Methods

Ab initio calculations[12] were carried out using the Spartan 4.0-5.0 molecular modeling and Gaussian 92/94 programs.[13,14] The STO-3G,[15,16] and split valence 3-21G,[17,18] and 6-31G*[19-23] basis sets were employed. The electron restricted and restricted open shell

Table 5.2: Products from a one-hour irradiation of 0.025 M chlorobenzene in cyclohexane.

Product[a]	Percent Yield of Product
Chlorocyclohexane	43
Benzene	70
HCl	35
Phenylcyclohexane	--[b]
Bicyclohexyl	42

[a]All yields are referred to the starting chlorobenzene. [b]Phenylcyclohexane was not discussed.[11]

Table 5.3: Irradiation of chlorobenzene in cyclohexane under various conditions.

	Percent Yield of Product[a,b]			
Product	**No Argon Bubbling**	**Argon Bubbling**	**No Cyclohexene**	**0.25 M Cyclohexene**
Chlorocyclohexane	42	21	31	48
Bicyclohexyl	55	54	40	20
HCl	--[c]	0	23	0

[a]All yields are referred to the starting chlorobenzene. [b]All reactions were done in cyclohexane solution. [c]HCl was not listed.[11]

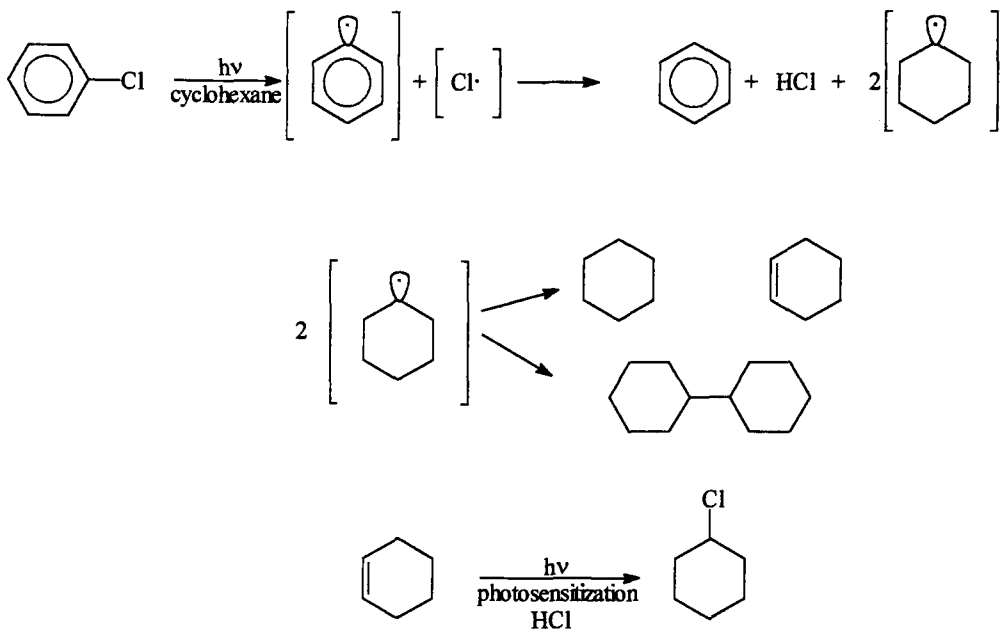

Scheme 5.3: Mechanistic scheme proposed by Arnold and Wong to explain product formation in the photolysis of chlorobenzene in cyclohexane.[11]

Hartree-Fock (HF) methods were used with the STO-3G basis set, the electron correlated Becke's three-parameter hybrid functional[24] combined with the Lee, Yang, and Parr (LYP) correlation functional, denoted B3LYP,[25] was used in calculations using the 3-21G and 6-31G* basis sets.[14,26] The optimized geometries from lower levels of theory were used as starting coordinates for higher level geometry optimizations. The "/" separates the method from the basis set; and "//" separates the computational level of the energy from the level of the geometry optimization in the following example: B3LYP/D95//B3LYP/D95. Frequency calculations were executed to ensure that no imaginary frequencies were present in any of the optimized geometries, and, no imaginary frequencies were found for the optimized structures discussed, *vide infra*.[26] The zero-point vibrational energies calculated at the B3LYP/6-31G* levels were scaled to 0.9613[26] and those calculated at the B3LYP/ 3-21G levels were not scaled.

Throughout this chapter, the changes in internal energy (ΔE_o) are calculated by subtracting the electronic energy plus the scaled zero point energy of the starting materials from the electronic energy plus the scaled zero point energy of the products.[21]

Experimental Methods

Materials

The chemicals were obtained from commercial sources except for 1, 2, 3, 5-tetra-chlorobenzene that was synthesized by a known method.[27] Hexachlorobenzene was purchased from Aldrich and was crystallized once from ethanol. Cyclohexane and methanol were used as obtained from Fisher Scientific. Tetramethylsilane, chloro-

cyclohexane, cyclohexene, bicyclohexyl, cyclohexyl benzene, cyclohexene, biphenyl, 1, 3, 5-trichlorobenzene, mercury thiocyanate, and iron (III) nitrate were obtained from the Aldrich Chemical Co. and were taken directly from the manufacturers' bottle. Azoxybenzene was acquired from Janssen Chimica and underwent no further purification. Pentachlorobenzene, 1, 2, 3, 4-tetrachlorobenzene, 1, 2, 4, 5-tetrachlorobenzene, 1, 2, 3-trichlorobenzene and 1, 2, 4-trichlorobenzene were also purchased from Aldrich Chemical company and were purified by preparative gas chromatography using a Varian 3700 Gas Chromatograph equipped with a thermal conductivity detector. The Varian 3700 gas chromatograph was equipped with a 4' × 1/8"-10% OV-101 on chromosorb and a 4' × 1/8"-Chromosorb W on 80/100 solid support reference column. All compounds were found to be greater than 99% pure by analysis on a Varian 3300 and/or a Varian 3400 gas chromatograph equipped with flame ionization detector, and a Varian 3400 gas chromatograph interfaced with a Finnigan 4023 mass spectrometer operating in electron capture chemical ionization mode.

General Procedure for Photolysis and Analysis of Organic Compounds

Hexachlorobenzene and chlorobenzene samples (2-3 mL) were placed in 170 mm x 15 mm pyrex and quartz phototubes, respectively, that were purchased from Ace Glass. The samples were degassed three times for a total of 30 minutes. The samples were sealed in vacuum with a nylon adapter that contained stopper valves. The photolyses of hexachlorobenzene and chlorobenzene were carried out in a Rayonet merry-go-round reactor purchased from the Southern New England Co. equipped with 300 nm and 253.7 nm Rull lamps, respectively. The temperature of the reactor was kept constant at 50°C and

20 °C under a fresh stream of air for photolyses carried out in cyclohexane and tetramethyl silane, respectively. After photolyses, HCl was carefully extracted by the following procedure. The samples were cooled in liquid nitrogen. Once the samples were frozen, deionized water (DI H_2O, ~ 1-2 mL) was added to the stopper valves, the stopper valves were pushed into the phototubes and the deionized water rushed into the samples that were in vacuum. As soon as the water was pulled into the frozen samples, the stopper valves were re-sealed. The samples were allowed to thaw in isopropyl alcohol. Once the samples were thawed, the phototubes were placed in an ice bath to minimize evaporation of tetramethyl silane (boiling point = 26-28 °C). Before the nylon adapters were removed the phototubes were inverted several times to ensure that the most of the HCl was extracted into the DI H_2O. The adapters were removed and the lower DI H_2O layers were extracted using Pasteur pipettes. The samples were extracted two more times with ~5 mL and ~2 mL DI H_2O , respectively. The organic layer of the photolysis samples was analyzed on a Varian 3400 gas chromatograph equipped with flame ionization detector. An Alltech 30 m x 0.25 mm x 0.25 μm EC-WAX capillary column (Econo-Cap) was used and the temperature of the column was held at 30 °C for 10 minutes, ramped to 250 °C at a rate of 10 °C/minute and held at 250 °C for 8 minutes. Dodecane was used as an internal standard. Azoxybenzene was used as an actinometer according to the procedure developed by Bunce and coworkers.[28] Standard samples of the compounds of interest found in the photolyzed reaction were run on the Varian 3400 gas chromatograph to check retention times, and response factors were determined using the flame ionization detector. A Varian 3400 gas

chromatograph interfaced with a Finnigan 4023 mass spectrometer, operating in electron capture chemical ionization mode, was used to verify the compounds in the reaction mixtures.

Procedure for HCl Analysis

An analytical procedure that is routinely used in flow injection analysis for analysis of chloride ion was implemented to analyze the HCl concentration.[29] This procedure was implemented because the HCl concentration in many of the photolyzed samples was very low and it was difficult to get reproducible results from standard methods such as titrations with NaOH. An indicator solution was made by dissolving 0.0262 g of mercury thiocyanate ($Hg(SCN)_2$), 3.03 g of iron (III) nitrate ($Fe(NO_3)_3$), 0.472 g of concentrated nitric acid and 15 mL of methanol in DI H_2O, making the final volume 100 mL. Standard HCl solutions ranging from 2 x 10^{-5} M to 2 x 10^{-3} M were extracted from both tetramethyl silane and cyclohexane solutions. The analytical procedure is based on the reactions presented in **equations 5.1** and **5.2.** The intensity of the red-colored

$$Hg(SCN)_2 + 2Cl^- \rightarrow HgCl_2 + 2SCN^- \qquad \textbf{Equation 5.1}$$

$$2SCN^- + Fe^{3+} \rightarrow Fe(SCN)_2^+ \ (\textit{red colored complex}) \qquad \textbf{Equation 5.2}$$

complex was measured spectrophotometrically at 460, 470 and 480 nm using an HP8452A Diode Array Spectrophotometer. To minimize human error in the absorbance measurements, a flow cell was connected to a peristaltic pump and acted as a sipper

system. The pump was allowed to sip the sample solution for 1 minute, the sample equilibrated for 15 seconds, then the absorbance was measured. A second measurement was executed ~ 15 seconds after the first reading.

The height of the absorbance peak is proportional to the concentration of chloride ion in the samples. Therefore, the concentration of the standard HCl solutions vs. the absorbance was plotted and a second order polynomial fit was applied to the data rather than a linear regression line because the higher HCl concentrations the correlation becomes non-linear, **Figures 5.1** and **5.2**. Absorbance measurements at 460, 470 and 480 nm of standard HCl solutions abstracted from tetramethyl silane and cyclohexane have R^2 values = 0.9999 and 0.9998, respectively. Since the measurements of absorbance at the all three wavelengths have high R^2 values, the equations for the second order polynomial fit at 470 nm were chosen to determine the concentration of the chloride ion. Once the intensities were measured for the DI H_2O layers extracted from samples photolyzed in tetramethyl silane and cyclohexane, the absorbance values at 470 nm were entered into **equation 5.3** and **equation 5.4**, respectively, to determine the chloride ion (Cl^-, i.e. HCl) concentrations.

$$[Cl^-] = 3.36\times10^{-4}x^2 + 7.98\times10^{-4}x - 1.99\times10^{-4} \qquad \textit{tetramethyl silane} \qquad \textbf{Equation 5.3}$$

$$[Cl^-] = 3.95\times10^{-4}x^2 + 7.37\times10^{-4}x - 1.92\times10^{-4} \qquad \textit{cyclohexane} \qquad \textbf{Equation 5.4}$$

Results and Discussion

Computations

Computations were undertaken to investigate the nature of the singlet π-chloro-benzene and singlet π-hexachlorobenzene intermediates. The computational results of the π-chlorobenzene intermediate will be discussed first. The starting geometry for the π-chlorobenzene was composed of the chlorine atom centered over the ring of the phenyl radical. The changes in internal energy (ΔE_o) are 5.8 and 3.3 kcal/mol at the B3LYP/ 3-21G//B3LYP/3-21G and B3LYP/6-31G*//B3LYP/6-31G* levels, respectively, for formation of π-chlorobenzene. Whereas at the HF/STO-3G//HF/STO-3G level the ΔE_o = 25.8 kcal/mol and is highly endothermic, **Table 5.4**. The decreased endothermicity at the higher computational levels may be due improvements using split valence sets and the inclusion of electron correlation. The overall structure at the HF/STO-3G//HF/STO-3G level including bond lengths, angles and natural charges is somewhat similar to the higher computational levels, although, the ΔE_o is so much larger that only the bond lengths, angles and natural charges at the B3LYP/3-21G//B3LYP/3-21Gand B3LYP/6-31G*//B3LYP/ 6-31G* levels will be listed in the figures and tables, *vide infra*. Similar results were obtained at both the B3LYP/3-21G//B3LYP/3-21G and B3LYP/6-31G*//B3LYP/6-31G* levels; thus, only the B3LYP/6-31G*//B3LYP/6-31G* level bond lengths, angles and natural charges will be discussed in the subsequent paragraphs.

The singlet π-chlorobenzene optimized at the B3LYP/6-31G*//B3LYP/6-31G* level revealed that the chlorine atom moved from the center of the phenyl ring to associate with the carbon atom number two (C2) of the phenyl ring that is directly opposite to the

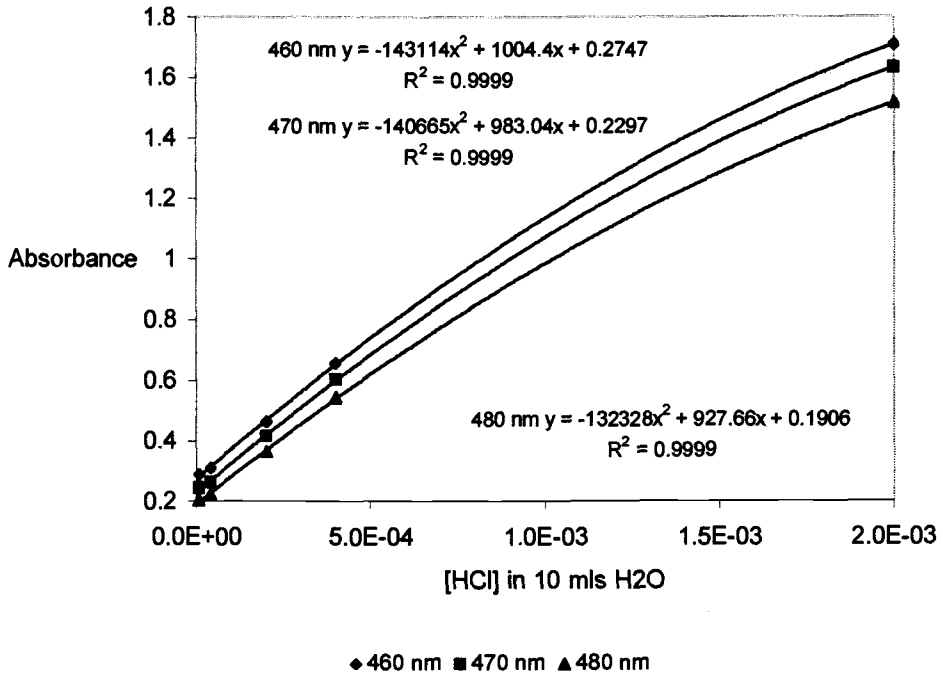

Figure 5.1: **HCl standards extracted from tetramethyl silane vs. absorbances at 460, 470 and 480 nm.**

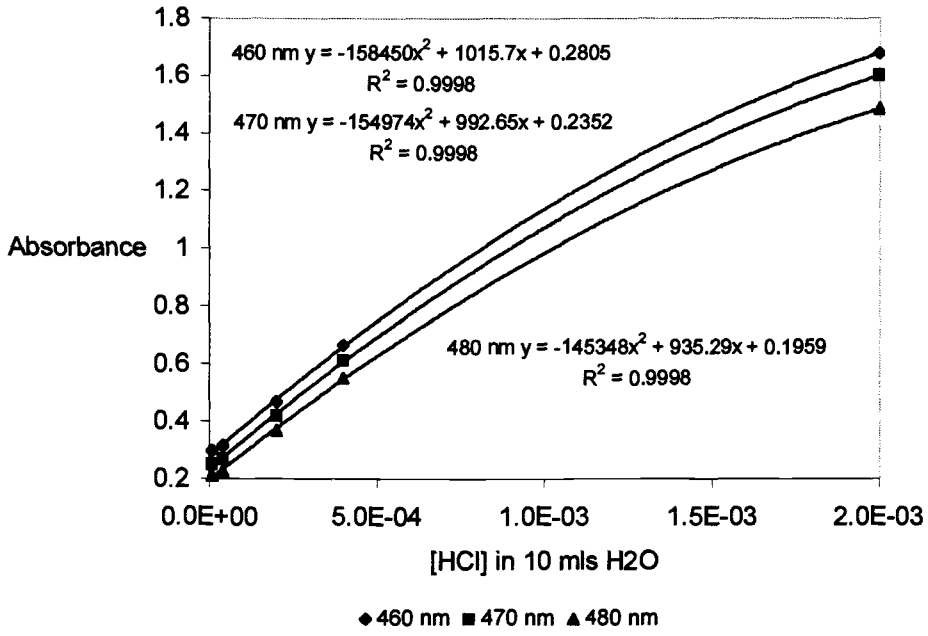

Figure 5.2: **HCl standards extracted from cyclohexane vs. absorbances at 460, 470 and 480 nm.**

radical center at C10, **Figure 5.3** and **Table 5.5**. The carbon-chlorine bond length is 1.913 Å at B3LYP/6-31G*//B3LYP/6-31G* level. The carbon-chlorine bond is much longer than standard sp^2 or sp^3 carbon-chlorine bond distances which are 1.73 Å and 1.79 Å,[31] respectively. The carbon-chlorine bond length is, nevertheless, much shorter than what has been found for carbon-chlorine bond where a chlorine molecule (Cl_2) is complexed with benzene.[30] The carbon-chlorine bond distances in this complex is > 3 Å at both the RHF/STO-3G//RHF/STO-3G and MP2/DZP+(d)//MP2/DZP+(d) levels.[39] The chlorine-carbon bond length in the triplet complex of chlorine atom and benzene is 2.599 Å at the B3LYP/3-21G//B3LYP/3-21G level which is much longer than the singlet chlorine atom phenyl radical complex. One similarity between the three complexes is that the chlorine molecule and chlorine atom moved from the center of the ring to associate with a carbon of the ring.[30] A difference between the π-chlorobenzene complex, and the complexes of Cl_2 with benzene and chlorine atom with benzene is that the latter two have benzene rings that are planar. The π-chlorobenzene carbon-hydrogen bond lengths are approximately the same length as benzene sp^2 carbon-hydrogen bond distances = 1.08 Å except for the C2-H1 bond which is 1.09 Å at the B3LYP/6-31G*//B3LYP/6-31G* level. The C2-H1 bond is the same length as a methane sp^3 carbon-hydrogen bond = 1.09 Å.[31] The elongation of this carbon-hydrogen bond is due to the association of Cl5 to C2. Furthermore, the C2 bond angles along with the bond angles at C10 (C3-C2-C4 = 114.64°, C3-C2-Cl5 = 108.98°, C4-C2-Cl5 = 108.98° and C6-C10-C7 = 117.22° at the B3LYP/6-31G*//B3LYP/6-31G* level) are moving in the direction of sp^3 carbon bond angles (109.5°).[31] The carbon-carbon bond lengths of C2-C4 = 1.479 Å and C2-C3 = 1.479 Å at the B3LYP/6-31G*//B3LYP/6-31G* level are much longer than a benzene carbon-carbon bond = 1.397 Å and are

approaching an average propene sp^3 carbon-sp^2 carbon bond distance = 1.51 Å.[31] In addition, C2 and C10 both moved out of the plane of the ring such that the phenyl ring looks more like a boat shaped 2,4-cyclohexadiene rather than a benzene ring with dihedral bond angles of C4-C2-C3-C7 = 9.41° and C2-C4-C10-C7 = 35.045°at the B3LYP/ 6-31G*//B3LYP/6-31G* level. The diene like structure is also reaffirmed by the bond distances of C4-C6 = 1.368 Å and C3-C7 = 1.368 Å at the B3LYP/6-31G*//B3LYP/ 6-31G* level are much shorter than the other benzene carbon-carbon bonds = 1.397 Å.[31] The structure of the π-chlorobenzene intermediate does not seem to be an association of the benzene ring π-system, but an association of the chlorine atom that involves direct σ bonding to a carbon of the benzene ring. The chlorine atom is bonded to C2 causing this carbon to become sp^3 like with elongation of the benzene carbon-carbon and carbon-hydrogen bonds, and reduction of the bond angles from 120° to an approximation of tetrahedral angle forming an isomeric chlorobenzene (*iso*-chlorobenzene) intermediate, **Table 5.5**.

The natural atomic charges of this singlet *iso*-benzene B3LYP/6-31G*//B3LYP/ 6-31G* level reveal that there is extra electron density on C2, C3, C4, Cl5, C6 and C7, **Table 5.6**. The negative charge resides mostly on the C2, C6 and C7. C10 has a slightly positive charge revealing a lack of electron density at this atom. The lack of electron density could be due to the electron withdrawing chlorine atom and/or the radical character of this carbon in the beginning and optimized structure. The diminished electron density at C10 and increased electron density at the other five carbons of the ring is also found in the geometry optimized at the B3LYP/6-31G*//B3LYP/6-31G* level of the triplet phenyl radical (with no chlorine atom complexation). In the singlet chlorine atom complexed with

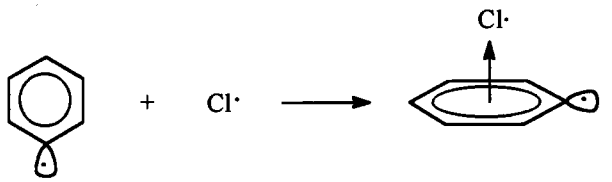

Table 5.4: The changes in internal energy (ΔE_0) at the HF/STO-3G//HF/STO-3G, B3LYP/3-21G//B3LYP/3-21G and B3LYP/6-31G*//B3LYP/6-31G* levels for the formation of singlet isomeric chlorobenzene.[a]

Method/Basis Set	ΔE_0
HF/STO-3G//HF/STO-3G	25.8
B3LYP/3-21G//B3LYP/3-21G	5.8
B3LYP/6-31G*//B3LYP/6-31G*	3.3

[a]All geometries are optimized and contain no imaginary frequencies.

A.

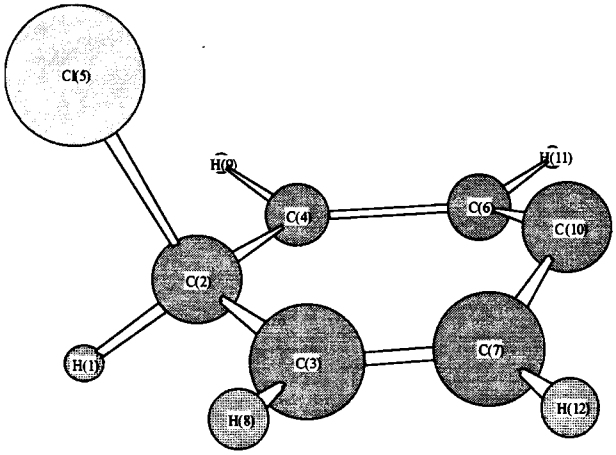

B.

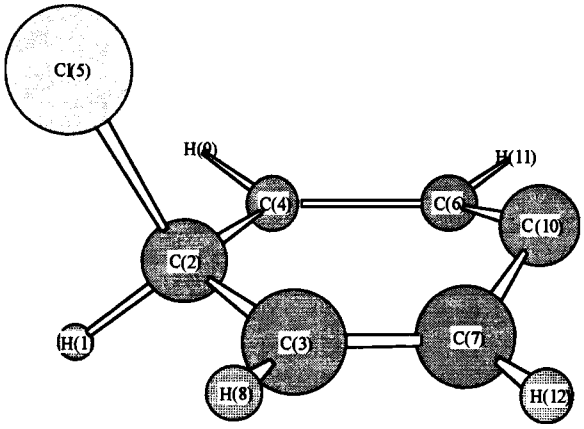

Figure 5.3: **The optimized geometry of singlet isomeric chlorobenzene at A) the B3LYP/3-21G//B3LYP/3-21G and B) the B3LYP/6-31G*//B3LYP/ 6-31G* levels with no imaginary frequencies.**

Table 5.5: The bond lengths and angles at the B3LYP/3-21G//B3LYP/3-21G and B3LYP/6-31G*//B3LYP/6-31G* levels of the singlet isomeric chlorobenzene.[a]

Bond Length(Å)/Bond and Dihedral Angles (°)[b]	B3LYP/3-21G// B3LYP/3-21G	B3LYP/6-31G*// B3LYP/6-31G*
C2-C3	1.480	1.479
C2-C4	1.479	1.479
C2-Cl5	1.947	1.913
C3-C7	1.370	1.368
C3-H8	1.084	1.087
C4-C6	1.370	1.368
C4-H(9)	1.085	1.088
C6-C10	1.423	1.419
C6-H(11)	1.085	1.089
C7-C10	1.423	1.419
C7-H12	1.085	1.089
C2-H1	1.092	1.095
C3-C2-C4	115.039	114.637
C3-C2-Cl5	107.534	108.982
C4-C2-Cl5	107.527	108.981
H1-C2-C3	112.492	111.463
H1-C2-C4	112.495	111.463
H1-C2-Cl5	100.446	100.299
C2-C3-C7	120.801	120.947
C2-C3-H8	117.461	117.435
C7-C3-H8	121.446	121.304
C2-C4-C6	120.816	120.968
C2-C4-H(9)	117.482	117.398
C6-C4-H(9)	121.407	121.315
C4-C6-C10	117.992	117.982
C4-C6-H(11)	120.201	119.732
C10-C6-H(11)	120.631	120.795
C3-C7-C10	117.998	118.013
C3-C7-H12	120.136	119.730
C10-C7-H12	120.669	120.780
C6-C10-C7	117.660	117.218
C4-C2-C3-C7	10.07	9.140
C3-C2-C4-C6	-10.092	-9.134
C2-C3-C7-C10	11.379	12.481
C2-C4-C6-C10	-11.343	-12.497
C2-C4-C10-C7	33.836	35.048
C3-C7-C10-C6	-33.852	-35.049

[a]All geometries are optimized at the B3LYP/3-21G//B3LYP/3-21G and B3LYP/6-31G*//B3LYP/6-31G* levels and contain no imaginary frequencies. [b]Average bond lengths: carbon-carbon: sp^3-sp^3 = 1.53 Å; sp^3-sp^2 = 1.51 Å; sp^3-sp = 1.47 Å; sp^2-sp^2 = 1.48 Å (e.g. butadiene); sp^2-sp^2 = 1.397 Å (e.g. benzene); sp^2-sp = 1.43 Å; and sp-sp = 1.38 Å. Carbon-hydrogen: sp^3-H and sp^2-H = 1.09 Å and sp-H = 1.08 Å. Carbon-chlorine: sp^3-Cl = 1.79 Å; sp^2-Cl = 1.73 Å; and sp-Cl = 1.63 Å.[31]

benzene there is a slightly greater negative charge on the carbon that is loosely bonded to the chlorine atom and the negative charge is slightly less at the carbon directly across from the carbon bonded to chlorine atom at the B3LYP/3-21G//B3LYP/3-21G level. Even though there are some similarities in natural charges for the isomeric chlorobenzene intermediate and the phenyl radical and the chlorine atom complexed with benzene, the optimized geometry of the phenyl radical and the chlorine atom complexed with benzene complex do not have any severe perturbations of the bond lengths and angles as in the isomeric chlorobenzene intermediate optimized geometry.

The computational results of the *iso*-hexachlorobenzene intermediate are somewhat similar to the results of *iso*-chlorobenzene. The starting geometry for the *iso*-hexachlorobenzene intermediate consisted of the chlorine atom centered over the ring of the pentachlorophenyl radical. The changes in internal energy (ΔE_o) are –7.5 and –6.3 kcal/mol at the B3LYP/3-21G//B3LYP/3-21G and B3LYP/6-31G*//B3LYP/6-31G* levels, respectively, for formation of the *iso*-hexachlorobenzene intermediate which are slightly exothermic, whereas at the HF/STO-3G//HF/STO-3G level the ΔE_o = 34.3 kcal/mol and is highly endothermic, **Table 5.7**. Once again the ΔE_o is larger at the HF/STO-3G//HF/STO-3G level than the other two computational levels, therefore, the bond lengths, angles and natural charges at the B3LYP/3-21G//B3LYP/3-21G and B3LYP/6-31G*//B3LYP/6-31G* levels will be listed in the following figures and tables, and the B3LYP/6-31G*//B3LYP/6-31G* level results will be discussed in the ensuing paragraphs.

Table 5.6: Natural charges of the isomeric chlorobenzene at the B3LYP/3-21G// B3LYP/3-21G and B3LYP/6-31G*//B3LYP/6-31G* levels.[a]

	B3LYP/3-21G//B3LYP/3-21G	B3LYP/6-31G*//B3LYP/6-31G*
Atom	**Natural Charges[b]**	**Natural Charges[b]**
H1	0.30285	0.29462
C2	-0.29828	-0.27370
C3	-0.17193	-0.17698
C4	-0.17193	-0.17698
Cl5	-0.12886	-0.12670
C6	-0.33891	-0.32300
C7	-0.33891	-0.32300
H8	0.25605	0.25030
H(9)	0.25605	0.25030
C10	0.10692	0.09194
H(11)	0.26347	0.25659
H12	0.26347	0.25659

[a]All geometries are optimized at the B3LYP/3-21G//B3LYP/3-21G and B3LYP/6-31G*// B3LYP/ 6-31G* levels and have no imaginary frequencies. [b]Natural charges from natural population analysis.[26]

The *iso*-hexachlorobenzene optimized geometries B3LYP/6-31G*//B3LYP/6-31G* level show that the chlorine atom migrated from the center of the ring of the pentachlorophenyl radical to C3 of the phenyl ring that is one carbon away from the radical center C10, **Figure 5.4** and **Table 5.8**. The carbon-chlorine C3-Cl7 bond length is 1.795 Å at the B3LYP/6-31G*//B3LYP/6-31G* level. The carbon-chlorine bond has been elongated because Cl9 has shifted from the center of the phenyl ring to associate (or bond) with C3. The distance between C3-Cl9 is 1.832 Å at the B3LYP/6-31G*//B3LYP/6-31G* level, and is again longer than standard sp^2 or sp^3 carbon-chlorine bond distances. Note that the carbon-chlorine bond length is much shorter than what has been found for the carbon-chlorine bond in the complexes of chlorine atom with benzene and Cl_2 with benzene as discussed previously.[30] Furthermore, the other carbon-chlorine bond distances are similar to average sp^2 carbon-chlorine bond lengths and range from 1.722-1.738 Å at the B3LYP/6-31G*//B3LYP/6-31G* level. The bond angles at C3 (C2-C3-C6 = 109.43 Å, C2-C3-Cl7 = 109.14 Å, C6-C3-Cl9 = 111.40 Å and Cl7-C3-Cl9 = 109.02 Å at the B3LYP/6-31G*//B3LYP/6-31G* level) have decreased from 120° to approximately sp^3 carbon type bond angles. In addition, C3 moved out of the plane of the ring with the dihedral angles of C4-C2-C3-C6 = 21.51°, C3-C2-C4-C5 = 10.36°,C2-C3-C6-C10 = –32.996° and C3-C6-C10-C5 = 12.99° at the B3LYP/6-31G*//B3LYP/6-31G* level such that the phenyl ring looks more like an allene rather than a benzene ring. The allene structure is also supported by the carbon-carbon bond lengths of C3-C6 = 1.538 Å and C2-C3 = 1.56 Å at the B3LYP/6-31G*//B3LYP/6-31G* level, which are much longer than a benzene carbon-carbon bond = 1.397 Å and are even longer than an average sp^3 carbon-

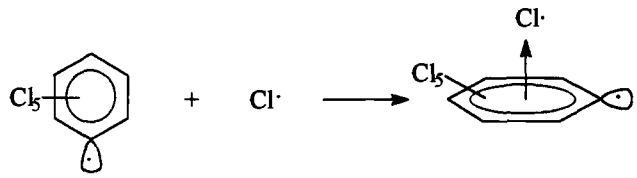

Table 5.7: **The changes in internal energy (ΔE_0) at the HF/STO-3G//HF/STO-3G, B3LYP/3-21G//B3LYP/3-21G and B3LYP/6-31G*//B3LYP/6-31G* levels for the formation of isomeric hexachlorobenzene.[a]**

Method/Basis Set	ΔE_0
HF/STO-3G//HF/STO-3G	34.3
B3LYP/3-21G//B3LYP/3-21G	-7.5
B3LYP/6-31G*//B3LYP/6-31G*	-6.3

[a]All geometries are optimized and contain no imaginary frequencies.

A.

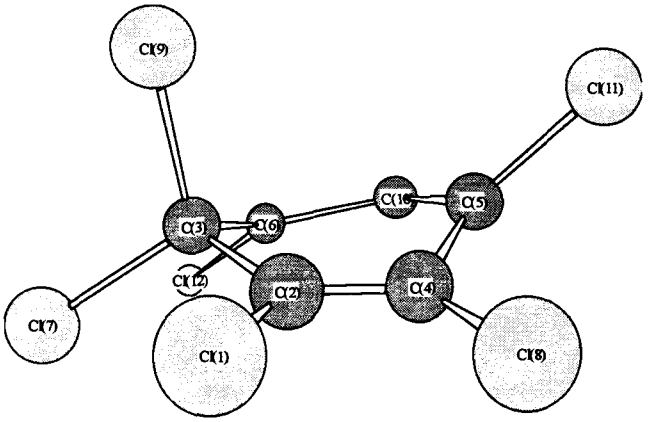

B.

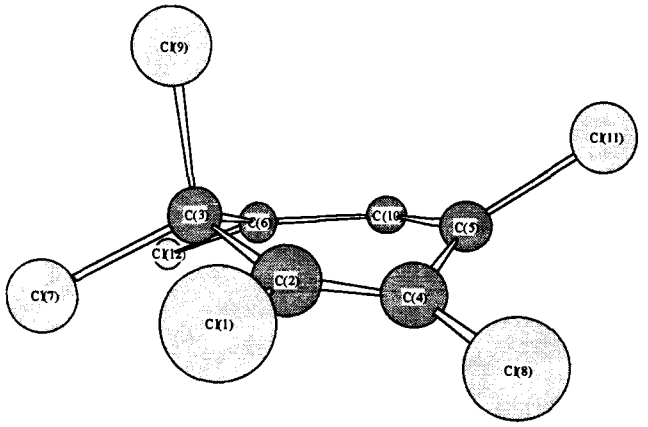

Figure 5.4: **The optimized geometry of singlet isomeric hexachlorobenzene at A) the B3LYP/3-21G//B3LYP/3-21G and B) the B3LYP/6-31G*//B3LYP/ 6-31G* levels with no imaginary frequencies.**

Table 5.8: **Bond lengths and angles of the isomeric hexachlorobenzene at the B3LYP/3-21G//B3LYP/3-21G and B3LYP/6-31G*//B3LYP/6-31G* levels.**

Bond Length(Å)/Bond and Dihedral Angles (°)	B3LYP/3-21G// B3LYP/3-21G	B3LYP/6-31G*// B3LYP/6-31G*
Cl(1)-C2	1.722	1.722
C2-C3	1.568	1.560
C2-C4	1.356	1.361
C3-C6	1.545	1.538
C3-Cl7	1.796	1.795
C3-Cl9	1.838	1.832
C4-C5	1.478	1.467
C4-Cl8	1.733	1.734
C5-C10	1.328	1.332
C5-Cl11	1.736	1.738
C6-Cl10	1.320	1.322
C6-Cl12	1.734	1.737
Cl(1)-C2-C3	116.599	116.830
Cl(1)-C2-C4	121.481	121.061
C3-C2-C4	121.778	121.998
C2-C3-C6	108.267	109.243
C2-C3-Cl7	110.017	109.140
C2-C3-Cl9	106.860	107.487
C6-C3-Cl7	111.217	110.479
C6-C3-Cl9	111.056	111.402
Cl7-C3-Cl9	109.323	109.016
C2-C4-C5	115.826	115.118
C2-C4-Cl8	123.096	123.165
C5-C4-Cl8	120.390	120.970
C4-C5-C10	115.392	116.403
C4-C5-Cl11	118.344	118.512
C10-C5-Cl11	124.418	123.474
C3-C6-Cl10	114.184	114.899
C3-C6-C12	121.087	121.322
C10-C6-Cl12	123.950	123.362
C5-C10-C6	128.898	127.796
C4-C2-C3-C6	24.583	21.510
C3-C2-C4-C5	8.255	10.364
C2-C3-C6-C10	-36.137	-32.996
C3-C6-C10-C5	15.966	12.993
C2-C4-C5-Cl11	133.025	132.393
Cl11-C5-C10-...	-143.778	-142.748
C2-C3-C6-Cl12	134.149	139.807
Cl12-C6-C10-...	-154.003	-159.646

[a]All geometries were optimized at the B3LYP/3-21G//B3LYP/3-21G and B3LYP/6-31G*//B3LYP/6-31G* levels and contain no imaginary frequencies. [b]Average bond lengths: carbon-carbon: sp^3-sp^3 = 1.53 Å; sp^3-sp^2 = 1.51 Å; sp^3-sp = 1.47 Å; sp^2-sp^2 = 1.48 Å (e.g. butadiene); sp^2-sp^2 = 1.397 Å (e.g. benzene); sp^2-sp = 1.43 Å; and sp-sp = 1.38 Å. Carbon-hydrogen: sp^3-H and sp^2-H = 1.09 Å and sp-H = 1.08 Å. Carbon-chlorine: sp^3-Cl = 1.79 Å; sp^2-Cl = 1.73 Å; and sp-Cl = 1.63 Å.[31]

Table 5.9: **Natural atomic and Mulliken charges of isomeric hexachlorobenzene at the B3LYP/3-21G//B3LYP/3-21G and B3LYP/6-31G*//B3LYP/6-31G* levels.[a]**

	B3LYP/3-21G//B3LYP/3-21G	B3LYP/6-31G*//B3LYP/6-31G*
Atom	**Natural Atomic Charges[b]**	**Natural Atomic Charges[b]**
Cl(1)	0.12520	0.12711
C2	-0.06924	-0.06345
C3	-0.16595	-0.16878
C4	-0.11577	-0.11621
C5	-0.09720	-0.09279
C6	-0.11293	-0.11673
Cl7	0.08006	0.07987
Cl8	0.09551	0.09601
Cl9	0.03393	0.03582
C10	0.02390	0.01915
Cl11	0.10169	0.10279
Cl12	0.10080	0.09720

[a]All geometries are optimized at the B3LYP/3-21G//B3LYP/3-21G and B3LYP/6-31G*//B3LYP/6-31G* levels and have no imaginary frequencies. [b]Natural charges from natural population analysis.[26]

sp^3 carbon bond = 1.53 Å.[31] The bond lengths of C6-C10 = 1.322 Å , and C2-C4 = 1.361Å, at the B3LYP/6-31G*//B3LYP/6-31G* level are similar to an ethylene sp^2 carbon-sp^2carbon bond = 1.32 Å.[31] The C5-C10 bond length = 1.332 Å at the B3LYP/6-31G*// B3LYP/6-31G* level approaches the carbon-carbon double bond in ethylene and C4-C5 = 1.467 Å at B3LYP/6-31G*//B3LYP/6-31G* level is close to typical values for an sp^2-sp^2 single bond in butadiene.[31] Plus, the chlorines that straddle C10 are moved above and below the plane of the ring with dihedral angles of C2-C4-C5-Cl11 = 132.39 Å, Cl11-C5-C10-... = –142.748 Å, C2-C3-C6-Cl12 = 139.81 Å, and Cl12-C6-C10-... = -159.646 Å at B3LYP/6-31G*//B3LYP/6-31G* level, which is reasonable for an allene attempting to move towards the perpendicular plane for the two π-bonds in unstrained allene. Overall, the structure of the *iso*-hexachlorobenzene intermediate is not an association of the pentachlorophenyl ring π-system with the chlorine atom, but rather a species exhibiting a σ-bonded chlorine atom to a ring carbon of benzene. The bonding of the chlorine atom to C3 causes this carbon to become sp^3 like with elongation of the benzene carbon-carbon and carbon-hydrogen bonds along with a reduction of the bond angles from 120° to approximately 109.5° forming an isomeric hexachlorobenzene intermediate, **Table 5.8**.

The natural charges at the B3LYP/6-31G*//B3LYP/6-31G* level reveal that there is extra electron density on C2, C3, C4, C5, and C6, **Table 5.9**. The negative charge resides mostly on the C3, C4 and C6. C10 has a slightly positive charge revealing a lack of electron density at this atom. The lack of electron density at C10 and increased electron density at the other five carbons of the ring is similar to the geometry optimized at the B3LYP/6-31G*//B3LYP/6-31G* level of the phenyl radical as well as the *iso*-chloro-

benzene discussed above. The chlorine atom-benzene complex reveals an increased amount of electron density at the carbon complexed with the chlorine atom at the B3LYP/3-21G//B3LYP/3-21G. Similarities exist between the natural charges for the isomeric hexachlorobenzene intermediate, the phenyl radical, and chlorine atom and benzene complex, although, once gain, no severe perturbations of the bond lengths and angles are present in the optimized geometry of the phenyl radical.

In conclusion, the calculations reveal that the formation of the isomeric chlorobenzene is slightly endothermic at the B3LYP/3-21G//B3LYP/3-21G and the B3LYP/6-31G*//B3LYP/6-31G* levels, while the formation of the isomeric hexachloro-benzene intermediate is slightly exothermic at the same levels of theory and basis sets. The optimized geometries at the B3LYP/3-21G//B3LYP/3-21G and the B3LYP/6-31G*// B3LYP/6-31G* levels suggest that the chlorine atom does not associate with the benzene discussed above. The chlorine atom-benzene complex reveals an increased amount of electron density at the carbon complexed with the chlorine atom at the B3LYP/3-21G//B3LYP/3-21G. Similarities exist between the natural charges for the isomeric hexachlorobenzene intermediate, the phenyl radical, and chlorine atom and benzene complex, although, once gain, no severe perturbations of the bond lengths and angles are present in the optimized geometry of the phenyl radical.

Photolysis Experiments

It would be interesting to find out if other chlorinated benzenes besides chlorobenzene could form products via an *iso*-polychlorobenzene intermediate in both cyclohexane and in a solvent that does not readily undergo disproportionation. Would the

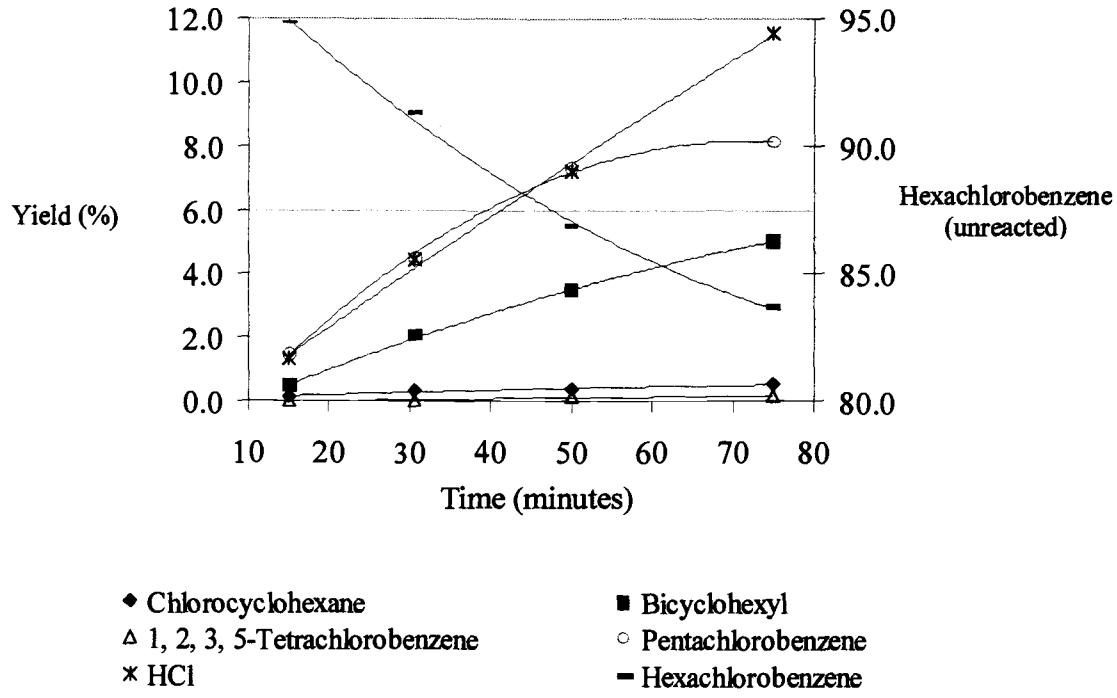

Figure 5.5: **Product distribution of an irradiated solution of hexachlorobenzene in cyclohexane vs. irradiation time.**

Table 5.10: **Percent yield of products in the irradiations of 0.00078 M hexachlorobenzene in cyclohexane at 300 nm.**

	Photolysis Time (minutes)			
Compound	**15**	**30.5**	**50**	**75**
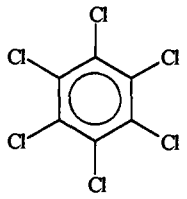 (unreacted)	94.81 ± 5.45	91.28 ± 0.67	86.85 ± 2.5	83.68 ± 1.95
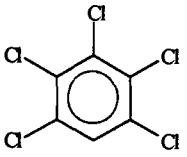	1.50 ± 0.08	4.48 ± 0.14	7.3 ± 0.13	8.1 ± 0.43
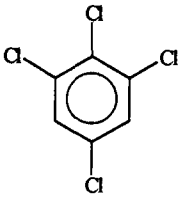	---	---	0.13 ± 0.03	0.14 ± 0.03
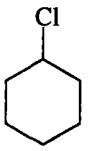	0.13 ± 0.05	0.34 ±0.07	0.37 ± 0.004	0.52 ± 0.18
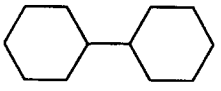	0.46 ± 0.04	2.03 ± 0.07	3.47 ± 0.014	5.02 ± 0.9
HCl	1.32 ± 0.79	4.46 ± 0.36	7.23 ± 0	11.54 ± 1.78

[a]All yields are referred to the starting concentration of hexachlorobenzene.

other products be similar to what Lemal and Arnold found?[10,11] Photolysis experiments of hexachlorobenzene in cyclohexane and tetramethyl silane were undertaken to see what percentage of products came about from the *iso*-hexachlorobenzene intermediate. Irradiations of chlorobenzene in tetramethyl silane were also conducted to make sure that the ratio of products is not much different than photolyses in neopentane.

When 0.0078 M hexachlorobenzene is irradiated at 300 nm in cyclohexane for 15 to 75 minutes the major products are HCl, pentachlorobenzene and bicyclohexyl, **Figure 5.5** and **Table 5.10**. The minor products are chlorocyclohexane and 1, 2, 3, 5-tetra-chlorobenzene. The percent conversion of hexachlorobenzene is < 15 %, therefore, we can assume that the majority of the products are due to reactions of hexachlorobenzene, although pentachlorobenzene did undergo dehalogenation to form a small amount of 1, 2, 3, 5-tetrachlorobenzene as the photolysis time increased to 50 and 75 minutes. Most significant for the present discussion is the presence of chlorocyclohexane. The formation of chlorocyclohexane is an indication that the *iso*-hexachlorobenzene is forming in the photolysis of hexachlorobenzene in cyclohexane. To be able to calculate the minimum involvement of the non-traditional mechanism we assume that the photosensitized reaction of the HCl addition to cyclohexene contributes minimally to the formation of chlorocyclohexane. The fraction of recombination and diffusion is unknown, although literature suggests that it would be diffusion controlled.[32-34] The minimum percent involvement of the non-traditional mechanism can be calculated by dividing the concentration of chlorocyclohexane by the concentration of HCl plus chlorocyclohexane multiplied by one hundred (i.e. the non-traditional pathway divided by the sum of the

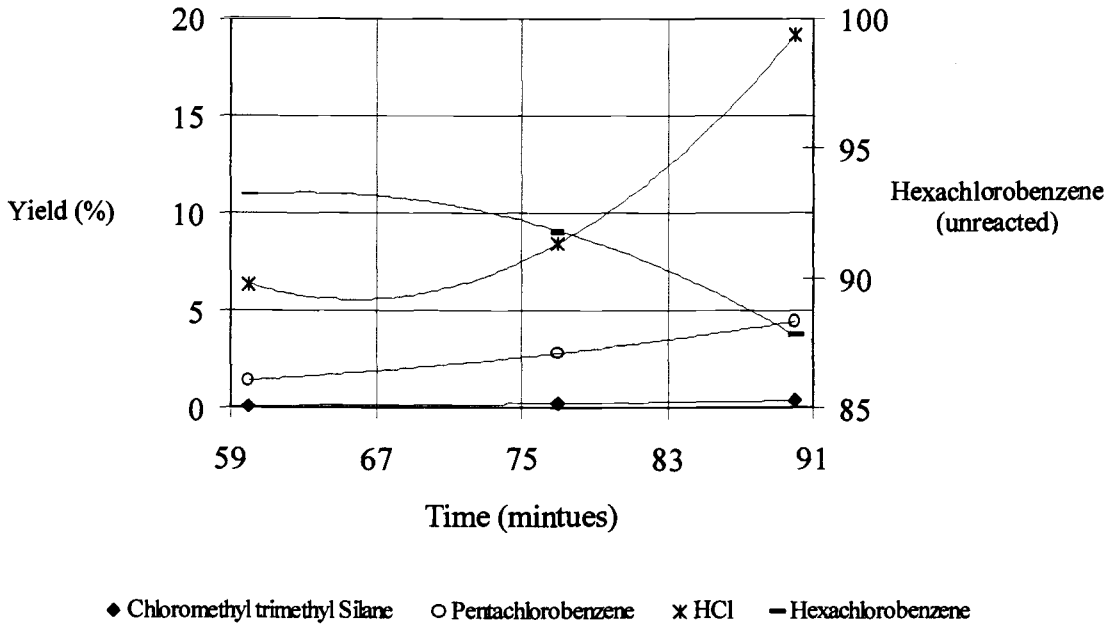

Figure 5.6: Product distribution of irradiated solution of hexachlorobenzene in tetramethyl silane vs. irradiation time.

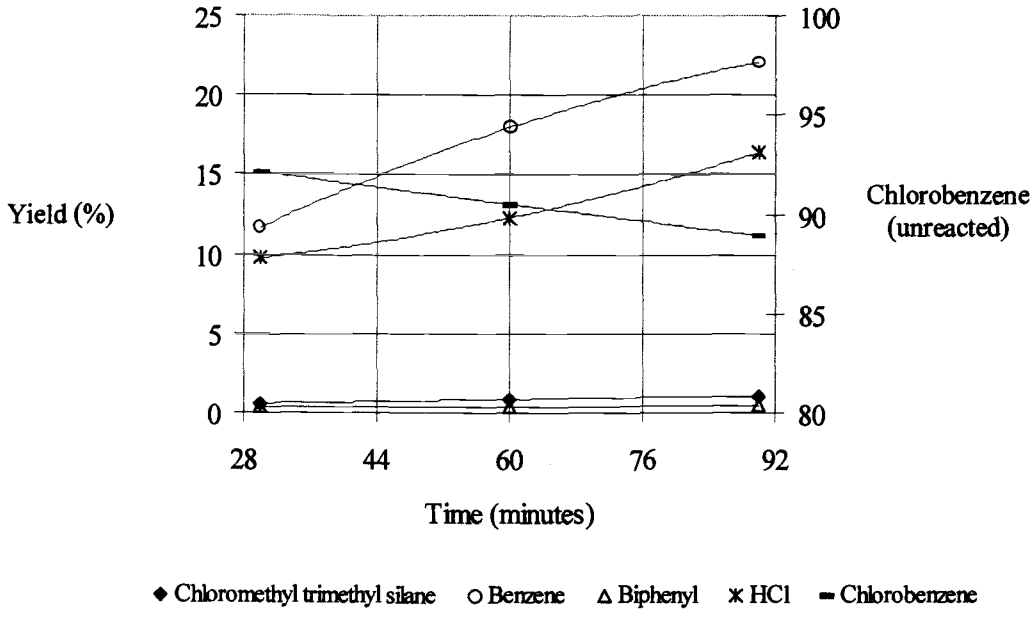

Figure 5.7: Product distribution of irradiated solution of chlorobenzene in tetramethyl silane vs. irradiation time.

traditional and non-traditional pathways). The minimum percent involvement of *iso*-hexachlorobenzene is 9%, 7.1%, 4.9% and 4.3% in the 15, 30.5, 50 and 75 minute photolyses, respectively. These photolysis experiments provide evidence for the involvement of *iso*-hexachlorobenzene.

Since cyclohexane can undergo disproportionation, chlorocyclohexane may have come about from the photosensitized addition of HCl to cyclohexene. To further assess the involvement of *iso*-hexachlorobenzene in the irradiation of hexachlorobenzene, hexachlorobenzene was irradiated in a solvent that does not readily undergo disproportionation. Arnold and Wong used neopentane ($C(CH_3)_4$) and found that < 5% of products arose from *iso*-chloro-propylbenzene.[11] Neopentane is no longer commercially available, therefore, tetramethyl silane was used because of the similarities of the silicon-carbon (Si-C) single bond and the carbon-carbon (C-C) single bond.[33,34] The boiling point of tetramethyl silane (26-28°C) is much higher than neopentane (~9.5°C) making it much easier to work with in the laboratory. Plus, it has been found that many Si-C containing molecules undergo chlorination, bromination, diazotisation, nitration and coupling of the organic groups without Si-C bond cleavage.[34]

Dilute solutions of 0.0013 M hexachlorobenzene were irradiated in tetramethyl silane for 60, 77 and 90 minutes. The gas chromatogram traces were not very complex and (chloromethyl) trimethylsilane, pentachlorobenzene and HCl were formed **Figure 5.6**. The minimum percent contribution of the alternative mechanism is 1.5%, 2.5% and 1.9% in the 60, 77 and 90 minute photolyses, respectively, assuming the chlorine atom and trimethylsilylmethyl radical react in cage and do not diffuse away from each other. The presence of (chloromethyl) trimethyl silane provides evidence that the *iso*-hexa-

chlorobenzene pathway is involved in the photolyses of hexachlorobenzene in tetramethyl silane.

Chlorobenzene (0.02 M) was irradiated in tetramethyl silane to ensure that the product yields did not differ greatly from the photolyses in neopentane. The gas chromatogram traces revealed a complex mixture of products and the following products were identified: HCl, biphenyl, benzene, (chloromethyl) trimethylsilane and unreacted chlorobenzene. The product of most interest in the comparison to the results of Arnold and Wong[11] is (chloromethyl) trimethylsilane, which is the product that is the equivalent to neopentyl chloride, **Figure 5.7**. The yield percent in the 30, 60 and 90 minute photolyses is 0.6%, 0.89% and 1.1%, respectively. The yield percent is slightly less than experiments in neopentane because the researchers photolyzed for approximately 2 hours so that almost all of the *o*-chloropropylbenzene had disappeared. The percent conversions of chlorobenzene in the photolyses in tetramethylsilane are < 15 %. The minimum percent involvement of the *iso*-chlorobenzene pathway is 5.8%, 6.7% and 6.3% in the 30, 60 and 90 minute photolyses, respectively. The formation of chloromethyltrimethylsilane provides a clue that the alternative mechanism is occurring in the irradiations.

Conclusion

The computations conducted at both B3LYP/3-21G//B3LYP/3-21G and B3LYP/ 6-31G*//B3LYP/6-31G* levels reveal that both chlorobenzene and hexachlorobenzene may form *iso*-chlorobenzene and *iso*-hexachlorobenzene complexes. The computations suggest that the complexes are not an association of the chlorine atom with the π-system of the benzene ring as originally thought by researchers in the 1970s,[10,11] but rather involve

direct σ bonding to a carbon of the benzene ring. Evidence for a minor, but notable pathway involving *iso*-polychlorinated benzene is based upon the formation of (chloromethyl) trimethylsilane in our photolysis experiments. The average minimum percent contribution of the minor mechanism responsible for products in the photolyses of hexachlorobenzene and chlorobenzene in tetramethyl silane is 2% and 6.3%, respectively.

Acknowledgements

I would like to thank Dr. Jaromir Růžička and Armando Herbelin (University of Washington, Seattle) for their informative discussions on flow injection chloride analysis methods.

Support for this research by the Environmental Health Sciences, Oregon State University Chemistry Department and the N. L. Tarter fellowship is gratefully acknowledged.

References

1. Freeman, P.K.; Srinivasa, R.; Campbell, J.-A.; Deinzer, M.L. *J. Am. Chem. Soc.*, 1986, *108*, 5531-5536.

2. Crosby, D. G.; Hamadmad, N. *J. Agr. Food Chem.* 1971, *19*, 1171-1174.

3. Crosby, D. F. Moilanen, K. W.; Wong, A. S. *Eviron. Health Perspect.* 1973, *5*, 259-266.

4. Freeman, P. K.; Ramnath, N. *J. Org. Chem.* 1988, *53*, 148-152.

5. Freeman, P. K.; Ramnath, N.; Richardson, A. D. *J. Org. Chem.* 1991, *56*, 3643-3646.

6. Freeman, P. K.; Ramnath, N. *J. Org. Chem.* 1991, *56*, 3646-3651.

7. Freeman, P. K.; Jang, J-S.; Haugen, C.M. *Tetrahedron* 1996, *52*, 8397-8406.

8. Bunce, N.L.; Hayes, P.J.; Lemke, M.E. *Can. J. Chem.* 1983, *61*, 1103-1104.

9. Åkermark, B.; Baeckström, P.; Westlin, U.E.; Göthe, R.; Wachtmesiter, C. *Acta Chem. Scand. B.* 1976, *30*, 49-52.

10. Fox, M.A.; Nichols, Jr., W.C; Lemal, D.M. *J. Am. Chem. Soc.* 1973, *95*, 8164-8166.

11. Arnold, D.R.; Wong, P.C. *J. Am. Chem. Soc.* 99, *1977*, 3361-3366.

12. Hehre, W.J.; Radom, L.; Schleyer, P.v.R.; Pople, J.A. *Ab Initio Molecular Orbital Theory*; Wiley: New York, 1986.

13. *Spartan*, versions 4.1-5.0; Wavefunction, Inc.: Irvine, CA, 1993-1997.

14. *Gaussian 92*, Revision G.4, M. J. Frisch, G. W. Trucks, M. Head-Gordon, P. M. W. Gill, M. W. Wong, J. B. Foresman, B. G. Johnson, H. B. Schlegel, M. A. Robb, E. S. Replogle, R. Gomperts, J. L. Andres, K. Raghavachari, J. S. Binkley, C. Gonzalez, R. L. Martin, D. J. Fox, D. J. Defrees, J. Baker, J. J. P. Stewart, and J. A. Pople, Gaussian, Inc., Pittsburgh PA, 1992. *Gaussian 94*, Revisions C.2 and E.1, M. J. Frisch, G. W. Trucks, H. B. Schlegel, P. M. W. Gill, B. G. Johnson, M. A. Robb, J. R. Cheeseman, T. Keith, G. A. Petersson, J. A. Montgomery, K. Raghavachari, M. A. Al-Laham, V. G. Zakrzewski, J. V. Ortiz, J. B. Foresman, J. Cioslowski, B. B. Stefanov, A. Nanayakkara, M. Challacombe, C. Y. Peng, P. Y. Ayala, W. Chen, M. W. Wong, J. L. Andres, E. S. Replogle, R. Gomperts, R. L. Martin, D. J. Fox, J. S. Binkley, D. J. Defrees, J. Baker, J. P. Stewart, M. Head-Gordon, C. Gonzalez, and J. A. Pople, Gaussian, Inc., Pittsburgh PA, 1995.

15. Hehre, W.J.; Stewart, R.J.; Pople, J.A. *J. Chem. Phys.* 1969,*51*, 2657.

16. Collins, J.B.; Schleyer, P.v.R.; Binkley, J.S.; Pople, J.A. *J. Chem. Phys. 1976,* 64, 5142.

17. Binkley, J.S.; Pople, J.A.; Hehre, W.J. *J. Am. Chem. Soc.* 1980, *102*, 939.

18. Dobbs, K.D.; Hehre, W.J. *J. Comp. Chem.* 1987, *8*, 880.

19. Ditchfield, R.; Hehre, W.H.; Pople, J.A. *J. Chem. Phys.* 1971, *54*, 724.

20. Hehre, W.H.; Ditchfield, R.; Pople, J.A. *J. Chem. Phys.* 1972, *56*, 2257.

21. Hariharan, P.C.; Pople, J.A. *Mol. Phys.* 1974, *27*, 209.

22. Gordon, M.S. *Chem. Phys. Lett.* 1980, *76*, 163.

23. Hariharan, P.C.; Pople, J.A. *Theo. Chim. Acta.* 1973, *28*, 213.

24. Becke, A.D. *J. Chem. Phys.* 1993, *98*, 5648.

25. Lee, C.; Yang, W.; Parr, R.G. *Phys. Rev. B.* 1988, *37*, 785.

26. Forseman, J.B.; Frisch, Æ. *Exploring Chemistry with Electronic Methods*, 2nd Ed.; Gaussian, Inc.: Pittsburgh, PA, 1995-96.

27. Bulliard, C.; Allan, M.; Haselbach. E. *J. Phys. Chem.* 1994, *98*, 11040-11045.

28. Bunce, N.J.; LaMarre, J.; Baish, S.P. *Photochem. Photobiol.* 1984, *39*, 531.

29. Růžička, J.; Hansen, E.H. *Flow Injection Analysis*, 2nd ed.; Winefordner, J.D., Kolthoff, I.M., Eds.; Chemical Analysis: A Series of Monographs on Analytical Chemistry and Its Applications; Wiley and Sons: New York, NY, 1988; Vol. 62, 302.

30. Matsuzawa, H.; Osamura, Y. *Bull. Chem. Soc. Jpn.* 1997, *70*, 1531-1537.

31. March, J. Advanced Organic Chemistry. *Reactions Mechanisms and Structure*, 4th Ed.: Wiley and Sons: New York, NY, 1992.

32. Perkins, M.J. *Radical Chemistry;* Mellor, J., Ed.; Ellis Horwood Series in Organic Chemistry; Ellis Horwood: New York, NY, 1994.

33. Fritz, G.; Matern, E. *Carbosilanes: Synthesis and Reactions*; Springer-Verlag: New York, NY, 1986.

34. Pawlenko, S. *Organosilicon Chemistry*; Walter de Gruyter: New York, NY, 1986.

Chapter 6: Conclusion

Sharon Maley Herbelin

Mechanistic studies have been conducted on polyhalogenated benzenes. These prevalent environmental pollutants have been analyzed by an electron monochromator mass spectrometer system. It has been found that the EM/MS is a very powerful analytical tool that can be implemented to distinguish electronegative compounds (especially isomers) by observing transient negative ions (TNIs) of the same mass but differing energies and/or the formation of distinct TNIs of different masses for each electronegative compound. Therefore, in unknown samples, the presence of these compounds could be validated. *Ab initio* molecular orbital calculations provide insight into groups of molecular orbitals that may be capturing the electrons by directly comparing the energies of the TNIs and chloride ions and the eigenvalues of the optimized geometries of the neutral molecules. The implementation of Koopman's theorem results in calculated attachment energies that are very close to experimental values.

Calculations have also been performed to understand the mechanisms that may take place in the electron capture chemical ionization mass spectrometry experiments, and the non-photochemical and photochemical reactions of the polyhalogenated benzenes. The computations qualitatively support the results from the GC/ECCI/MS experiments, and the photochemical and non-photochemical experiments of many of the polyhalogenated benzenes in the presence of electron transfer reagents. Furthermore, insight has been provided into which chlorines are cleaved preferentially and which methods and basis sets are most appropriate to model radical anion cleavage pathways of polychlorinated benzenes.

Direct probe insertion electron capture chemical ionization mass spectrometry (DP/ECCI/MS) experiments reveal that the bromine and chlorine addition adducts are not due to impurities in the sample. The results of the DP/ECCI/MS experiments and

calculations reveal that typical reactions, plus, atypical reactions involving sequential "positive halogen transfers" and hydrogen abstractions to form ions with one to three bromines added to the starting material may be occurring in the ionization chamber.

Finally, experiments were conducted to see if a minor, but important pathway that involves a "π-polychlorobenzene intermediate" is taking part in the photo-dehalogenation of two polychlorinated benzenes, chlorobenzene and hexachlorobenzene. Calculations suggest that the complexes are not an association of the chlorine atom with the π-system but rather involve direct σ bonding to a carbon of the benzene ring forming *iso*-chloro-benzene and *iso*-hexachlorobenzene complexes. Evidence for a minor, but notable pathway involving *iso*-polychlorinated benzene is based upon the formation of chloromethyltrimethylsilane in our photolysis experiments. The average minimum percent contribution of the minor mechanism responsible for products in the photolyses of hexachlorobenzene and chlorobenzene in tetramethyl silane is 2% and 6.3%, respectively.

Bibliography

Åkermark, B.; Baeckström, P.; Westlin, U.E.; Göthe, R.; Wachtmesiter, C. *Acta Chem. Scand. B.* **1976**, *30*, 49-52.

Arnold, D.R.; Wong, P.C. *J. Am. Chem. Soc.* **99**, *1977*, 3361-3366.

Atkins, P.W. *Physical Chemistry*, 4th Ed.; W.H. Freeman and Company: New York, 1990.

Atkins, P.W. *Physical Chemistry*, 4th ed.; W.H. Freeman and Company: New York, 1990.

Barofsky, D.F.; Deinzer, M.L. *Mass Spectrometry of Organic Molecules (AC637/CH537)*, Fall **1992**, Class Notes, Oregon State University.

Becke, A.D. *J. Chem. Phys.* **1993**, *98*, 5648.

Berkout, V.D.; Mazurkiewicz, P.; Deinzer, M.L. *Anal. Chem.* in press, 1998.

Bieniek, D.; Bahadir, M.; Korte, F. *Heterocycles*, **1989**, *28*, 719-722.

Binkley, J.S.; Pople, J.A.; Hehre, W.J. *J. Am. Chem. Soc.* **1980**, *102*, 939.

Bulliard, C.; Allan, M.; Haselbach. E. *J. Phys. Chem.* **1994**, *98*, 11040-11045.

Bunce, N.J.; LaMarre, J.; Baish, S.P. *Photochem. Photobiol.* **1984**, *39*, 531.

Bunce, N.L.; Hayes, P.J.; Lemke, M.E. *Can. J. Chem.* **1983**, *61*, 1103-1104.

Bunnett, J.F. *Acc. Chem. Res.* **1972**, *5*, 139-147.

Bunnett, J.F.; Moyer, Jr., C.E. *J. Am. Chem. Soc.*, **1971**, 93, 1183-1205.

Burrow, P.D.; Modelli, A.; Jordan, K.D. *Chem. Phys. Lett.* **1986**, *132*, 441.

Carey, F.A.; Sunberg, R.J. *Advanced Organic Chemistry Part A: Structure and Mechanisms*, 3rd ed.; Plenum Press, NY, 1990.

Chlorinated Organic Micropollutants; Hester, R.E., Harrison, R.M., Eds.; Issues in Environmental Science and Technology 6; Royal Society of Chemistry: Cambridge, UK, 1996.

Clarke, D.D.; Coulson, C.A. *J. Chem. Soc. A*, **1969**, 169.

Collins, J.B.; Schleyer, P.v.R.; Binkley, J.S.; Pople, J.A. *J. Chem. Phys. 1976,* **64**, 5142.

Couch, T.L. Ph.D. Thesis, Oregon State University, Corvallis, OR, 1997.

Crosby, D. F. Moilanen, K. W.; Wong, A. S. *Eviron. Health Perspect.* **1973**, *5*, 259-266.

Crosby, D. G.; Hamadmad, N. *J. Agr. Food Chem.* **1971**, *19*, 1171-1174.

Ditchfield, R.; Hehre, W.H.; Pople, J.A. *J. Chem. Phys.* **1971**, *54*, 724.

Dobbs, K.D.; Hehre, W.J. *J. Comp. Chem.* **1987**, *8*, 880.

Dressler, R; Allan, M.; Haselbach, E. *Chimia,* **1985**, *39*, 385.

Energetics of Organic Free Radicals; Simões, J.A.M., Greenberg, A., Liebman, J.F.Eds.; Structure Energetics and Reactivity in Chemistry Series (SEARCH); Liebman, J.F., Greenberg, A., Eds.; Blackie Academic and Professional: NY, 1996; Vol. 4.

Forseman, J.B.; Frisch, Æ. *Exploring Chemistry with Electronic Methods*, 2nd Ed.; Gaussian, Inc.: Pittsburgh, PA, 1995-96.

Fox, M.A.; Nichols, Jr., W.C; Lemal, D.M. *J. Am. Chem. Soc.* **1973**, *95*, 8164-8166.

Freeman, P. K.; Jang, J-S.; Haugen, C.M. *Tetrahedron* **1996**, *52*, 8397-8406.

Freeman, P. K.; Ramnath, N. *J. Org. Chem.* **1988**, *53*, 148-152.

Freeman, P. K.; Ramnath, N. *J. Org. Chem.* **1991**, *56*, 3646-3651.

Freeman, P. K.; Ramnath, N.; Richardson, A. D. *J. Org. Chem.* **1991**, *56*, 3643- 3646.

Freeman, P.K.; Lee, Y-S. Masters Thesis, Oregon State University, Corvallis, OR, 1987.

Freeman, P.K.; Srinivasa, R.; Campbell, J.-A.; Deinzer, M.L. *J. Am. Chem. Soc.*, **1986**, *108*, 5531-5536.

Fritz, G.; Matern, E. *Carbosilanes: Synthesis and Reactions*; Springer-Verlag: New York, NY, 1986.

Gaussian 92, Revision G.4, M. J. Frisch, G. W. Trucks, M. Head-Gordon, P. M. W. Gill, M. W. Wong, J. B. Foresman, B. G. Johnson, H. B. Schlegel, M. A. Robb, E. S. Replogle, R. Gomperts, J. L. Andres, K. Raghavachari, J. S. Binkley, C. Gonzalez, R. L. Martin, D. J. Fox, D. J. Defrees, J. Baker, J. J. P. Stewart, and J. A. Pople, Gaussian, Inc., Pittsburgh PA, 1992. *Gaussian 94*, Revisions C.2 and E.1, M. J. Frisch, G. W. Trucks, H. B. Schlegel, P. M. W. Gill, B. G. Johnson, M. A. Robb, J. R. Cheeseman, T. Keith, G. A. Petersson, J. A. Montgomery, K. Raghavachari, M. A. Al-Laham, V. G. Zakrzewski, J. V. Ortiz, J. B. Foresman, J. Cioslowski, B. B. Stefanov, A. Nanayakkara, M. Challacombe, C. Y. Peng, P. Y. Ayala, W. Chen, M. W. Wong, J. L. Andres, E. S. Replogle, R. Gomperts, R. L. Martin, D. J. Fox, J. S. Binkley, D. J. Defrees, J. Baker, J. P. Stewart, M. Head-Gordon, C. Gonzalez, and J. A. Pople, Gaussian, Inc., Pittsburgh PA, 1995.

Glukhovtsev, M. N.; Bach, R.D.; Laiter, S. *J. Org. Chem.* **1997**, 62, 4036-4046.

Gordon, M.S. *Chem. Phys. Lett.* **1980**, *76*, 163.

Hariharan, P.C.; Pople, J.A. *Mol. Phys.* **1974**, *27*, 209.

Hariharan, P.C.; Pople, J.A. *Theo. Chim. Acta.* **1973**, *28*, 213.

Harrison, A.G. *Chemical Ionization Mass Spectrometry*, 2nd Ed.; American Chemical Society: Washington, DC, 1997.

Hehre, W.H.; Ditchfield, R.; Pople, J.A. *J. Chem. Phys.* **1972**, *56*, 2257.

Hehre, W.J.; Radom, L.; Schleyer, P.v.R.; Pople, J.A. *Ab Initio Molecular Orbital Theory*; Wiley: New York, 1986.

Hehre, W.J.; Stewart, R.J.; Pople, J.A. *J. Chem. Phys.* **1969**,*51*, 2657.

ISOPRO - Isotopic Abundance Simulator, version 2.0; M.W. Senko: Department of Chemistry, Cornell University, Ithaca, NY.

Jennings, K.R.; Dolnikowski, G.G. *Methods in Enzymology.* **1990**, 193, 37-61.

Klusmeier, W.; Vögler, P.; Ohrback, K.-H.; Weber, H.; Kettrup, A. *J. Anal. App. Pyrolysis*, **1988**, *13*, 277-285.

Laramée, J. A.; Kocher, C. A.; Deinzer, M. L. *Analytical Chemistry* **1992,** *64,* 2316-2322.

Laramée, J.A.; Mazurkiewicz, P.; Berkout, V.D.; Deinzer, M.L. *unpublished manuscript* 1996.

Lee, C.; Yang, W.; Parr, R.G. *Phys. Rev. B.* **1988**, *37*, 785.

Leffler, J.E. *An Introduction to Free Radicals*; John Wiley and Sons: New York, NY, 1993.

Lowry, T.H.; Richardson, K.S. *Mechanism and Theory in Organic Chemistry*, 3rd ed.; Harper & Row, Publishers: New York, 1987.

Mach, M.H.; Bunnett, J.F. *J. Org. Chem.*, **1980**, *45*, 4660-4666.

March, J. *Advanced Organic Chemistry. Reactions Mechanisms and Structure*, 4th Ed.: Wiley and Sons: New York, NY, 1992.

Matsuzawa, H.; Osamura, Y. *Bull. Chem. Soc. Jpn.* **1997**, *70*, 1531-1537.

McLafferty, F.W.; Tureček, F. *Interpretation of Mass Spectra*, 4th Ed., **1993**, University Science Books, Mill Valley, CA, pp. 339-342.

McQuarrie, D.A. *Quantum Chemistry*; University Science Books: Mid Valley, California, 1983.

Olthoff, J.K.; Tossell, J.A.; Moore, J.H. *J. Chem. Phys.* **1985**, *83*, 5627.

Oster, T.; Kühn, A.; Illenberger, E. *Int. J. Mass Specctrom. Ion Proc.*, **1989**, *89*, 1-72.

Pawlenko, S. *Organosilicon Chemistry*; Walter de Gruyter: New York, NY, 1986.

Perkins, M.J. *Radical Chemistry;* Mellor, J., Ed.; Ellis Horwood Series in Organic Chemistry; Ellis Horwood: New York, NY, 1994.

Růžička, J.; Hansen, E.H. *Flow Injection Analysis*, 2nd ed.; Winefordner, J.D., Kolthoff, I.M., Eds.; Chemical Analysis: A Series of Monographs on Analytical Chemistry and Its Applications; Wiley and Sons: New York, NY, 1988; Vol. 62, 302.

Raunhut, G.; Pulay, P. *J. Am. Chem. Soc.*, **1995**, 117, 4167-4172.

Spartan, versions 4.1-5.0; Wavefunction, Inc.: Irvine, CA, 1993-1997.

Staley, S.W.; Strnad, J.T. *J. Phys. Chem.* **1994**, *98*, 116-121.

Stricklett, K.L.; Chu, S.C.; Burrow, P.D. *Chem. Phys. Lett.* **1986**, *131*, 279.
Time-of-Flight Mass Spectrometry; Cotter, R.J., Ed.; ACS Symposium Series 549; American Chemical Society: Washington, DC, 1994.

Watanabe, I.; Kashimoto, T.; Tatsukawa, R. *Bull. Envrion. Contam. Toxicol.*, **1986**, *36*, 778-784.

Watson, T.T. *Introduction to Mass Spectrometry*, 3rd ed.; Lippincott-Raven: New York, 1997.

White, F.A.; Wood, G.M. *Mass Spectrometry: Applications in Science and Engineering*; Wiley and Sons: New York, 1986.

Appendix A: Example Spectra of the DP/ECCI/MS Experiments

Sharon Maley Herbelin

Appendix A contains example spectra from direct probe electron capture chemical ionization mass spectrometry (DP/ECCI/MS) experiments of the dibromobenzenes, tribromobenzenes, and a mixture of 1, 2, 3-trichlorobenzene and 1, 2, 3-tribromobenzene. The y-axis of many of the spectra has been expanded. The m/z value of 127 corresponds to an impurity in the mass spectrometer, iodide (I^-). The mass calibration for m/z values > 50 was correct at the time of these experiments, however, the low mass calibration (m/z < 50) was inaccurate; thus, the m/z value for the chloride ion (Cl^-) is 41 instead of 35.

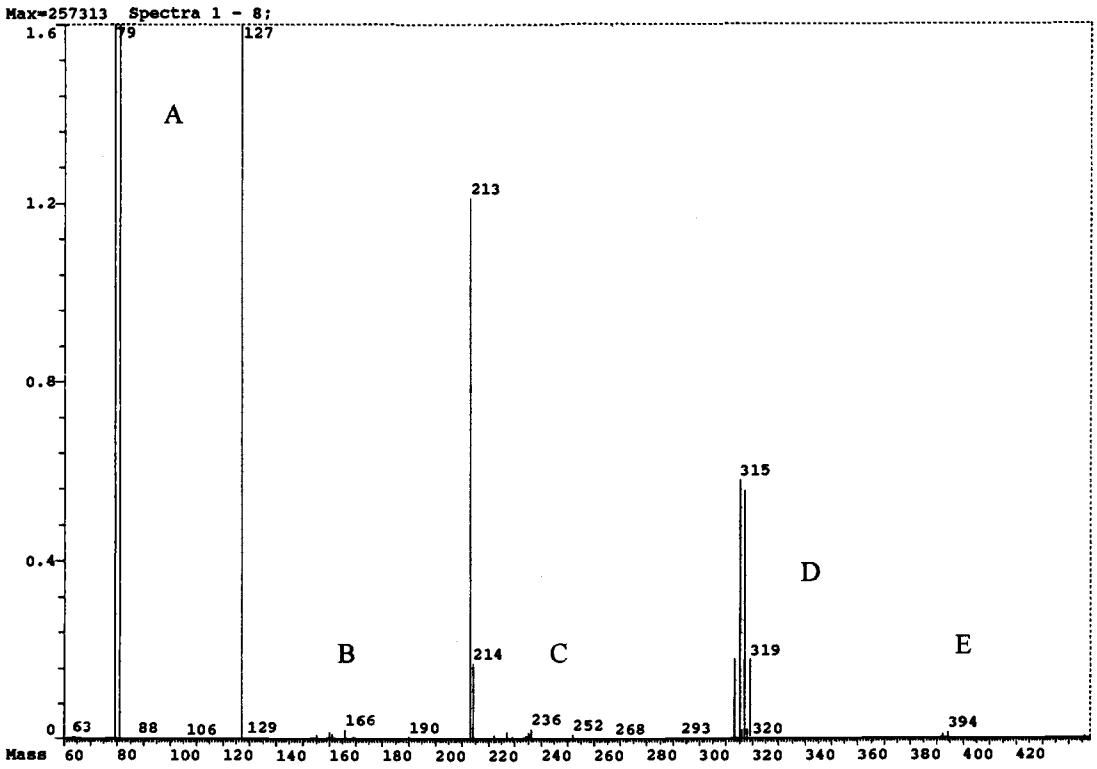

A. Br^- B. $(M-Br)^-$ C. $M^{-\cdot}$ and $(M-H)^-$ D. $(M+Br)^-$ E. $(M+2Br-2H)^-$

Figure A.1: Spectrum from the third run of 1, 2-dibromobenzene.

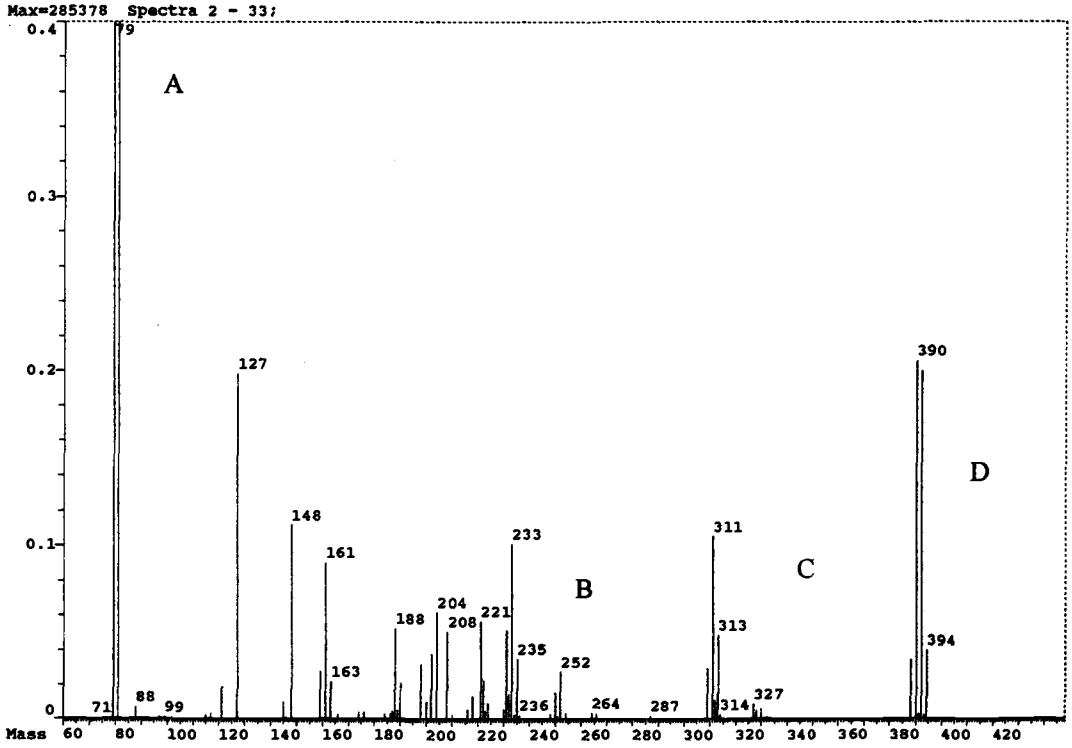

A. Br^- B. $(M-H)^-$ C. $(M+Br-2H)^-$ D. $(M+2Br-2H)^-$

Figure A.2: Spectrum from the first run of 1, 3-dibromobenzene.

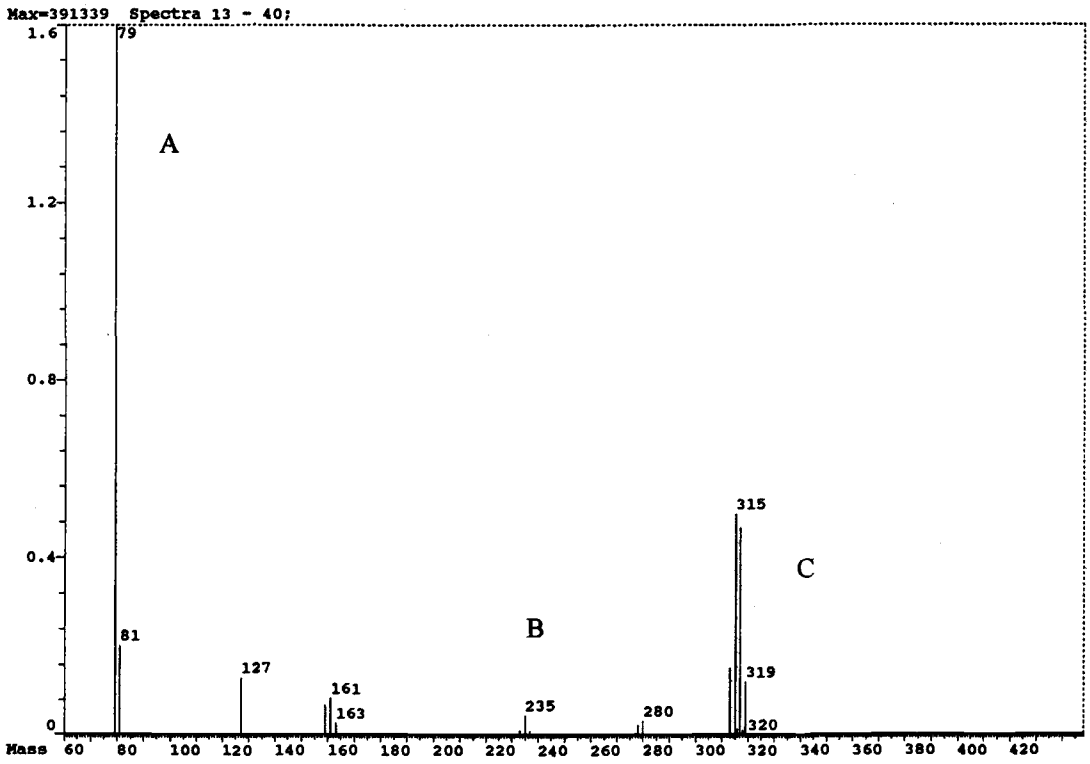

A. Br^- B. $(M-H)^-$ C. $(M+Br)^-$

Figure A.3: Spectrum from the beginning of the TIC from the first run of 1, 4-dibromobenzene.

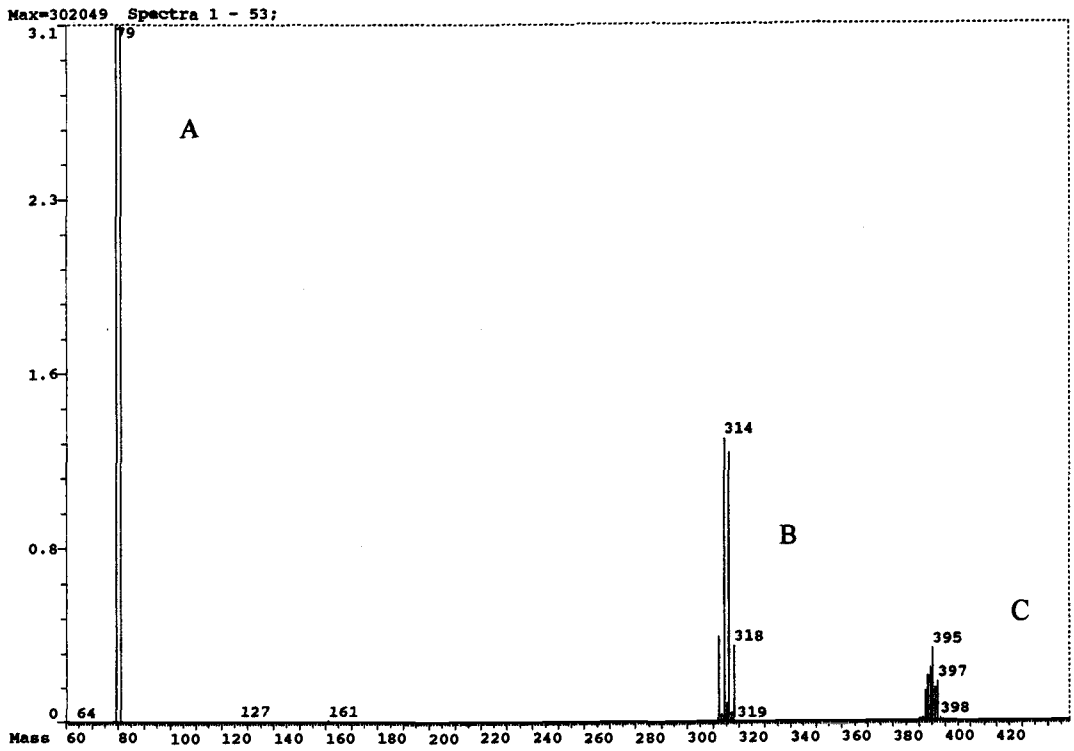

A. Br^- B. M^- C. $(M+Br)^-$ and $(M+Br-H)^-$

Figure A.4: Spectrum from the first run of 1, 2, 4-tribromobenzene.

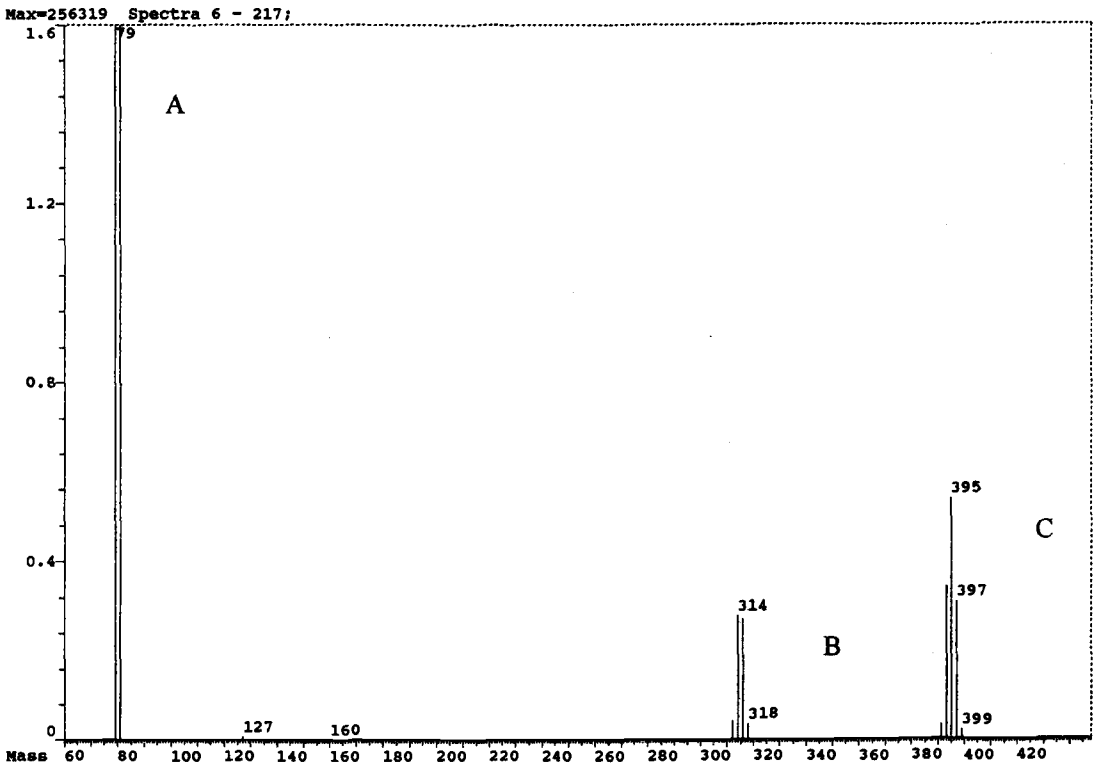

A. Br^- B. $M^{-\cdot}$ C. $(M+Br)^-$

Figure A.5: Spectrum of the beginning of the TIC from the second run of 1, 2, 3-tribromobenzene.

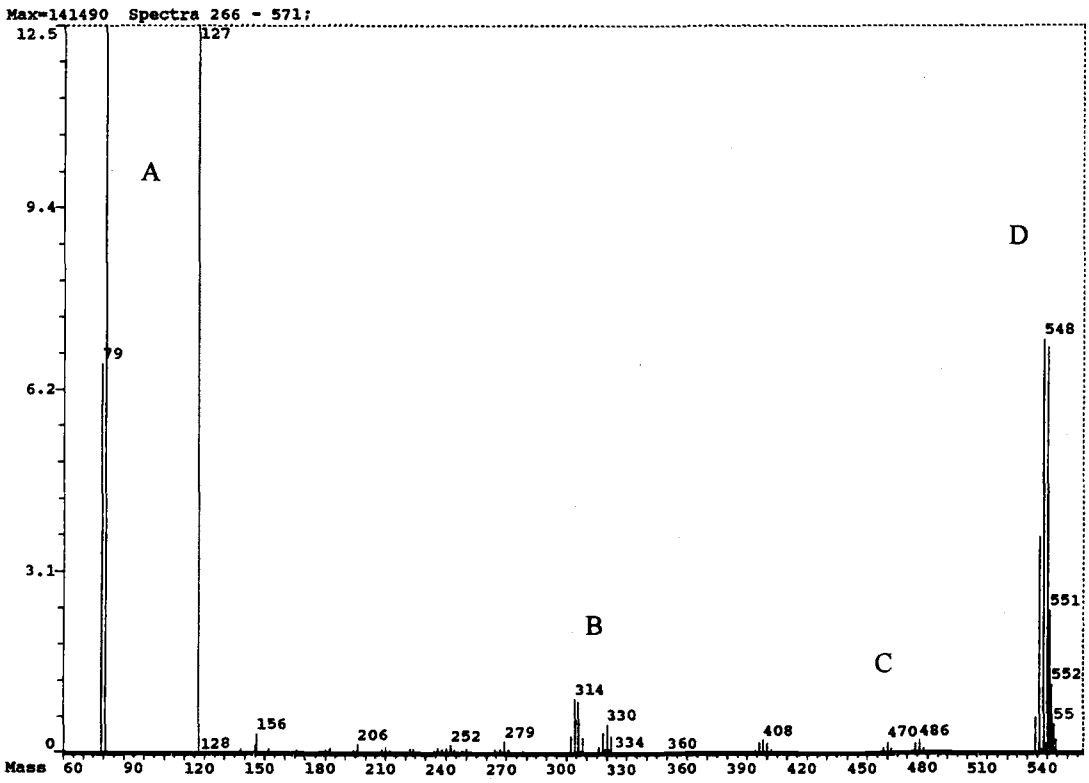

A. Br^- B. $M^{-\cdot}$ C. $(M+Br-3H)^-$ D. $(M+3Br-3H)^-$

Figure A.6: Spectrum from the end of the TIC from the first run of 1, 3, 5-tribromobenzene.

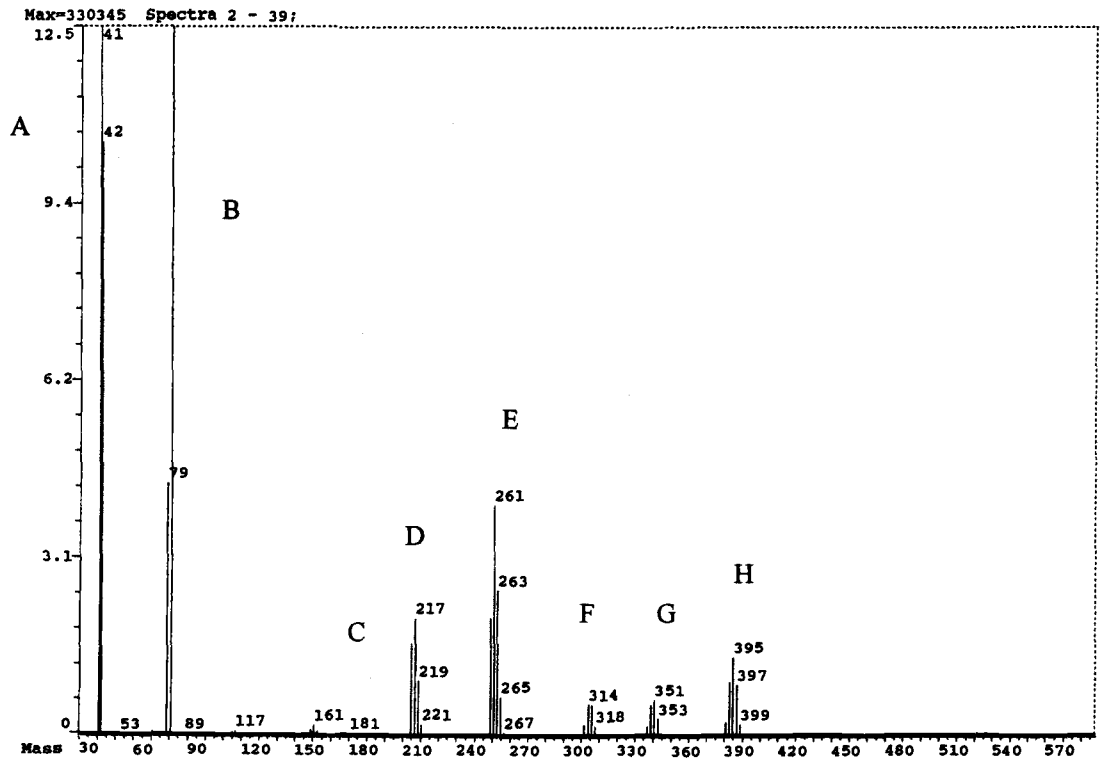

A. Cl^- B. Br^- C. $(M-H)^-$ D. $(M+Cl)^-$
E. $(M+Br)^-$ F. $m^{-\cdot}$ G. $(m+Cl)^-$ H. $(m+Br-2H)^-$

Figure A.7: Spectrum from the beginning of the TIC from the second run of the 1, 2, 3-trichlorobenzene (M) and 1, 2, 4-tribromobenzene (*m*) mixture.